2-1-2012

Characterization of traffic load and local calibration of the MEPDG for New Mexico

Jose Ivan Rodriguez Ruiz

José Iván Rodríguez Ruiz
Candidate

Civil Engineering
Department

This thesis is approved, and it is acceptable in quality and form for publication:

Approved by the Thesis Committee:

Dr. Rafiqul A. Tarefder , Chairperson

Dr. James D. Brogan

Dr. Tang-Tat Ng

CHARACTERIZATION OF TRAFFIC LOAD AND LOCAL CALIBRATION OF THE MEPDG FOR NEW MEXICO

BY

JOSÉ IVÁN RODRÍGUEZ RUIZ

B.S., CIVIL ENGINEERING, UNIVERSIDAD DE GRANADA, 2009
M.S., CIVIL ENGINEERING, UNIVERSITY OF NEW MEXICO, 2011

THESIS

Submitted in Partial Fulfillment of the
Requirements for the Degree of

Master of Science
Civil Engineering

The University of New Mexico
Albuquerque, New Mexico

December, 2011

DEDICATION

To my beloved brother Francisco Javier "El Rodri"

ACKNOWLEDGEMENTS

First, I would like to thank my family. In particular, my father Antonio, my mother Loli, and my sister Mariló for caring about me every day without exception and for missing me so much. Rosalba, my girlfriend, and her daily support have been very important to me during the last two years. Her help in formatting this manuscript was really useful. Then, I am very thankful to my advisor, Dr. Rafiqul Tarefder, for funding my graduate studies and for the time he has spent with me supervising this work. I would like to show gratitude to my colleagues Mesbah, Mostaqur, Sumee, Faisal, Damien, Mekdim, Anthony, Saleh, Meghan, Courtney, Mohiuddin, Rashad, Inram, Bayo, Jared, Ulises, Claudia, Joan, and Carolin for being such a good friends. Also, the rest of my family and friends which are in Spain for being always there for me. And finally, the faculty and staff of the Department of Civil Engineering for giving me an exceptional treatment.

CHARACTERIZATION OF TRAFFIC LOAD AND

LOCAL CALIBRATION OF THE MEPDG FOR NEW MEXICO

by José Iván Rodríguez Ruiz

B.S., Civil Engineering, Universidad de Granada, 2009

M.S., Civil Engineering, University of New Mexico, 2011

ABSTRACT

In the Mechanistic-Empirical Pavement Design Guide (MEPDG), traffic loading is more complex and precise than in the old AASHTO 1993 Guide. Traffic load in MEPDG is characterized by a larger number of traffic inputs such as Annual Average Daily Truck Traffic (AADTT), traffic growth, traffic directional distribution, lane distribution, vehicle class distribution, hourly distribution, monthly distribution, axle load spectra, number of axles per truck class, traffic wander, speed, and tire pressure. Many of these inputs can only be obtained from Weigh-in-Motion (WIM) data. There are about 15 WIM stations in New Mexico. Data from these WIM sites are evaluated for their use for local calibration of the MEPDG. An algorithm is developed in Visual Basic Application (VBA) to check the quality of WIM data. In essence, frequency distributions of the gross vehicle weight and the front steering axle weight are calculated and compared to the criteria recommended by the Traffic Monitoring Guide (TMG). It is observed that only three WIM sites have consistent and reliable weight data. The reasons for the inconsistency in collected WIM data are found to be lack of calibration and bad condition of the pavement

surface near WIM sites. Also, axle load spectra are developed for all WIM data using an algorithm implemented in VBA. The influence of axle load spectra on pavement performance is predicted using MEPDG. For the sections analyzed, it is shown that the effect of axle load spectra is very high on fatigue cracking, moderate on permanent deformation, and non-existent on thermal cracking and roughness.

In this study, local data related to traffic, climate, pavement structure, materials, and distress are collected from different NMDOT sources and stored in MEPDG Oracle database. A total of 29 New Mexico pavement sections are found to have all MEPDG inputs, however data lack from quantitative distress values required for MEPDG calibration. This is because New Mexico has collected qualitative distress data rather than actual measurements of rut depth and crack length over the past years. Instead of using these 29 sections, only 11 sections from the Long Term Pavement Performance (LTPP) database located in New Mexico are used for local calibration. The permanent deformation, alligator cracking, and longitudinal cracking models are calibrated. In calibration methodology, the target is fixed to reduce the residual sum of squared errors, defined by the difference between predicted and measured distress, so that any bias is eliminated and precision is increased. The optimized calibration coefficients are: β_{r1} = 1.0, β_{r2} = 0.9, β_{r3} = 1.2, β_{GB} = 0.8, β_{SG} = 0.8 for the rutting model; C_1 = 0.73, C_2 = 0.09, C_3 = 7200 for alligator cracking; and C_1 = 5.5, C_2 = 2.56, C_3 = 1000 for longitudinal cracking. It is concluded that the newly developed calibration coefficients reduce the error in the MEPDG prediction and are beneficial for designing pavements using MEPDG in New Mexico.

TABLE OF CONTENTS

LIST OF FIGURES

LIST OF TABLES

Chapter 1

INTRODUCTION

1.1 Problem Statement

The new Mechanistic-Empirical Pavement Design Guide (MEPDG) represents a recent breakthrough in the analysis and design of pavement structures. Unlike the previous 1993 AASHTO Guide for Pavement Design that was purely empirical, the MEPDG uses mechanistic principles for determining the stresses and strains in the pavement structure (asphalt concrete, granular bases, and subgrade). Then, empirically-based models are used in MEPDG for predicting distresses such as permanent deformation, cracking, or roughness and performance during the pavement design life. The MEPDG does not only require a much larger number of inputs, but also these are more complex in general. There are three main groups of inputs: traffic loading, environmental conditions, and material properties.

Traffic loading is one of the most important inputs of MEPDG. The MEPDG uses a rather complex approach to characterize the traffic loading. Traffic loading constitutes the magnitude and frequency of the load applied on the pavement during its design life. In addition, MEPDG requires a series of frequency distributions such as directional distribution, lane distribution, truck class distribution, monthly distribution, hourly distribution, axle load spectra, and traffic growth. The development of these inputs is very important to perform level one design, and thus, for the implementation of MEPDG in New Mexico.

Axle load spectra comprise the weight frequency distributions of single, tandem, tridem, and quad axles for every truck class. There are 10 truck classes (4 to 13) according to the FHWA classification scheme. This input can only be obtained by processing the weight data collected at Weigh-In-Motion (WIM) sites. There are different technologies used in WIM stations to collect continuous weight data. These include the use of piezoelectric sensors, piezoquartz sensors, kistler sensors, bending plates or load cells. Each technology has a particular accuracy, or random error in the measurement, plus a systematic bias due to the lack of calibration that drifts over time. Therefore, it is critical to provide a procedure for examining the quality of WIM data and ensure the development of MEPDG traffic inputs from only reliable WIM data.

The traffic inputs obtained from reliable WIM data are needed in the local calibration of the MEPDG for New Mexico conditions. The empirical models or transfer functions that relate stresses and strains to the pavement performance were calibrated globally at a national level. A representative sample of pavement sections from the Long Term Pavement Performance program (LTPP) around North America were used for national calibration at level 3. This suggests that predictions of MEPDG with default empirical models match the average distresses observed in the field around the country, but MEPDG may not predict accurately the field distresses observed locally (i.e. New Mexico) under local conditions of traffic, climate, and materials. There is a need for local calibration of the distress models using pavement sections within New Mexico to allow MEPDG to predict the distresses actually observed in the field under New Mexico conditions.

1.2 Hypotheses

Hypothesis One: Very few software packages are available today for quality control of WIM data and development of traffic MEPDG inputs (*TrafLoad, 2004; PrepME, 2009*). Available software packages are not compatible with the WIM data collected by the New Mexico Department of Transportation (NMDOT). Considering the collection of WIM data for pavement design, a positive weight measurement bias produces a positively biased axle load spectra. During the MEPDG simulation, this results in over-prediction of pavement distress and pavement thickness, and thus, in unnecessary costs of construction. Similarly, a negative bias in axle load spectra results in under-prediction of pavement thickness, and thus, in unnecessary costs of rehabilitation.

Hypothesis Two: If a procedure can be developed to check the quality of WIM data, it will prevent under or over-design and save costs of construction and rehabilitation. A set of subroutines to develop axle load spectra and other traffic inputs are needed to check WIM data quality and accomplish the implementation of MEPDG in New Mexico.

Calibration of the MEPDG has to be performed under local conditions of traffic, climate, and materials. This means that there is a need for determining a set of calibration coefficients for every distress transfer function such that the residual error (difference between the predicted distress and the actual value observed in the field) is minimized. This process requires the collection of accurate input data related to traffic, climate, and materials, for a sufficient number of pavement sections including LTPP sections located in New Mexico.

1.3 Objectives

Under the first hypothesis, the objectives are to:

- Provide a procedure to examine the quality of WIM data in New Mexico.
- Develop axle load spectra and other truck traffic distributions for implementation of MEPDG in New Mexico.
- Study the influence of axle load spectra and WIM data quality on pavement performance.

Under the second hypothesis, the objectives are to:

- Gather data for all MEPDG inputs (traffic, climate, and materials) for a sufficient number of pavement sections throughout New Mexico.
- Determine a set of calibration coefficients that minimize the residual errors for a specific distress model such as rutting and fatigue cracking models.
- Validate the effectiveness of these calibration coefficients for a number of pavement sections that were not included in the local calibration process.

1.4 Thesis Outline

- Chapter 1 – Introduction
- Chapter 2 – Literature Review
- Chapter 3 – Characterization of Traffic Load for MEPDG
- Chapter 4 – Local Calibration of the MEPDG for Flexible Pavement in New Mexico
- Chapter 5 – Conclusions and Recommendations

Chapter 2

LITERATURE REVIEW

2.1 Traffic Loading Characterization in the MEPDG

2.1.1 Introduction

Traffic is one of the most important inputs required for the design of pavement structures. Traffic load constitutes the magnitude and frequency of the loads applied during the design life of a pavement. The AASHTO 1993 Guide for Pavement Design characterized traffic by defining the equivalent single axle load (ESAL). On the other hand, MEPDG uses a more complex approach, requiring a larger number of traffic inputs which are listed below (*MEPDG Documentation, 2004*):

- Base year two-way Annual Average Daily Truck Traffic (AADTT)
- Truck-traffic directional and lane distribution factors
- Truck operational speed
- Vehicle class distribution factors
- Monthly truck-traffic distribution factors
- Hourly truck-traffic distribution factors
- Truck-traffic growth factors
- Axle load distribution factors
- Axle and wheelbase configurations
- Tire characteristics and inflation pressure
- Truck lateral distribution factor

2.1.2 Hierarchical Approach in Traffic Characterization

The MEPDG adopts a hierarchical approach for the design inputs, defining three levels of traffic data input (Levels 1 through 3) on the basis of available data accuracy and reliability. This is because all state transportation agencies do not have the needed resources to collect detailed traffic data. The three levels can be defined as (*MEPDG Documentation, 2004*):

- Level 1 – Very good understanding of traffic characteristics. It is the most accurate and it requires historical site-specific truck traffic volume and axle weight distributions (measured along or near the roadway segment to be designed).
- Level 2 – Moderate understanding of traffic characteristics. It is reasonably accurate and based on regional and statewide truck volume and load data for the roadway to design.
- Level 3 – Poor understanding of traffic characteristics. It is based on default values from national databases or little truck volume and weight data are available (e.g., an average annual daily traffic (AADT), a truck percentage, or no segment specific axle load distribution). Also an estimate based on local experience is considered Level 3.

In this thesis, level 2 analysis is performed.

2.1.3 Data Sources in Traffic Characterization

In this section, the main traffic volume and load data sources used for traffic characterization in MEPDG are described. The input data hierarchical level depends on

the source of the traffic information collected. The input is Level 1 only when the data is site or segment specific, Level 2 when it is regional default data, and Level 3 when it is national default summaries (*MEPDG Documentation, 2004*).

WIM Data

For each vehicle weighed, the Weigh-in-Motion (WIM) station produces a tabulation of the vehicle type (FHWA class 4 through 13) and the number, spacing, and weight of axles. WIM data are required to determine the normalized axle load distribution or spectra for each axle type within each truck class. Processing and analysis of the WIM data to obtain the normalized axle load spectra is external to MEPDG. WIM data is specific to a site or roadway location.

AVC Data

Over a period of time, the Automatic Vehicle Classifier (AVC) produces a tabulation of the number and types of vehicles (FHWA class 4 through 13). AVC data are used to determine the normalized truck class distribution by performing a process which is external to MEPDG. Again, the level of AVC data depends on the specific location of the station (site-specific, regional/statewide, or national). AVC data cannot produce weight or axle load spectra.

Vehicle Counts

Vehicle counts data include the total number of vehicles classified in passenger vehicles (FHWA class 1 through 3), buses (FHWA class 4), and trucks (FHWA class 5 through 13). Vehicle counts can be continuous (365 days a year, the most accurate type); seasonal (from 2 to 12 times a year for periods of time ranging from 24 hours to 2 weeks); or short duration (ranging from 6 hours to 7 days). Vehicle counts provide Level 1, 2 and 3 traffic

volume inputs depending on the specific location where data are collected (site-specific, regional/statewide, or national).

Traffic Forecasting and Trip Generation Models

Traffic forecasting and trip generation models are based on turning movement studies, origin and destination studies, license plate surveys, etc., and they are very useful in urban areas. Traffic forecasting and trip generation models calibrated with site-specific or regional/statewide data can provide Level 1 or 2 traffic inputs. Their application is beyond the scope of this study.

2.1.4 Inputs for Traffic Characterization

Detailed traffic characterization requires four types of traffic data (*MEPDG Documentation, 2004*):

- Type 1 - Base year truck traffic volume
- Type 2 - Traffic volume adjustment factors
    - Vehicle class distribution factors
    - Monthly distribution factors
    - Hourly distribution factors
    - Traffic growth factors
- Type 3 - Axle load distribution factors
- Type 4 - General traffic inputs
    - Traffic wander standard deviation
    - Number of axle types per truck class
    - Axle configuration
    - Wheelbase

- Tire dimensions and inflation pressures

All these inputs are considered Level 1 when the value is determined through direct measurement on site-specific segments, Level 2 when a regional or statewide value from roadways with similar traffic characteristics is used (i.e. similar volume, composition of traffic, and loading patterns), and Level 3 if the default value provided in the software is adopted (*MEPDG Documentation, 2004*).

2.1.4.1 Base Year Truck Traffic Volume

The base year is defined as the year when the roadway is open to traffic for first time. The following base year information is required (*MEPDG Documentation, 2004*):

- Two-way Annual Average Daily Truck Traffic (AADTT)
- Number of lanes in the design direction
- Percent of trucks in the design direction
- Percent of trucks in the design lane
- Truck operational speed

Two-Way Annual Average Daily Truck Traffic

Two-way AADTT is the average volume of truck traffic (classes 4 to 13) passing a road segment in both directions during 24 hours. It is obtained from traffic counts during a time period (between 1 day and 1 year) by using WIM, AVC, vehicle counts, or traffic forecasting and trip generation models. It is recommended to use as the base year AADTT the average of the three most recent years with adequate data.

Number of Lanes in the Design Direction

It represents the total number of lanes in one direction and is a design specification.

Percent of Trucks in the Design Direction

The directional distribution factor (DDF) is defined as the percentage of trucks in the design direction and quantifies any difference in the volume of trucks in both directions. It is commonly assumed to be 50 percent but this is not always the case, for instance, when the route used for transporting goods to and from areas is different. According to the Long Term Pavement Performance (LTPP) database, usually the mean directional distribution factor for total truck traffic has a value of 0.525. It is suggested to use the truck DDF for the most common truck type (class 9) if detailed site-specific or regional/statewide truck traffic data are not available.

Percent of Trucks in the Design Lane

The truck lane distribution factor (LDF) is defined as the percentage of trucks in the design lane and quantifies the distribution of truck traffic between the lanes in one direction. For one lane in one direction, this factor is 1.0. In accordance to the LTPP database, the mean lane distribution factor for all trucks is 0.79 for a four lane roadway and 0.45 for a six lane roadway.

Vehicle Operational Speed

The vehicle operational speed is the average travel speed of trucks and depends on many factors, such as the roadway facility type (Interstate or otherwise), terrain, percentage of trucks, etc. The default operational speed value in MEPDG is 60 mph.

2.1.4.2 Truck Traffic Volume Adjustment Factors

Detailed traffic characterization requires four types of truck traffic volume adjustment factors (*MEPDG Documentation, 2004*):

- Vehicle class distribution factors

- Monthly distribution factors
- Hourly distribution factors
- Traffic growth factors

Vehicle Class Distribution Factors

The normalized vehicle class distribution represents the percentage of each truck class (classes 4 through 13) within the AADTT for the base year. Summing the percent of AADTT for all truck classes should equal 100. The definitions of the standard vehicle classes that are commonly used in the collection of traffic data are included in Table 2.1 (*Traffic Monitoring Guide, 2001*).

The formula used to compute the vehicle class distribution factors for each vehicle class is following:

$$VCDF_i = \frac{AADTT\ for\ class\ i}{Total\ AADTT} \times 100 \qquad \text{Eq. 2.1}$$

where i represents each FHWA vehicle class from 4 to 13.

The data required for vehicle class distributions are obtained from WIM, AVC, and vehicle counts. The most usual vehicle classification counting programs are of short duration. Also, MEPDG contains default vehicle class distribution factors (Level 3) based on the Roadway Functional Classification and the combination of the Truck Traffic Classification (TTC) groups that best describe the expected traffic stream (*MEPDG Documentation, 2004*).

Monthly Distribution Factors

Truck traffic monthly distribution factors (MDF) represent the percentage of the annual truck traffic for a given truck class that occurs in a specific month. They depend on

factors such as land use and roadway location. MEPDG assumes that the monthly distribution of truck traffic is constant during the pavement design life.

The monthly distribution factor for a specific month can be calculated as the monthly truck traffic for the given class divided by the total truck traffic for that truck class for the entire year. The following equation can be used to compute monthly distribution factors:

$$MDF_{ij} = \frac{Truck\ Traffic\ for\ class\ i\ during\ month\ j}{Annual\ Truck\ Traffic\ for\ class\ i} \times 12 \qquad \text{Eq. 2.2}$$

where i represents the vehicle class from 4 to 13 and j the month of the year from 1 (January) to 12 (December).

The sum of the monthly distribution factors of all months must equal 12. Also, MEPDG includes default monthly distribution factors which is a Level 3 input and is based on the LTPP database.

Hourly Distribution Factors

The hourly distribution factors (HDF) represent the percentage of the AADTT within each hour of the day. The sum of the percentage of average daily truck traffic for each hour within the whole day must equal 100%. Usually, hourly distribution factors are computed by using truck traffic data obtained from continuous 24-hours duration counting programs.

The following formula is applied to calculate the hourly distribution factors:

$$HDF_i = \frac{Annual\ Truck\ Traffic\ during\ hour\ i}{Total\ AADTT} \times 100 \qquad \text{Eq. 2.3}$$

where i represents each hour of the day from 0 (00:00) to 23 (23:00).

The MEPDG includes default truck hourly distribution factors (Level 3) that are based on the LTPP database.

Traffic Growth Factors

Traffic growth factors represent the percentage of the previous year AADTT that the current year average daily truck traffic is expected to increase. The best way to estimate the traffic growth factors at a particular site is by collecting continuous traffic count data. The data should be reliable and the differences from year to year should be due to growth. Also traffic growth factors can be obtained from short duration count data but are not as accurate.

In the computation of growth factors, it is recommended to use data from the same location collected during several years. Thus, error due to the inaccuracy of the AADTT estimate tends to self-correct.

The three different traffic growth functions used in MEPDG to forecast the growth or decay of truck traffic over time are described as follows (*MEPDG Documentation, 2004*):

- No Growth Model:

$$AADTT_X = 1.0 \times AADTT_{BY} \quad \text{Eq. 2.4}$$

- Linear Growth Model:

$$AADTT_X = GR \times AGE + AADTT_{BY} \quad \text{Eq. 2.5}$$

- Compound Growth Model:

$$AADTT_X = ADTT_{BY} \times GR^{AGE} \quad \text{Eq. 2.6}$$

where AADTTX is the annual average daily truck traffic at age X, AADTTBY is the base year annual average daily truck traffic, AGE is the number of years of forecasting, and GR is the traffic growth rate. The Design Guide allows users to choose a common growth function for all truck classes, or different functions for the different truck classes.

2.1.4.3 Axle Load Distribution Factors

The axle load distribution factors or axle load spectra represent the percentage of the total axle applications within each load interval for a specific axle type (single, tandem, tridem, and quad) and vehicle class (classes 4 through 13).

For single axles the load intervals are defined from 3,000 to 40,000 lb at 1,000 lb intervals; for tandem axles from 6,000 to 80,000 lb at 2,000 lb intervals; and for tridem and quad axles from 12,000 to 102,000 lb at 3,000 lb intervals.

The following equation is used to compute the axle load distribution factors:

$$ALDF_{ijk} = \frac{No.\ of\ axles\ for\ class\ i,\ \ month\ j,\ \ and\ load\ range\ k}{Total\ No.\ of\ axles\ for\ class\ i\ and\ month\ j} \times 100 \qquad \text{Eq. 2.7}$$

Where i represents the vehicle class (4 through 13), j the month (1 through 12) and k the load range (3,000 to 40,000 lb at 1,000 lb intervals for single axles). This is done for each axle type (single, tandem, tridem, and quad).

MEPDG allows users to input the axle load distribution factors for each axle type (single, tandem, tridem, and quad) within each load interval and for all truck classes (classes 4 to 13) and months of the year (January to December). But also, MEPDG includes default axle load distribution factors for each axle type and truck class that can be used as Level 3 inputs. MEPDG assumes the axle load spectra to be constant during the pavement design life.

2.1.4.4 General Traffic Inputs

Most of these inputs, except the number of axles by axle type per truck class and the wheelbase, define the axle load configuration for calculating the pavement response (*MEPDG Documentation, 2004*). They are explained as follows:

- Mean Wheel Location: It is the distance from the outer edge of the right wheel to the pavement marking.
- Traffic Wander Standard Deviation: This is the standard deviation of the lateral traffic wander (fluctuation of the wheel path around the mean location).

  These last two inputs are used to determine the number of axle load applications over a same point for predicting distress and performance.
- Design Lane Width: It is the distance between the lane markings on either side of the design lane.
- Axle Configuration: This input includes several values such as the average axle width, the dual tire spacing, and the axle spacing. It is needed to describe the configuration of the typical tire and axle loads.
- Number of Axles by Axle Type per Truck Class: This input represents the average number of axles of each axle type (single, tandem, tridem, and quad) for each truck class (Classes 4 to 13).
- Wheelbase: It includes the average axle spacing, and the percentage of trucks in classes 8 through 13 with the short, medium, and long axle spacing.

  The last two inputs are used in the traffic volume calculations.
- Tire Dimensions and Inflation Pressures for performance prediction models.

2.1.5 Quality Control Procedures for Weigh-in-Motion Data

Weigh-in-motion monitoring sites provide large datasets including date and time for most vehicles crossing the WIM sensors, counts of each vehicle's axles, and measurements of the individual axle loads and spacings. By processing this information we can get very

important characteristics of the traffic flow such as annual average daily traffic for each vehicle class, time histories of gross vehicle weights by class, frequency distributions of the traffic by vehicle class and axle load spectra.

The quality of collected WIM data is affected by many factors such as the site selection, the pavement condition, the system calibration, the system monitoring, the sensor technology and the driver behavior. Therefore, data errors are captured and quality control techniques are essential for ensuring good quality WIM data.

State agencies use proprietary software or develop their own software to validate WIM data. These programs flag any individual vehicle record that does not accomplish certain user defined rules and generate summary reports on flagged vehicles.

A multitude of possible validation rules were developed under the Transportation Pooled-Fund Study SPR-2 (182) titled “Traffic Data Editing Procedures: Traffic Data Quality (TDQ)” (*Flinner et al, 1995*). This project planned to develop standard software for traffic data quality control (TDQ), but it could not meet yet all the expected objectives because of funding constraints.

There are two commonly used procedures to test the quality of weight data collected from WIM stations: the steering axle load test and the gross vehicle weight test (*Traffic Monitoring Guide, 2001*). The first method is the steering axle load test which is performed by checking whether or not the steering axle weights of class 9 trucks fall in the range of 8,000 to 12,000 lbs. The second one is the gross vehicle weight test which is performed by checking whether the gross vehicle weights are in the range of 28,000 to 36,000 lbs for unloaded class 9 trucks and 72,000 to 80,000 lbs for loaded class 9 trucks.

2.1.6 Recent Studies

After describing and analyzing the different traffic inputs required for accurate analysis and design of pavements, we proceed to review the most significant research and studies related to this topic that have been performed recently:

Ramachandran, A. N., Taylor, K. L., Stone, J. R., and Sajjadi, S. S. (2011) performed research to check the quality of the WIM data collected by the North Carolina Department of Transportation after the data had been converted from the vendor format to the ASCII text format. The quality control procedures identify incomplete datasets, out of range values for individual vehicle classes, misclassified vehicles, and other possible data problems. The NCDOT requires that all data with quality problems be excluded from datasets used for planning and design. These quality control checks and methods are mainly based on the LTPP procedure and they were programmed in Access by using SQL queries in linked Access database tables including visual interpretation of the data to apply local knowledge. The program is a collection of auto-applied rules as shown in Tables 2.2 and 2.3 that identify invalid entries for the fields checked and that automatically exclude erroneous records into the exclusion tables. Weight QC is performed first because weight measurements are more likely to cause error than class data. The output of the QC database application is a table of accepted data for use in MEPDG and a table of excluded data for each data type. Weight plots sorted by class 4 through 13 are also outputs of the program that provide a graphical representation of how trucks are loaded and allow the user to identify appropriate peaks at weight ranges that correspond to empty and fully loaded conditions as recommended in Table 2.4. Data

collected immediately after installation, calibration, and validation of new sensors were used to ensure high quality data to support MEPDG development. After applying quality control to twelve consecutive months of data for 45 WIM stations, the results confirmed that NCDOT equipment provided reliable WIM data to develop Level 1 and Level 2 traffic inputs for MEPDG. Vehicle class and weight checks generate 0.97% and 6.42% anomalies respectively, most of them caused due to vehicle misclassifications. Finally, the authors recommend incorporating the following improvements to the QC procedure:

- Explore statistical data sampling methods to reduce the size of databases to a manageable extent.
- Assign a severity level (high, medium, or low) to data which are potentially invalid based on QC rules.
- Create a more robust database in Oracle or Microsoft SQL Server for long term WIM data storage and analysis.

Tran, N. H., and Hall, K. D. (2007a) performed research for the Arkansas State Highway and Transportation Department (AHTD) to develop statewide truck traffic volume adjustment factors (class, monthly, and hourly distribution factors) and evaluate the significance of these inputs. The AHTD performs a traffic-monitoring program in accordance with the guidelines of the 2001 Traffic Monitoring Guide, so weigh-in-motion (WIM) stations collect continuously traffic volume, vehicle classification, and vehicle weight data throughout the state. Therefore, the AHTD provided classification data in the C-record format found in the TMG, collected at 55 WIM sites. But the traffic records were evaluated according to the quality control procedures recommended by

LTPP and FHWA, and only 23 WIM sites provided suitable classification records due to missing and inaccurate data. Software was created to process the vehicle classification data and develop the corresponding statewide monthly, hourly, and class distribution factors for the state of Arkansas. The statewide vehicle class, monthly, and hourly distribution factors were developed based on classification data collected at WIM stations, while the default values provided in MEPDG were based on LTPP data collected throughout the US. Then, they did analyses in MEPDG showing that site-specific class distribution factors have a significant effect on predicted pavement performance, compared with predictions generated by default distribution values. MEPDG software was configured for these analyses, with an assumed 20 years design life, national calibration parameters for pavement performance prediction models without adjustment, and new flexible pavement with AADTT of 10,000. Total rutting and fatigue cracking are the two predicted distresses considered in this study. However, the effect of using site-specific monthly and hourly distribution factors on predicted pavement performance was not significant. Therefore, they recommended using site-specific class distribution factors with default monthly and hourly distribution factors in MEPDG. Also, they encouraged state agencies to review and update statewide class distribution factors frequently.

Tran, N. H., and Hall, K. D. (2007b) also conducted research sponsored by the Arkansas State Highway and Transportation Department (AHTD) to develop statewide axle load spectra and evaluate its importance in MEPDG. The AHTD performs a traffic-monitoring program in accordance with the guidelines of the 2001 Traffic Monitoring Guide, so WIM stations collect continuously traffic volume, vehicle classification, and vehicle

weight data throughout the state. Therefore, the AHTD provided weight data in the weight record file format (W-record) from only 10 weigh-in-motion stations, because most of the WIM sites did not collect complete and accurate data and did not pass the quality control procedure recommended by LTPP and FHWA. A computer program was developed to process the vehicle weight data from the 10 WIM sites and generate statewide axle load spectra for single, tandem, and tridem axles for the state of Arkansas. There were not enough quad axle data. The statewide axle load spectra were developed on the basis of weight data collected at WIM stations, while the default values provided in MEPDG were developed on the basis of LTPP data collected throughout the US. In this study, analyses were performed to determine the differences between both inputs. MEPDG software was configured with an assumed 20 year design life, national calibration parameters for pavement performance prediction models without adjustment, and new flexible pavement with AADTT of 10,000. Total rutting and fatigue cracking were the two predicted distresses considered in this study. Sensitivity analysis showed important differences in predicted pavement performance resulting from the statewide and MEPDG default axle load spectra. Thus, they highly recommended the development of state-specific axle load spectra and their frequent update.

Smith, B. C., and Diefenderfer, B. K. (2010) determined and analyzed the differences in the distresses predicted by MEPDG between site-specific and default traffic inputs for flexible pavements in Virginia. A continuous 1-week period for each month for twelve consecutive months of data from eight interstate weigh-in-motion sites in Virginia was used to develop axle load spectra, monthly adjustment factors, vehicle class distribution

factors, and number of axles per truck. A MATLAB program was developed to process the raw WIM data and before accuracy and quality control is performed in accordance with the 2001 Traffic Monitoring Guide, so bad records are removed. A typical pavement section from Virginia was selected, and the distresses predicted by MEPDG using these site-specific traffic inputs were compared to those obtained using default traffic inputs. Longitudinal cracking, fatigue cracking, asphalt rutting, and total rutting were the main load-related distresses compared by using a normalized difference statistic and the coefficient of variation for each traffic input and pavement distress model. Also, the predicted time to failure for each pavement condition using site-specific traffic data inputs was compared to the predicted time to failure using the default traffic data inputs. Overall, the results showed that the effect of the site-specific traffic inputs was not very important. However, when total rutting is considered, the predicted time to failure using site-specific axle load spectra was found to be significant for all sites when compared to the default axle load spectra. Therefore, it is recommended that the state highway agencies collect and develop site-specific axle load spectra inputs for analysis of flexible pavements, and default inputs can be used for the remaining parameters. Because each state has a particular local combination of traffic, materials, climate, and pavement structures, each agency may need to perform a similar study in order to get their own conclusions.

Ishak, S., Shin, H. C., Sridhar, B. K., and Zhang, Z. (2010) studied the traffic data requirements of MEPDG for future implementation in Louisiana. They developed the truck axle load spectra from WIM data and proposed improvements in the current data

collection techniques. Currently, traffic loading data is collected using portable WIM stations in Louisiana, which collect data continuously for two consecutive days. Quartz piezoelectric sensors are used in these stations to collect weight data. Since they are temperature sensitive and not regularly calibrated, error can cause overestimation or underestimation of axle load spectra. The quality of data collected from permanent and portable WIM sites was assured by performing two QC tests. The first test is the steering axle load test which is performed by checking whether or not the steering axle weights of class 9 trucks fall in the range of 8,000 to 12,000 lbs. The second one is the gross vehicle weight test which is performed by checking whether the gross vehicle weights were in the range of 28,000 to 36,000 lbs for unloaded class 9 trucks and 72,000 to 80,000 lbs for loaded class 9 trucks. Only 51 sites out of 96 passed both quality tests, and therefore, they were used to develop single, tandem, and tridem axle load spectra. Cluster analysis was used to group the WIM sites with similar vehicle class distribution in order to reduce the number of axle load spectra proposed. The degree of similarity between two different distributions from two sites was measured by the sum of squared differences. If this value is small, the two distributions are very similar and can be clustered and combined into one group. For each group, one vehicle class distribution and one axle load spectra was developed. The dominant vehicle class for single and tandem axle loads was 9, while the majority of tridem axles belonged to vehicle class 10. The developed single axle load spectra were very similar to the default values. Both developed tandem and tridem axle load spectra were significantly different from the default values. The truck traffic classification (TTC) instead of the roadway functional classification was recommended for grouping the WIM sites. The researchers recommended collection of traffic data

during longer monitoring periods and more frequent calibration of WIM stations. Also, a strategic plan for installing more permanent WIM sites was encouraged.

Haider, S. W., Harichandran, R. S., and Dwaikat, M. B. (2010) performed research to investigate the impact of uncertainty in axle load spectra on the performance of both flexible and rigid pavements and their design reliabilities. The characterization of traffic loading is very important in pavement design. Indeed, axle load spectra are one of the most critical inputs in the new MEPDG and have a significant impact on the predicted pavement performance. The weigh-in-motion data necessary to develop axle load spectra often presents an uncertain quality due to inaccuracy and systematic bias. This inaccuracy depends upon the sensor technology, and systematic bias is introduced by calibration error and its drift over time. This study provided an overview of WIM data accuracy and calibration and the impact of these inherent uncertainties on the pavement design process. A typical axle load spectra from the specific pavement sections of the LTPP study was adopted as reference. A bimodal distribution was fitted to the reference axle load spectra, and the corresponding cumulative distribution function was obtained. The error distribution was simulated by assuming different values of systematic error (bias) and random error (accuracy). Monte Carlo simulation was used to generate axle load spectra for different combinations of random and systematic errors. The simulated axle load spectra that included measurement errors were used to predict pavement performance through correlation. This direct correlation process was validated using MEPDG. The results showed that cracking is the distress most impacted by variations of axle load spectra, while rutting is moderately affected. For both flexible and rigid pavements,

cracking performance was significantly affected in particular by negative weight measurement bias. In order to assess the impact of measurement errors on the reliability of designed pavements, each distress type was predicted at 95% reliability using the MEPDG procedure for the axle load spectra generated previously. The MEPDG reliability analysis can compensate for this negative measurement bias for most of the distresses by providing conservative estimates, but a lower threshold is needed for the case of cracking.

2.2 Local Calibration of the MEPDG

2.2.1 Introduction

The new Mechanistic-Empirical Pavement Design Guide (MEPDG) for new and rehabilitated pavement structures is based on both mechanistic and empirical principles. The design procedure assumes that pavement can be modeled as a multi-layered elastic structure and performs a time-stepping process. At every time step, structural analysis is done to estimate critical stresses and strains within the structure; then, empirical models are used to compute incremental distresses such as rutting, cracking, and roughness based on the stresses and strains calculated previously. This cycle is repeated through the pavement design life (*MEPDG Documentation, 2004*).

The pavement distress prediction models, also called transfer functions, are key components of the mechanistic-empirical procedure. Calibration of these models with local data sets is necessary to obtain an acceptable correlation between levels of distress observed in the field and those levels predicted with the MEPDG. The validation of the performance prediction models is a very important step to establish confidence before adopting them for design purposes. Calibration is the mathematical process in which the

total residual error (difference between observed and predicted values of distress) is minimized. Validation is the process to confirm that the calibrated model can predict distresses accurately for other cases not used in the calibration (*AASHTO Guide for Local Calibration of MEPDG, 2010*).

The calibration-validation process requires the use of precision and bias statistics. The concept of accuracy, or the exactness of a prediction to the actual value, encompasses both precision and bias. A prediction model is said to be precise when it can give repeated estimates that correlate strongly with the observed values. On the other hand, a model that is biased systematically over-predicts or under-predicts observed distresses; this means the prediction is consistently higher or lower than the observed value as distinct from random error (*AASHTO Guide for Local Calibration of MEPDG, 2010*).

The standard error of the estimate is a statistic that measures the amount of dispersion of the data points around the line of equality between the observed and predicted values of distress. In calibration, the total standard error of a pavement performance model presents four major components: measurement error, input error, model or lack-of-fit error, and pure error. The measurement error is caused by inaccuracies in the measure of distress along the pavement sections used in the calibration process. The input error is caused by variations in laboratory and field measurements when estimating the MEPDG inputs. Pure error is the random or normal variation due to replication. The model or lack-of-fit error is the portion of the total variance caused by inadequate theory and algorithms or incorrect model form. Understanding the contribution of each of these variance sources to the total standard error is critical in order to have the greatest effectiveness in the calibration refinement process (*AASHTO Guide for Local Calibration of MEPDG, 2010*).

Local calibration is performed to reduce bias and increase precision of the MEPDG prediction models. A biased model consistently produces over-designed or under-designed pavements with important cost consequences. A model with lack of precision leads to inconsistency in design effectiveness. Validation of the MEPDG prediction models is necessary to ensure that the calibrated models produce robust and accurate predictions of pavement distresses for cases other than those used in calibration. Typically, the split sample approach 80/20 is used with 80 percent of the data used for calibration and 20 percent used for validation (randomly chosen). Successful validation requires that the bias and precision statistics of the validation data sets are similar to those obtained from calibration (*AASHTO Guide for Local Calibration of MEPDG, 2010*).

The performance models of MEPDG were calibrated at a global scale using a representative number of pavement sections from the Long Term Pavement Performance (LTPP) program throughout North America. Local calibration factors are included in the MEPDG to consider the differences in construction practices, maintenance policies, and material specifications across the United States. The objective of the local calibration process is to find appropriate calibration factors such that significant bias is eliminated, standard error is minimized, and precision maximized. This will consequently reduce construction and maintenance costs at the same reliability level (*AASHTO Guide for Local Calibration of MEPDG, 2010*).

2.2.2 Distress or Performance Indicators in the MEPDG

The following indicators of distress and performance of flexible pavements are predicted by the MEPDG, and therefore, their definitions are provided next (*AASHTO Guide for Local Calibration of MEPDG, 2010*):

- Rutting or Rut Depth: It is a longitudinal depression of the surface in the wheel path due to plastic or permanent deformation in each layer of the pavement (asphalt concrete, granular base, and subgrade). It is measured in the field as the maximum vertical distance between the transverse profile of the pavement surface and a wire-line across the lane width. The unit of rutting in the MEPDG is inches. A reasonable standard error of the estimate for total rutting is 0.10 in.
- Alligator Cracking: It is a series of interconnected cracks with a characteristic "alligator" pattern that initiate at the bottom of the asphalt concrete (AC) layer caused by fatigue. Alligator cracks initially start as multiple short cracks in the wheel path that eventually become interconnected under a continued traffic loading. The unit of alligator cracking in MEPDG is percent of total lane area. The MEPDG does not predict the severity of alligator cracking, but includes low, medium, and high in the definition. A reasonable standard error of the estimate for alligator cracking is 7%.
- Longitudinal Cracking: It is a series of cracks parallel to the pavement centerline that occur within the wheel path caused by fatigue. It initiates as short longitudinal cracks at the surface of the AC pavement that eventually become connected under continued loading. The unit of longitudinal cracking in MEPDG is feet per mile. The MEPDG does not predict severity of the longitudinal cracks, but includes low, medium, and high in the definition. A reasonable standard error of the estimate is 600 ft/mi.
- Transverse Cracking: Non-load related cracking that is perpendicular to the pavement centerline and caused by low temperatures or thermal cycling. The unit

of transverse cracking in the MEPDG is feet per mile or spacing of transverse cracks in feet. A reasonable standard error of the estimate is 250 ft/mi.

2.2.3 Recent Studies

The most significant research related to this topic that has been performed recently is described next:

Hoegh, K., Khazanovich, L., and Jensen, M. (2010) conducted research to evaluate and calibrate the MEPDG rutting prediction model using 12 hot mix asphalt (HMA) pavement sections from the full-scale pavement research facility MnROAD in Minnesota. This research project involved the following objectives: identify pavement sections where performance data is known, obtain MEPDG inputs for these MnROAD sections, run MEPDG to predict rutting, compare predicted and measured rutting at every section, and finally adjust the parameters of the MEPDG rutting model to reduce error. All data collected at the MnROAD facility is entered into a database for the Minnesota Department of Transportation (MnDOT). Rutting was measured by MnROAD staff three times per year manually using the straightedge method. Trenches were cut at the MnROAD sections to study the level of rutting occurring in individual layers of the pavement. It was observed that most of the rutting occurred in the HMA while the granular base and the subgrade were unaffected. The sections were subjected to the same environmental and traffic loading, but the following design variables were different: asphalt binder grade, mix design, air void content, HMA thickness, type and thickness of the base. MEPDG version 1.0 was used to predict the rutting performance of the test sections. The design guide calculates the rutting due to the asphalt concrete (AC) layer,

the granular base, and the subgrade; the summation of the three is the total rutting in the pavement:

$$Total\_Rutting = Rutting\_AC + Rutting\_Base + Rutting\_Subgrade \quad \text{Eq. 2.8}$$

The measured total rutting was compared to the MEPDG predicted value for all MnROAD pavement sections and it was observed that the predicted total rutting was always greater than the measured total rutting. In some sections, the predicted AC rutting was similar to the measured total rutting. Considering that forensic studies found that most of the measured rutting occurred in the AC layer, the MEPDG predicts accurately the rutting due to the AC, but the base and subgrade predictive models overestimate total rutting, and therefore, they should be modified. It was noticed that during the first month of the pavement design life, the MEPDG consistently predicts a huge accumulation of rutting in the base and subgrade layers which is not realistic. Therefore, it was recommended to subtract the base and subgrade rutting accumulated during the first month of pavement life from the MEPDG rutting prediction:

$$Total\_Rutting = Rutting\_AC + (Rutting\_Base - Rutting\_Base\_1st\_month) + (Rutting\_Subgrade - Rutting\_Subgrade\_1st\_month) \quad \text{Eq. 2.9}$$

With the application of the locally calibrated rutting prediction model, bias and the residual error were reduced significantly.

Li, J., Pierce, L. M., and Uhlmeyer, J. (2009) performed calibration of the MEPDG new flexible pavement distress models to Washington State local conditions using data obtained from the Washington State Pavement Management System (WSPMS). The sensitivity of required input data was analyzed as well. This paper proposes an

implementation plan for MEPDG that could replace the 1993 AASHTO Design Guide in Washington State Department of Transportation (WSDOT). Level 2 MEPDG inputs of traffic, climate, and pavement structure data were collected from a variety of sources. MEPDG software did not work properly when dynamic modulus data was used for mix design inputs (Level 1). More than 30 years of distress data were available from the WSPMS. The split-sample and the jackknife testing approaches were combined in the calibration process. The sensitivity of the design parameters was checked by varying the inputs and performing iterative runs. The following key observations were made:

- AC rutting is mostly influenced by climate, traffic loading, AC thickness and base type.
- Longitudinal cracking is strongly influenced by PG binder and AC thickness.
- Alligator cracking is mainly affected by the stiffness of the hot mix asphalt (HMA).
- Temperature is the most important factor in transverse cracking prediction.
- Roughness is influenced by climate, traffic loading, and base type.

From analyses, it was observed that default MEPDG tends to underpredict AC rutting, longitudinal cracking, and alligator cracking. Trenches in WSDOT routes have shown that very limited rutting occurs in the subgrade, therefore, the corresponding calibration coefficients were set to 0. The MEPDG transverse cracking prediction under default settings matched the WSPMS performance data, and thus, it is not necessary to calibrate this model. An elasticity analysis was conducted to describe the effects of the different calibration factors on the pavement distress predictions. Elasticity is an econometric parameter which is defined as follows:

$$E_{distress}^{C_i} = \frac{\partial(distress)/distress}{\partial(C_i)/C_i} \quad \text{Eq. 2.10}$$

where $E^{Ci}_{distress}$ is the elasticity of the calibration factor C_i for the associated distress. The elasticity can be zero, positive, or negative. Zero indicates that the calibration factor has no influence on the prediction, positive implies that the estimation increases as the factor increases, and negative means that the prediction decreases as the factor increases. The results showed the following conclusions: in the rutting model, the calibration factors β_{r2} and β_{r3} have more impact than β_{r1}; in the AC fatigue model, β_{f2} and β_{f3} are more influential than β_{f1}; C_2 is the most important factor in longitudinal cracking and C_1 in alligator cracking. During the calibration process, the user varies the calibration factors until the MEPDG distress prediction matches the actual pavement performance. Only one pavement section can be evaluated at a time in MEPDG software, therefore, few sections are carefully chosen to represent a larger group of WSDOT's pavements. The calibration factors were adjusted in order of high to low elasticity. The set of calibration factors with the least error between the MEPDG prediction and the WSPMS measurements on all calibration and validation sections was selected as the final result:

- Rutting: $\beta_{r1} = 1.05$; $\beta_{r2} = 1.109$; $\beta_{r3} = 1.1$; $\beta_{s1} = 0$.
- Fatigue: $\beta_{f1} = 0.96$; $\beta_{f2} = 0.97$; $\beta_{f3} = 1.03$.
- Longitudinal Cracking: $C_1 = 6.42$; $C_2 = 3.596$; $C_3 = 0$; $C_4 = 1{,}000$.
- Alligator Cracking: $C_1 = 1.071$; $C_2 = 1$; $C_3 = 6{,}000$.

The IRI model could not be calibrated because of bugs in the MEPDG software. These calibration factors can be used to predict more accurately flexible pavement performance.

Banerjee, A., Aguiar-Moya, J. P., and Prozzi, J. A. (2009) carried out an extensive local effort with the objective of calibrating the MEPDG permanent deformation performance model for five different regions in the state of Texas. The focus of this study was to find a set of two calibration factors of the asphalt concrete (AC) permanent deformation model per region by minimizing the sum of squared errors (SSE) between observed and predicted pavement distresses. A joint optimization approach was adopted to obtain Level 2 calibration factors for every region. At the end all of them would be averaged to come up with a set of Level 3 calibration factors for the state of Texas. If this approach were used with all the pavement sections at once, the results obtained would be more accurate, but the computational process would required more time. A total of 18 sections were obtained from the LTPP database. These experiments were representative of five regions with different environmental conditions: wet-warm, wet-cold, dry-warm, dry-cold, and mixed. The number is not sufficient and the researchers recommend monitoring at least 100 new sections and storing the data in the Texas Flexible Pavement Database. The data required to simulate the 18 pavement sections in the MEPDG (traffic, layers, materials, and performance) was obtained from the LTPP database. The MEPDG analysis was initiated with default calibration parameters and then adjusted such that the difference between the observed and the predicted distress values is reduced progressively. The optimal solution minimizes the SSE. For this calibration, the factor β_{r2} was kept constant. The calibration coefficient β_{r1} that captures the influence of the HMA layer thickness and β_{r3} that captures the impact of the number of load repetitions were optimized. The calibration factor β_{s1} controlling the rutting in the subgrade was preset to regional defaults (0.3 for West Texas and 0.7 for East Texas) that were determined on the basis of

average moisture content of the subgrade soil. It was observed that the distress predictions were more sensitive to β_{r3} than β_{r1}, and for this reason a higher precision was used for β_{r3}. The final Level 3 calibration coefficients obtained for the state of Texas were: β_{r1} = 2.39, β_{r3} = 0.856, and β_{s1} = 0.5. The standard error of the calibrated permanent deformation model was found to be less than 0.1 in. which is a good result.

Muthadi, N. R., and Kim, Y. R. (2008) performed research to calibrate the MEPDG permanent deformation and alligator cracking models for local materials, conditions, and practices used in flexible pavements in North Carolina. A total of 53 pavement sections were selected: 30 from the LTPP database (16 new flexible and 14 rehabilitated) and 23 from the North Carolina Department of Transportation (NCDOT) databases. The data collection effort included the gathering of MEPDG inputs related to materials, traffic, climate, and pavement structure. The performance data obtained from the Pavement Management Unit used a nonnumeric rating format which consisted of none, low, medium, or severe level of distress. This data was converted to MEPDG format to be able to compare measured and predicted distress values. The first step of the local calibration process was to perform verification runs on the pavement sections with default MEPDG models. It was observed that NCDOT sections introduced significant error and inconsistency because of their nonnumeric distress measurement technique. Thus, only LTPP sections were used in the calibration of the permanent deformation model. The second step was to calibrate the model coefficients to reduce the bias and the standard error. For the permanent deformation model, the Microsoft Excel Solver program was used to optimize the coefficients β_{r1}, β_{GB}, and β_{SG} (β_{r2} and β_{r3} were not calibrated)

separately for each layer. Since pavement trenches and cores were not available, the total measured rutting was distributed to each layer according to the ratio of predicted total rutting to the predicted permanent deformation in each layer. For the bottom-up cracking model, the coefficients C_1 and C_2 of the corresponding transfer function were optimized using Microsoft Excel Solver. Both LTPP and NCDOT sections were used for the alligator cracking calibration. In the final step, validation was performed to check for the reasonableness of the performance predictions. The split-sample approach was used where 80% of the sections were randomly selected for calibration and 20% were kept aside for validation. The following calibration factors were obtained and proposed to use until a more robust calibration process with more sections is achieved in the future:

- Rutting: $\beta_{r1} = 1.017$, $\beta_{r2} = 1$, $\beta_{r3} = 1$, $\beta_{GB} = 0.778$, $\beta_{SG} = 0.818$.
- Alligator Cracking: $C_1 = 0.437$; $C_2 = 0.151$; $C_3 = 6{,}000$.

The standard error of the calibrated permanent deformation model was reduced from 0.154 to 0.109. Similarly, the standard error of the calibrated alligator cracking model was reduced from 6.02 to 3.64. The last model presented a poor precision perhaps because the NCDOT sections were included in its calibration. The researchers recommended the use of the LTPP distress identification manual for the measurement of distress in the pavement sections.

Hall, K. D., Xiao, D. X., and Wang, K. C. (2010) conducted the calibration and validation of the MEPDG performance prediction models to local traffic, climate, materials, and practices in Arkansas. A total of 26 pavement sections were obtained from two sources: the LTPP database and the Pavement Management System (PMS) of the Arkansas State

Highway and Transportation Department (AHTD). All pavement sections were distributed across the five different regions of Arkansas. The PMS sections had a construction date later than 1996 when the Superpave HMA mixture design system was implemented. 20 sites (80%) were randomly selected for calibration and the other 6 (20%) were preserved for validation. The data required such as traffic, climate, structure, materials, and pavement performance were collected from LTPP and AHTD databases. Verification runs were performed with default calibration coefficients and it was observed that measured and predicted distresses did not match well for longitudinal and alligator cracking. The calibration coefficients were obtained by minimizing the sum of squared error between predicted and measured distresses. The Microsoft Excel Solver function was used to optimize the coefficients of the alligator cracking and longitudinal cracking models. Iterative runs of MEPDG were performed with different combinations of coefficients to optimize the rutting model. It was assumed that rutting would occur only in the HMA layer and in the subgrade, thus the coefficient β_{GB} for the granular base was not calibrated. The transverse cracking model was not calibrated because its MEPDG prediction is zero when properly selected Performance-Graded (PG) binders are used. The IRI model was not calibrated either because it is a function of other predicted distresses. The following calibration coefficients were obtained:

- Rutting: $\beta_{r1} = 1.2$, $\beta_{r2} = 1$, $\beta_{r3} = 0.8$, $\beta_{base} = 1$, $\beta_{subgrade} = 0.50$.
- Alligator Cracking: $C_1 = 0.688$, $C_2 = 0.294$, $C_3 = 6000$.
- Longitudinal Cracking: $C_1 = 3.016$, $C_2 = 0.216$, $C_3 = 0$, $C_4 = 1000$.

The calibrated models were validated by running MEPDG on the remaining sites and it is evident that local calibration reduces the difference between predicted and measured distress.

The methodology, procedures, and analyses necessary to accomplish the goals of this study are described in detail in the next chapters.

Table 2.1 Definition of the vehicle classes (*Traffic Monitoring Guide, 2001*)

FHWA Vehicle Class	Description
1	Motorcycles
2	Passenger Cars
3	Two Axles and Four Tire Single Units
4	Buses
5	Two Axles and Six Tire Single Units
6	Three Axle Single Units
7	Four or More Axle Single Units
8	Four or Less Axle Single Trailers
9	Five Axle Single Trailers
10	Six or More Axle Single Trailers
11	Five or Less Axle Multi-Trailers
12	Six Axle Multi-Trailers
13	Seven or More Axle Multi-Trailers

Table 2.2 Quality Control Rules List for Weight Data (*Ramachandran et al, 2011*)

Order	Description of the problem	Criteria
1	Any field with a null value	Field Value ≠ Null
2	Invalid hour	HOUR ≠ (0 - 23)
3	Invalid month	MONTH ≠ (1 – 12)
4	Invalid vehicle class code	VHCL_CLASS ≠ (4 - 13)
5	Invalid FIPS Code	STATE_CD ≠ 37 (North Carolina)
6	Invalid station ID	STATION_ID ≠ Expected station identifier
7	Invalid direction for station	DRCTN_CD ≠ Valid values for station
8	Invalid lane number for station	TRVL_LN_NBR ≠ Valid values for station
9	Invalid year	YEAR ≠ Valid year for date range captured
10	Invalid day	DAY ≠ Valid date for the MONTH
11	Hour without any weight records. A full day of data may not be available for all lanes	Manual audit of hours without weight records
12	Axle count inconsistent with number of axle spacings	AXLE_COUNT ≠ (# of spacings +1)
13	Axle count inconsistent with number of axle weights	AXLE_COUNT ≠ # of axle weights
14	GVW is inconsistent with sum of axle weights	TOTAL_WGHT ≠ Sum of axle weights
15	Axle weight is out of acceptable range	441 lb (200 kg) < (X)_WGHT < 44,100 lb (20,003.4 kg)
16	Axle spacing is out of acceptable range	1.97 ft (0.6 m) < (X)_(Y)_SPACING < 49.2 ft (15 m)

Table 2.2 (cont.) Quality Control Rules List for Weight Data (*Ramachandran et al, 2011*)

17	Sum of axle spacings exceeds maximum wheelbase	Sum of axle spacings > 98.2 ft (29.93 m)
18	Review Average DOW volumes by month for unusual patterns	A pattern deviates significantly from other months
19	Review GVW plots by class by month for unusual patterns	A pattern deviates significantly from other months

Table 2.3 Quality Control Rules List for Class Data (*Ramachandran et al, 2011*)

Order	Description of the problem	Criteria
1	Any field with a null value	Field Value = Null
2	Invalid month	MONTH ≠ (1 – 12)
3	Invalid hour	HOUR ≠ (0 – 23)
4	Total lane volume exceeds max. limit	TOTAL_VOL > 3000
5	Invalid FIPS Code	STATE_CD ≠ 37 (North Carolina)
6	Invalid station ID	STATION_ID ≠ Expected station identifier
7	Invalid direction for station	DRCTN_CD ≠ Valid values for station
8	Invalid lane number for station	TRVL_LN_NBR ≠ Valid values for station
9	Invalid year	YEAR ≠ Valid year for date range captured
10	Invalid day	DAY ≠ Valid date for the MONTH
11	A full day of data is not available for a day for all lanes	Manual audit of hours and days
12	Class volume exceeds maximum limit	CLS_CNT_## = TOTAL_VOL
13	1AM total lane volume exceeds 1PM total lane volume	HOUR(1) TOTAL_VOL > HOUR(13) TOTAL_VOL
14	Static total lane volume for four consecutive hours	HOUR(X) TOTAL_VOL = HOUR(X+1,+2,+3) TOTAL_VOL
15	Review Avg. DOW volumes by month for unusual patterns	A pattern deviates significantly from other months
16	Review Class Distribution by month for unusual patterns	A pattern deviates significantly from other months

Table 2.3 (cont.) Quality Control Rules List for Class Data (*Ramachandran et al, 2011*)

17	Review Class % Distributions for unusual patterns	The summary data exhibits an unusual pattern

Table 2.4 Gross Vehicle Weight Ranges for Peaks (Ramachandran et al, 2011)

Vehicle Class	Typical Weight Ranges for Peaks (lbs)
4	One peak at 20,000
5	One peak at 10,000
6	One peak at 20,000 to 25,000 and Other at 45,000 to 55,000
7	One peak at 50,000 to 60,000
8	One peak at 30,000 to 35,000
9	One peak at 30,000 to 35,000 and Other at 70,000 to 80,000
10	One peak at 40,000 to 45,000 and Other at 75,000 to 85,000
11	One peak at 55,000 to 60,000
12	One peak at 55,000 to 65,000
13	Straight Line (Constant weight range with very low frequency of trucks)

Chapter 3

CHARACTERIZATION OF TRAFFIC LOAD FOR MEPDG

3.1 Introduction

Traffic is one of the most important inputs required for the design and analysis of pavements. It represents the magnitude and frequency of the loads applied during the pavement design life. The 1993 AASHTO Guide for Pavement Design characterized traffic using the number of equivalent single axle loads (ESALs) which is the number of standard axle loads applied during the pavement design life. However, MEPDG uses a more complex approach that requires a larger number of traffic inputs. One of these inputs is the axle load spectra which can be only obtained from weigh-in-motion data. Therefore, it is critical for highway state agencies to collect and process high quality WIM data (*Guide for Design of Pavement Structures, 1993*).

WIM systems are installed in suitable road sections to collect classification and weight traffic data which are stored in C-files and W-files respectively. Classification data consists of a tabulation containing the total number of vehicles that pass through the WIM site in every lane and every direction during every hour of the day, and the distribution of these vehicles by FHWA vehicle class. In addition, for each truck passing, these equipment record a tabulation formed with the FHWA vehicle class and the number, spacing, and weight of axles, which constitutes the weight data.

There are different technologies for WIM systems such as load cells, bending plates, kistler lineas, and piezo sensors. The dynamic weight measured by these systems is not

the same as the actual static weight, because there is an error associated with any measure and also a systematic bias whether the equipment is not well calibrated. Each one of them has a particular accuracy. Unlike random error that may distort the weight measurement on any one occasion but balances out on the average, systematic bias produces a significant distortion from the actual value that is consistently positive or negative.

The equipment required to collect weigh-in-motion data is very expensive and often state highway agencies and their traffic monitoring programs are subjected to budget constraints. This usually results in lack of calibration of their WIM sites which directly leads to weight measurement bias and its consequences on the quality of data. Moreover, the type of sensor, the pavement condition, and the temperature in the case of piezo systems are factors affecting considerably the accuracy and reliability of WIM sites. Therefore, it is very important to provide state highway agencies with a procedure to evaluate the quality of WIM data for determining when a particular WIM site requires calibration, and to develop the required traffic data inputs for the future implementation of the MEPDG. Quality of weigh-in-motion data affects axle load spectra, and thus, there is a need to evaluate the effect of WIM data quality on mechanistic-empirical pavement design.

The following objectives are pursued within this chapter:

- Develop a set of subroutines to perform quality control of weigh-in-motion data and to obtain traffic inputs required for the future implementation of MEPDG.
- Determine the influence of weigh-in-motion data quality and axle load spectra on pavement design and predicted performance.

3.2 Weigh-in-Motion Data in New Mexico

Currently, thirteen WIM stations are collecting weight and classification data throughout New Mexico. These WIM sites are operated by NMDOT. Three of them use bending plate systems, and the remaining use piezoelectric sensors. Figure 3.1 shows the location and Table 3.1 the type of technology of each of the WIM sites.

The condition of the road surface, the calibration of the system, and the temperature in the case of piezoelectric sensors are factors that significantly affect the weight measurement. The three bending plate systems are being calibrated semiannually, while the remaining WIM sites are calibrated annually due to budget constraints. The data collected in the thirteen operative WIM sites during the year 2010 are used for these analyses.

3.3 Quality Control Rules and Algorithms

A series of validation rules are defined to check whether the weigh-in-motion data is consistent and acceptable from a quality point of view. A set of fourteen rules for classification data and another set of fifteen rules for weight data are implemented by means of subroutines developed in Microsoft Excel Visual Basic Application. This program allows importing the desired C-files and W-files and when it is run every single record has to pass each of these rules in order to be valid. If any of the rules are not fulfilled then an "ERROR" flag appears, and the user can remove that particular invalid record.

The fourteen rules used to check the quality of classification data are described below (*Ramachandran et al, 2011*):

1. The record belongs to a C-file, e.g. if Record Type ≠ C then "ERROR".

2. The record belongs to New Mexico, e.g. if State Code ≠ 35 then "ERROR".
3. The WIM site id is unique and correct, e.g. if Station Code ≠ 21020 then "ERROR".
4. The direction is correct, e.g. if Direction ≠ 1 or 5 then "ERROR".
5. The lane number is correct, e.g. if Lane Number ≠ 1 to 4 then "ERROR".
6. The year is unique and correct, e.g. if Year ≠ 10 then "ERROR".
7. The month is correct, e.g. if Month ≠ 1 to 12 then "ERROR".
8. The day is correct, e.g. if Day ≠ 1 to 31 then "ERROR".
9. The time is correct, e.g. if Hour ≠ 0 to 23 then "ERROR".
10. The total hourly volume per lane does not exceed the maximum limit, e.g. if Total Hourly Lane Volume > 3000 then "ERROR".
11. The total volume in the outside lanes collected between 1 am and 2 am does not exceed the same volume collected from 1 pm to 2 pm, e.g. if Hour 1 Total Lane Volume > Hour 13 Total Lane Volume then "ERROR".
12. The total outside lanes volume is not constant for four consecutive hours, e.g. if Hour X Total Lane Volume = Hour X+1 Total Lane Volume = Hour X+2 Total Lane Volume = Hour X+3 Total Lane Volume then "ERROR".
13. The percentage of motorcycles is less than 5%, e.g. if % Motorcycles > 5 then "ERROR".
14. The percentage of unclassified vehicles (classes 14 and 15) is less than 5%, e.g. if Percentage of Unclassified Vehicles > 5 then "ERROR".

The fifteen rules used to check the quality of weight data are described below (*Ramachandran et al, 2011*):

1. The year is unique and correct, e.g. if Year ≠ 10 then “ERROR”.
2. The month is correct, e.g. if Month ≠ 1 to 12 then “ERROR”.
3. The day is correct, e.g. if Day ≠ 1 to 31 then “ERROR”.
4. The time is correct, e.g. if Hour ≠ 0 to 23 then “ERROR”.
5. The WIM site id is correct, e.g. if Station Code ≠ 21020 then “ERROR”.
6. The direction is correct, e.g. if Direction ≠ 1 or 5 then “ERROR”.
7. The lane number is correct, e.g. if Lane Number ≠ 1 to 4 then “ERROR”.
8. The vehicle class is correct, e.g. if Vehicle Class ≠ 4 to 13 then “ERROR”.
9. The number of axles is consistent with the number of axle spaces, e.g. if Number of Axles ≠ Number of Axle Spaces + 1 then “ERROR”.
10. The number of axles is consistent with the number of axle weights, e.g. if Number of Axles ≠ Number of Axle Weights then “ERROR”.
11. The gross vehicle weight is consistent with the sum of axle weights, e.g. if Sum of Axle Weights ≠ GVW then “ERROR”.
12. The number of axles is consistent with the vehicle class, e.g. if Number of Axles ≠ Range of Axles for that vehicle class then “ERROR”.
13. The sum of axle spaces is consistent with the maximum length, e.g. if Sum of Axle Spaces > 115 ft (35 m) then “ERROR”.
14. The axle weights are within acceptable range, e.g. if Axle Weight ≠ 440 lbs (200 kg) to 33,000 lbs (15,000 kg) then “ERROR”.
15. The axle spaces are within acceptable range, e.g. if Axle Spacing ≠ 2 ft (0.6 m) to 50 ft (15 m) then “ERROR”.

The maximum vehicle length, axle weight, and axle spacing are based on the maximum values allowed by the Guide for Vehicle Weights and Dimensions to which an additional percentage of the original value is added to account for overloaded and oversized trucks (*Guide for Vehicle Weights and Dimensions, 2001*).

Finally, other algorithms are developed to make this program able to calculate the following frequency distributions which are critical for quality control of weigh-in-motion data:

- Gross Vehicle Weight Frequency Distribution by Class.
- Front Steering Axle Weight Frequency Distribution by Class.

In the last step of this process, the gross vehicle weight and steering axle weight frequency distributions are subjected to the following criteria provided by the TMG (*Traffic Monitoring Guide, 2001*):

- The class 9 gross vehicle weight distribution must have a peak due to unloaded vehicles within the range of 30,000 lbs (13,500 kg) to 40,000 lbs (18,000 kg) and another peak due to loaded trucks within the range of 70,000 lbs (31,500 kg) to 80,000 lbs (37,000 kg).
- The class 9 front steering axle weight distribution must have the majority of axles within the range of 8,000 lbs (3,600 kg) to 12,000 lbs (5,400 kg).

3.4 Quality Control Analysis

Both sets of quality control rules are applied to the weigh-in-motion data. All WIM sites have less than 1% of invalid weight records, except Tucumcari that presents almost 6%. The classification data does not present any invalid records. Table 3.2 shows the total number of trucks recorded in each WIM site during 2010, and the corresponding number

and percentage of erroneous data. The invalid records are removed, and the program calculates the gross vehicle weight and front steering axle weight frequency distributions.

The gross vehicle weight frequency distributions for class 9 vehicles are plotted in Figures 3.1 (a) and 3.1 (b) for functional roadway classes 1 and 2, respectively. This vehicle class comprises almost 70% of the total traffic stream. The graph is divided in two parts according to the functional class of the roads where the WIM sites are located. Only the three bending plate systems (San Ysidro, Cuba and Bloomfield) present a distribution with peaks for unloaded and loaded trucks in the middle of the ranges recommended by the TMG. The remaining piezoelectric sites only have one single peak which indicates that these WIM sites are assigning either a too low or too high weight to every truck passing, probably due to a malfunction of the system. Although the site at Rincon presents two peaks, these are out of range, and thus, it is not acceptable (*Traffic Monitoring Guide, 2001*).

The front steering axle weight frequency distributions for class 9 vehicles are shown in Figures 3.2 (a) and 3.2 (b) for functional roadway classes 1 and 2, respectively. The graph is divided in two parts by functional class as well. For the case of San Ysidro, Cuba, and Bloomfield (bending plates), and also Hatchita and Tucumcari, most of the frequencies fall within the range recommended by the TMG. The curves of the remaining piezoelectric systems are out of the acceptable range (*Traffic Monitoring Guide, 2001*).

These results denote that the piezo sites are not providing good weigh-in-motion data, perhaps due to the lack of calibration or the effect of surface condition and temperature in piezoelectric sensors. On the other hand, San Ysidro, Cuba and Bloomfield are collecting

acceptable WIM data. Only these bending plate systems fulfill the two criteria recommended by the TMG, and therefore, are used to develop axle load spectra.

3.5 Development of Traffic Volume MEPDG Inputs

Two subroutines have been created in Visual Basic Application to process classification WIM data. These subroutines first import the C-file, and then process all classification data to calculate several traffic volume inputs and distributions that are required in the MEPDG. The outputs of these scripts are listed next:

- Average Daily Traffic (ADT)
- Average Daily Truck Traffic (ADTT)
- Percentage of Trucks
- Directional Distribution
- Lane Distribution
- Vehicle Class Distribution
- Truck Class Distribution
- Monthly Distribution by Vehicle Class
- Vehicle Hourly Distribution
- Truck Hourly Distribution

These subroutines are applied to the classification data collected during all of 2010 by the thirteen operative WIM sites. Table 3.3 includes the average daily traffic, the average daily truck traffic, and the percentage of trucks. The average daily traffic ranges from 2,000 vehicles per day to 34,000 depending on the functional class of the road, and the percentage of trucks varies from 17% up to 61%.

The vehicle class distribution of each WIM station is shown in Figures 3.3 (a) and 3.3 (b) for functional roadway classes 1 and 2, respectively. In general, classes 5 and 9 comprise around 80% of the total truck traffic stream, being the individual contribution of these two classes around 40% for functional class 2 roads. But for the case of functional class 1, only class 9 comprises almost 80% of the total heavy traffic. This indicates consistency of data since rural interstates usually are supposed to present larger trucks. The pattern observed at Rincon is unusual presenting 60% of class 5 vehicles and 25% of class 9 trucks; perhaps there is a problem with the classifier of this WIM station.

The directional distributions are shown in Figures 3.4 (a) and 3.4 (b) for functional roadway classes 1 and 2, respectively. The directional distribution factor is around 50% at all WIM sites except Lemitar, a trend to be expected on rural highways. This means that the weigh-in-motion equipment worked correctly in both directions. The case of Lemitar would require further examination to determine whether there is more volume in one direction than in the other.

Similarly, Figures 3.5 (a) and 3.5 (b) show the lane distribution of WIM sites for functional roadway classes 1 and 2, respectively. The lane distribution factors are around 45% for the outside lanes and 5% for the inside lanes. This is a typical pattern in New Mexico rural highways. The interpretation is that the weigh-in-motion equipment worked properly in every lane during the year and the data should be consistent.

The monthly volume distributions of Hatchita, Tucumcari, Tularosa, and San Ysidro sites are plotted in Figures 3.6 (a) and 3.6 (b) for functional roadway classes 1 and 2, respectively. Only these four stations had collected twelve months of data during 2010. It

seems that the months of July and August present traffic slightly higher than the average. This is a feature typically observed.

Also, the hourly volume distributions of Hatchita, Tucumcari, Tularosa, and San Ysidro are shown in Figures 3.7 (a) and 3.7 (b) respectively for functional roadway classes 1 and 2. The distributions are very similar in the four cases presenting maximum traffic between 9 am and 4 pm, a pattern which is common in New Mexico.

3.6 Development of Axle Load Spectra

Weigh-in-motion data is processed in order to obtain axle load spectra - one of the most important inputs to the MEPDG. This process is external to the Design Guide. TrafLoad v1.0.8 is software for processing and analyzing WIM data that was created under NCHRP Project 1-39. In this case TrafLoad cannot import successfully New Mexico WIM data, and therefore is not effective to produce axle load spectra (*TrafLoad's User Manual, 2004*).

Therefore, an algorithm has been implemented in Visual Basic Application to process WIM data and to compute the corresponding axle load spectra. This algorithm is based on the spacing between axles and the weight of each axle. A limit spacing value is defined such that when there are two, three or four consecutive axles separated by a distance smaller than the limit spacing value, then these axles are considered as tandem, tridem or quad respectively. A single axle is separated from the surrounding axles by a distance greater than the limit spacing.

The aforementioned subroutines are used to obtain the axle load spectra for single, tandem, tridem and quad axles. Figures 3.8 (a), 3.8 (b) and 3.8 (c) show respectively the single, tandem and tridem axle load spectra. San Ysidro, Cuba and Bloomfield sites

present very similar axle load spectra since the three WIM stations are located on the same highway. These axle load spectra are used in the next sections to evaluate the effect of weight measurement bias on the pavement performance predicted by MEPDG.

3.7 Simulating the Weight Measurement Bias

The weight measured in dynamic conditions by a WIM system is not the actual static weight. There is always some error. Part of this error is random due to the inherent deviation associated with any measurement process. Also, error can be produced by bias in the apparatus due to lack of calibration. The systematic bias results in a positive or negative consistent deviation for any weight measured and can be quantified as a percentage of the actual value.

A subroutine has been developed in Visual Basic Application to simulate the systematic bias in a weigh-in-motion site due to lack of calibration. This subroutine increases or decreases the weight data collected at the WIM site by a given percentage. The algorithm is used to apply a positive and negative bias of 10%, 20%, and 30% to the weigh-in-motion data, and thus to the axle load spectra of San Ysidro, Cuba, and Bloomfield WIM sites.

The single, tandem and tridem axle load spectra at San Ysidro for the cases of no bias and positive and negative 20% bias are respectively plotted in Figures 3.9 (a), 3.9 (b) and 3.9 (c). As expected, a positive bias produces a displacement of the curve to the right and a negative bias a displacement to the left. The displacement of the curve is larger for the heaviest axles since the increase or decrease applied is a percentage of the weight.

3.8 Prediction of Pavement Performance

The MEPDG version 1.100 is used to predict the pavement performance of typical sections on US-550 which are located close to the San Ysidro, Cuba, and Bloomfield WIM sites. These data are obtained from the Long Term Pavement Performance (LTPP) online database. The simulations are carried out for a design life that goes from the road construction date to the year 2011 (*LTPP Database Reference Manual, 2006*).

All inputs are kept constant except the axle load spectra which are varied to evaluate the influence of positive and negative 10%, 20%, and 30% bias on the predicted pavement distresses. Table 3.4 contains the percentage of variation of total rutting, asphalt concrete rutting, and IRI due to bias with respect to the initial no bias case. The values obtained for San Ysidro, Cuba, and Bloomfield are averaged.

As in the previous table, the percentage of distress variation due to 10%, 20%, and 30% positive and negative bias is calculated for longitudinal, alligator, and transverse cracking and included in Table 3.5. In both tables, the percentage of variation per one percent bias is calculated from the average values of the three WIM sites. The effect of weight measurement bias on predicted distresses are analyzed thoroughly in the next section.

3.9 Influence on Pavement Performance

The sensitivity of total and AC permanent deformation to weight measurement bias is plotted in Figures 3.10 (a) and 3.10 (b), respectively. The sensitivity of both rutting distresses is exactly the same, and equal for the three WIM sites. A positive or negative bias of 1% results in an increase or decrease in the predicted rutting of 1%, respectively. Also, it is interesting that the relationship between bias and variation of rutting is linear.

In this case the effect of weight measurement error on predicted permanent deformation is considerable but not critical.

Longitudinal cracking is the only distress producing failure of the pavement sections corresponding to the San Ysidro and Bloomfield sites. Figures 3.11 (a) and 3.11 (b) show the variation of longitudinal and alligator cracking versus weight measurement bias. In these two distresses, the relationship between cracking and bias is nonlinear in such a way that the influence of positive bias triples that of negative bias. A negative weight measurement bias of 1% produces an average decrease in longitudinal cracking of 3.69%, while a positive bias of 1% results in an average increase of 9.21%. Similarly, a negative bias of 1% results in an average decrease in alligator cracking of 3.08% and a positive bias of 1% produces an average increase of 5.94%. As shown, weight measurement bias affects dramatically the predicted longitudinal and alligator cracking. Therefore, erroneous weigh-in-motion data can lead to overestimated and underestimated pavement thickness, and thus, to unnecessary costs of construction and maintenance.

The influence of weight measurement bias on transverse cracking and IRI can be analyzed in Figures 3.12 (a) and 3.12 (b). As expected, weight measurement bias has no effect on transverse cracking because this type of distress depends upon temperature rather than load. Similarly, the effect of bias on the international roughness index is negligible since 1% bias produces a variation of 0.1%.

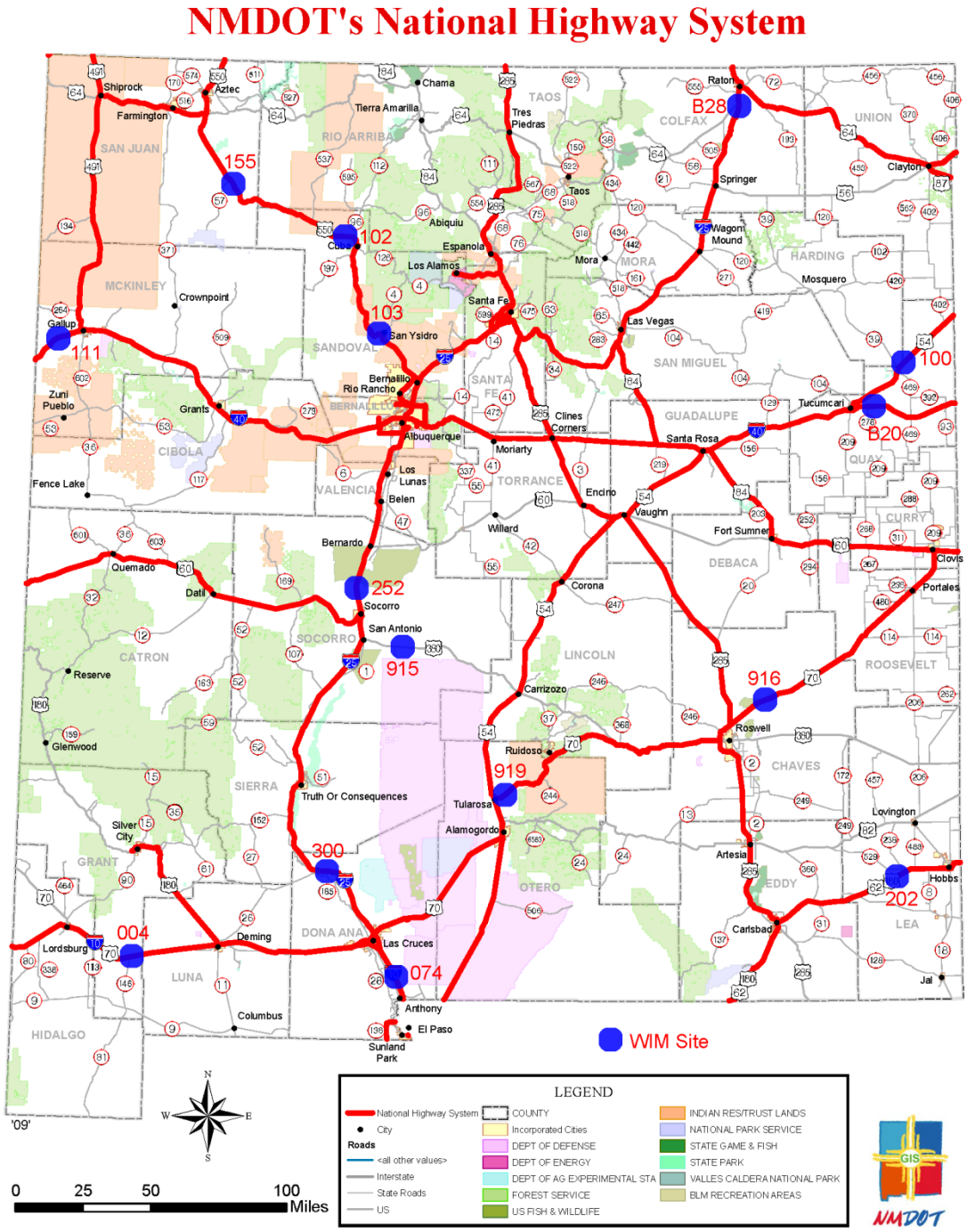

Figure 3.1 Location of WIM sites in New Mexico

Table 3.1 WIM sites location and type of technology

Site Name	Site Code	County	Road Name	Milepost	Type of Technology
HATCHITA	4	Grant	I-10	50.05	Piezo
VADO	74	Doña Ana	I-10	155.6	Piezo
RINCON	300	Doña Ana	I-25	37.2	Piezo
LEMITAR	252	Socorro	I-25	158.8	Piezo
RATON *	B28	Colfax	I-25	445	Piezo
GALLUP	111	McKinley	I-40	10.7	Piezo
TUCUMCARI	B20	Quay	I-40	340.9	Piezo
LOGAN *	100	Quay	US-54	328	Piezo
HOBBS	202	Lea	US-62/180	84	Piezo
TULAROSA	919	Otero	US-70	231.65	Piezo
ROSWELL	916	Roosevelt	US-70	354.3	Piezo
SAN ANTONIO	915	Socorro	US-380	15.7	Piezo
SAN YSIDRO	103	Sandoval	US-550	24.738	Bending Plate
CUBA	102	Sandoval	US-550	71.051	Bending Plate
BLOOMFIELD	155	San Juan	US-550	121.5	Bending Plate

* These sites are currently not operating

Table 3.2 Number and percentage of invalid records

WIM Site	Months of Data	Total Number of Trucks Weighed	Invalid Records	% of Invalid Records
HATCHITA	12	1,962,777	23,930	1.22 %
VADO	4	925,353	3,789	0.41 %
RINCON	2	163,000	251	0.15 %
LEMITAR	3	72,879	388	0.53 %
GALLUP	10	2,069,164	498	0.02 %
TUCUMCARI	12	1,885,748	111,676	5,92 %
HOBBS	7	242,717	929	0.38 %
TULAROSA	12	370,163	645	0.17 %
ROSWELL	7	119,488	287	0.24 %
SAN ANTONIO	2	3,809	14	0.37 %
SAN YSIDRO	12	359,120	706	0.20 %
CUBA	11	255,719	158	0.06 %
BLOOMFIELD	11	307,603	1,565	0.51 %

Table 3.3 Traffic volume and percentage of trucks

WIM Site	Average Daily Traffic (ADT)	Average Daily Truck Traffic (ADTT)	Percentage of Trucks
HATCHITA	12,655	6,719	53.09 %
VADO	34,444	8,524	24.75 %
RINCON	6,466	2,989	46.22 %
LEMITAR	7,453	1,160	15.56 %
GALLUP	17,387	10,704	61.56 %
TUCUMCARI	11,767	6,204	52.72 %
HOBBS	3,503	1,477	42.17 %
TULAROSA	6,677	1,021	15.30 %
ROSWELL	1,969	733	37.24 %
SAN ANTONIO	3,077	539	17.53 %
SAN YSIDRO	5,176	1,168	22.56 %
CUBA	4,357	1,019	23.40 %
BLOOMFIELD	5,045	1,288	25.54 %

Table 3.4 Variation of predicted rutting and IRI due to weight measurement bias

TOTAL RUTTING (% variation)							
WIM site | % bias	-30	-20	-10	0	10	20	30
SAN YSIDRO	-29.02	-19.61	-9.80	0.00	9.80	19.22	29.41
CUBA	-30.04	-20.18	-9.87	0.00	9.87	19.73	29.60
BLOOMFIELD	-29.75	-19.83	-9.92	0.00	10.33	19.83	29.75
Average	-29.61	-19.87	-9.86	0.00	10.00	19.59	29.59
% variation / % bias	0.99	0.99	0.99		1.00	0.98	0.99
AC RUTTING (% variation)							
WIM site | % bias	-30	-20	-10	0	10	20	30
SAN YSIDRO	-28.70	-19.13	-9.57	0.00	9.57	19.13	29.57
CUBA	-29.63	-19.75	-9.88	0.00	9.88	19.75	29.63
BLOOMFIELD	-30.00	-20.00	-10.00	0.00	10.00	20.00	30.00
Average	-29.44	-19.63	-9.81	0.00	9.81	19.63	29.73
% variation / % bias	0.98	0.98	0.98		0.98	0.98	0.99
IRI (% variation)							
WIM site | % bias	-30	-20	-10	0	10	20	30
SAN YSIDRO	-3.04	-2.11	-1.10	0.00	1.18	2.36	3.72
CUBA	-2.25	-1.52	-0.80	0.00	0.72	1.44	2.17
BLOOMFIELD	-2.40	-1.48	-0.55	0.00	1.29	2.31	3.32
Average	-2.56	-1.70	-0.82	0.00	1.07	2.04	3.07
% variation / % bias	0.09	0.09	0.08		0.11	0.10	0.10

Table 3.5 Variation of predicted cracking due to weight measurement bias

LONGITUDINAL CRACKING (% variation)							
WIM site | % bias	-30	-20	-10	0	10	20	30
SAN YSIDRO	-86.09	-70.65	-43.05	0.00	68.71	154.60	259.92
CUBA	-88.00	-73.58	-46.63	0.00	77.89	198.95	381.05
BLOOMFIELD	-87.90	-73.27	-46.42	0.00	76.54	191.36	358.64
Average	-87.33	-72.50	-45.37	0.00	74.38	181.64	333.20
% variation / % bias	2.91	3.63	4.54		7.44	9.08	11.11
ALLIGATOR CRACKING (% variation)							
WIM site | % bias	-30	-20	-10	0	10	20	30
SAN YSIDRO	-77.48	-60.79	-35.43	0.00	49.61	117.32	203.94
CUBA	-77.54	-60.92	-35.62	0.00	50.00	116.15	202.31
BLOOMFIELD	-78.41	-61.81	-36.56	0.00	51.98	120.70	212.33
Average	-77.81	-61.17	-35.87	0.00	50.53	118.06	206.19
% variation / % bias	2.59	3.06	3.59		5.05	5.90	6.87
TRANSVERSE CRACKING (% variation)							
WIM site | % bias	-30	-20	-10	0	10	20	30
SAN YSIDRO	0	0	0	0	0	0	0
CUBA	0	0	0	0	0	0	0
BLOOMFIELD	0	0	0	0	0	0	0
Average	0	0	0	0	0	0	0
% variation / % bias	0	0	0		0	0	0

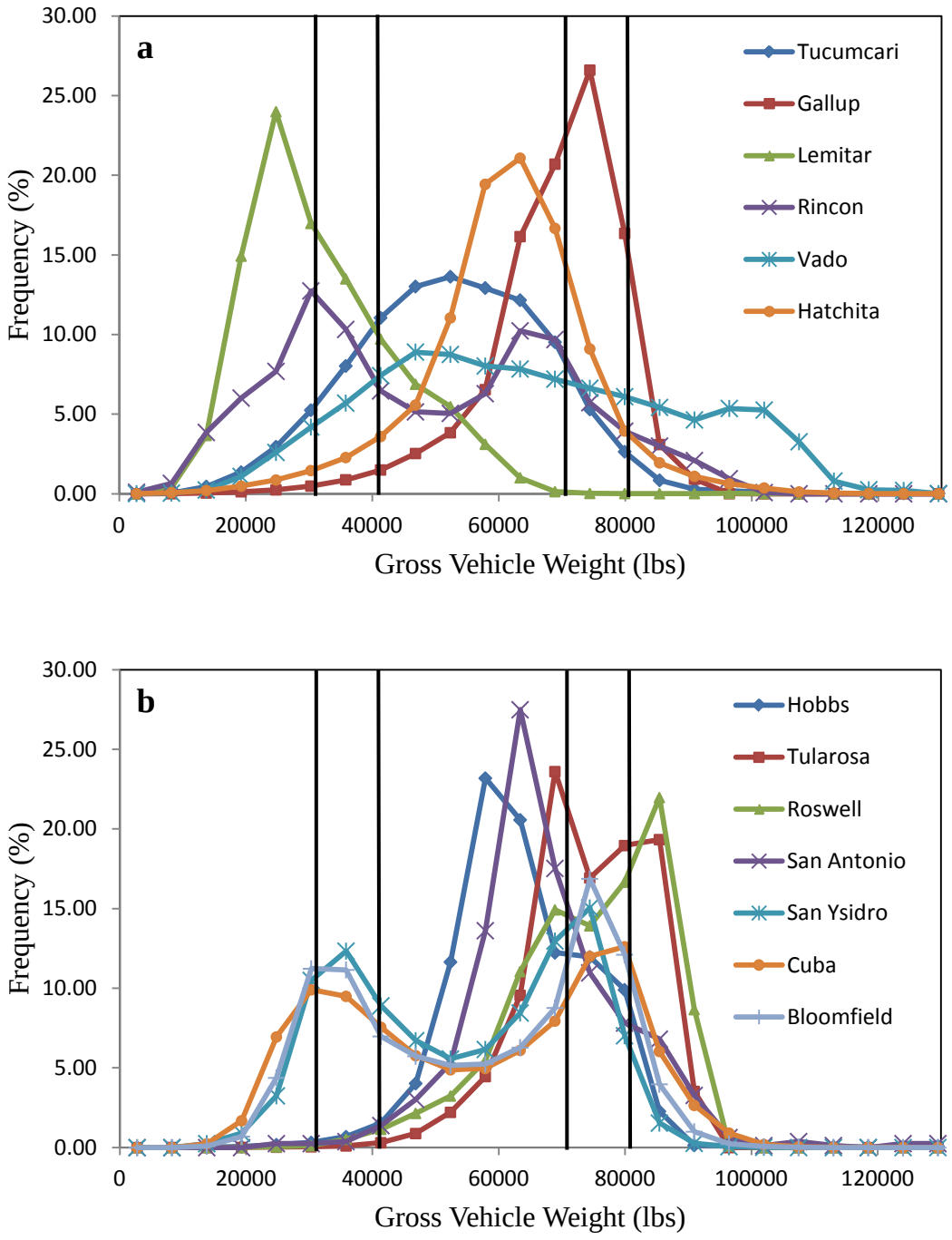

Figure 3.2 Class 9 gross vehicle weight frequency distribution: a) functional class 1, b) functional class 2

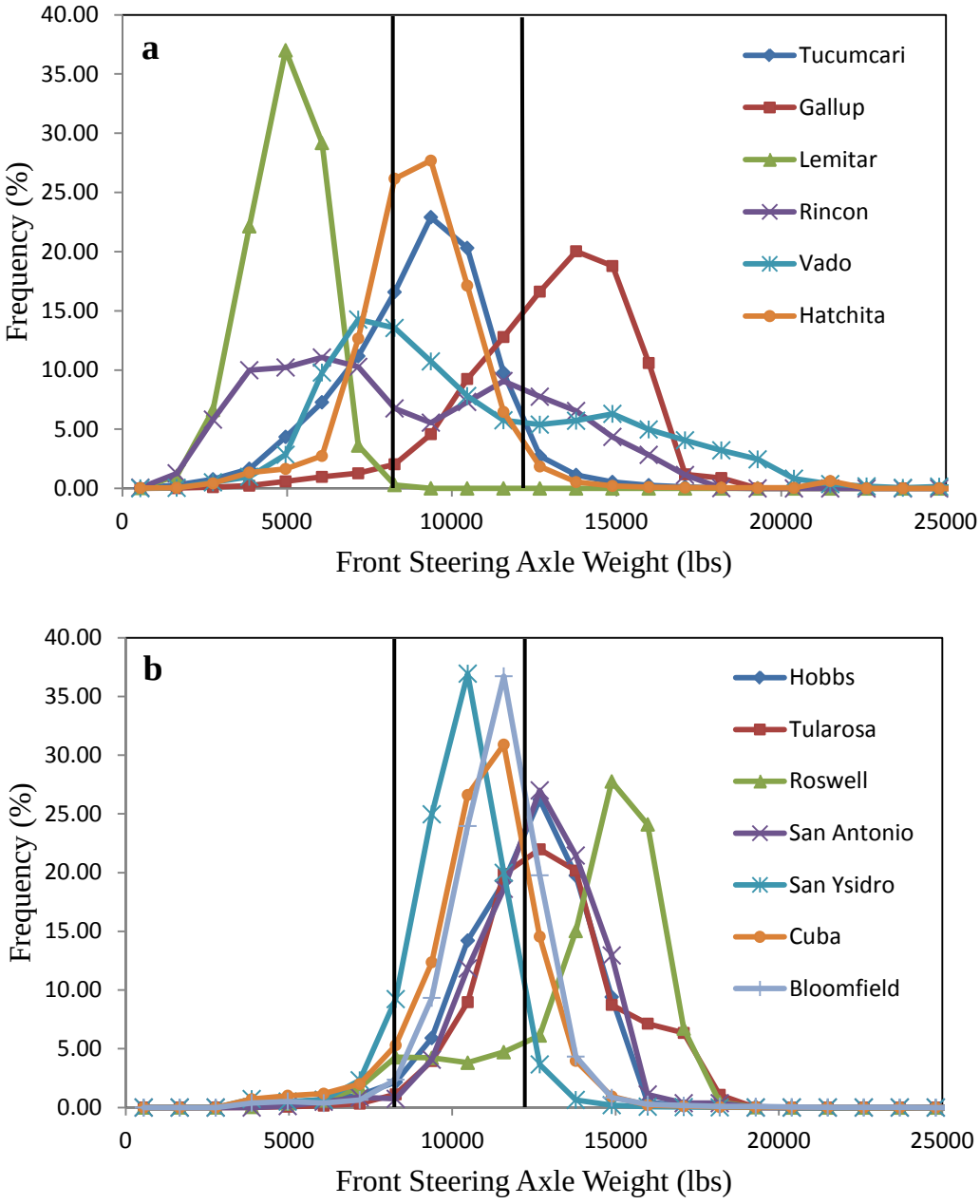

Figure 3.3 Class 9 steering axle weight frequency distribution: a) functional class 1, b) functional class 2

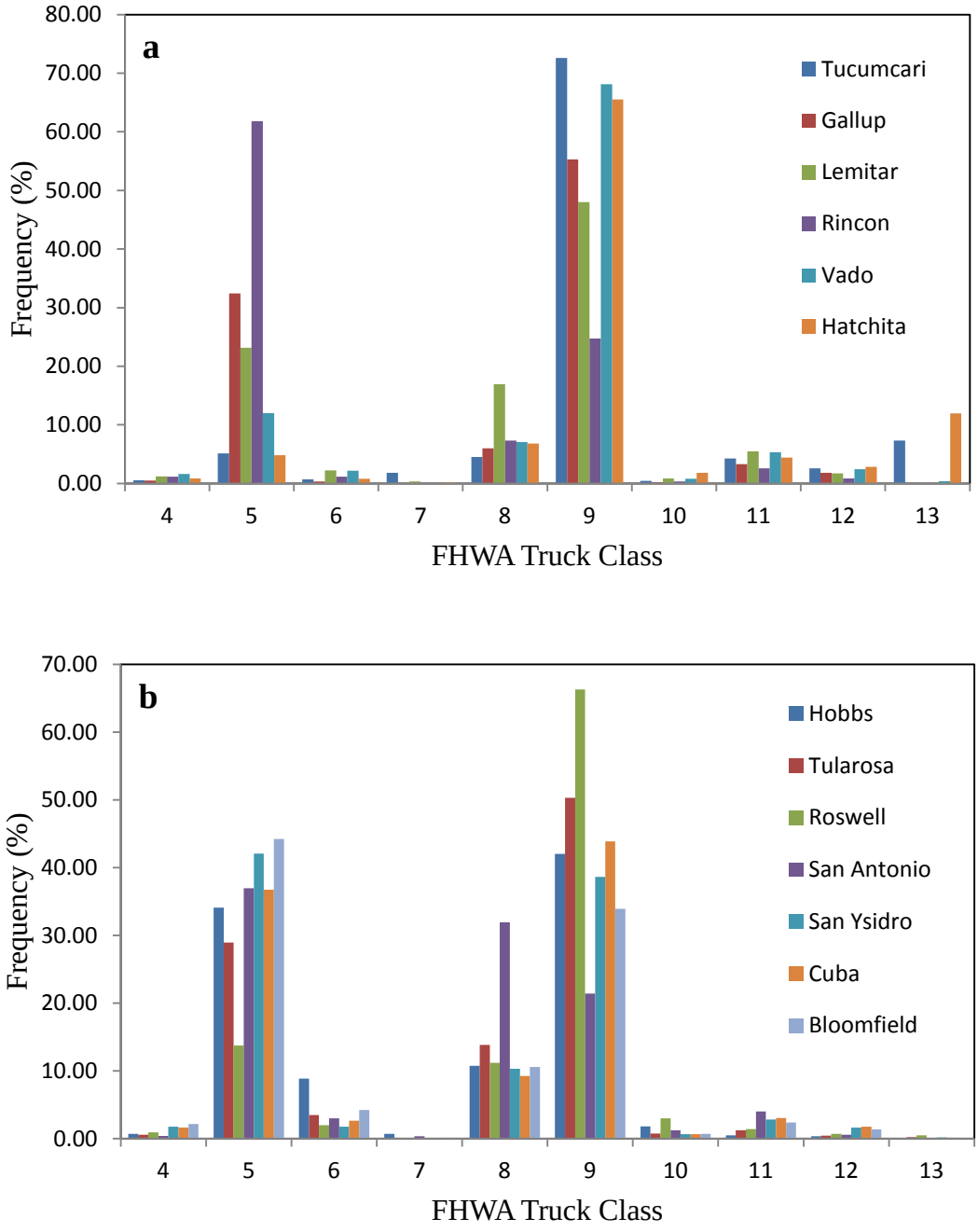

Figure 3.4 Vehicle class distribution: a) functional class 1, b) functional class 2

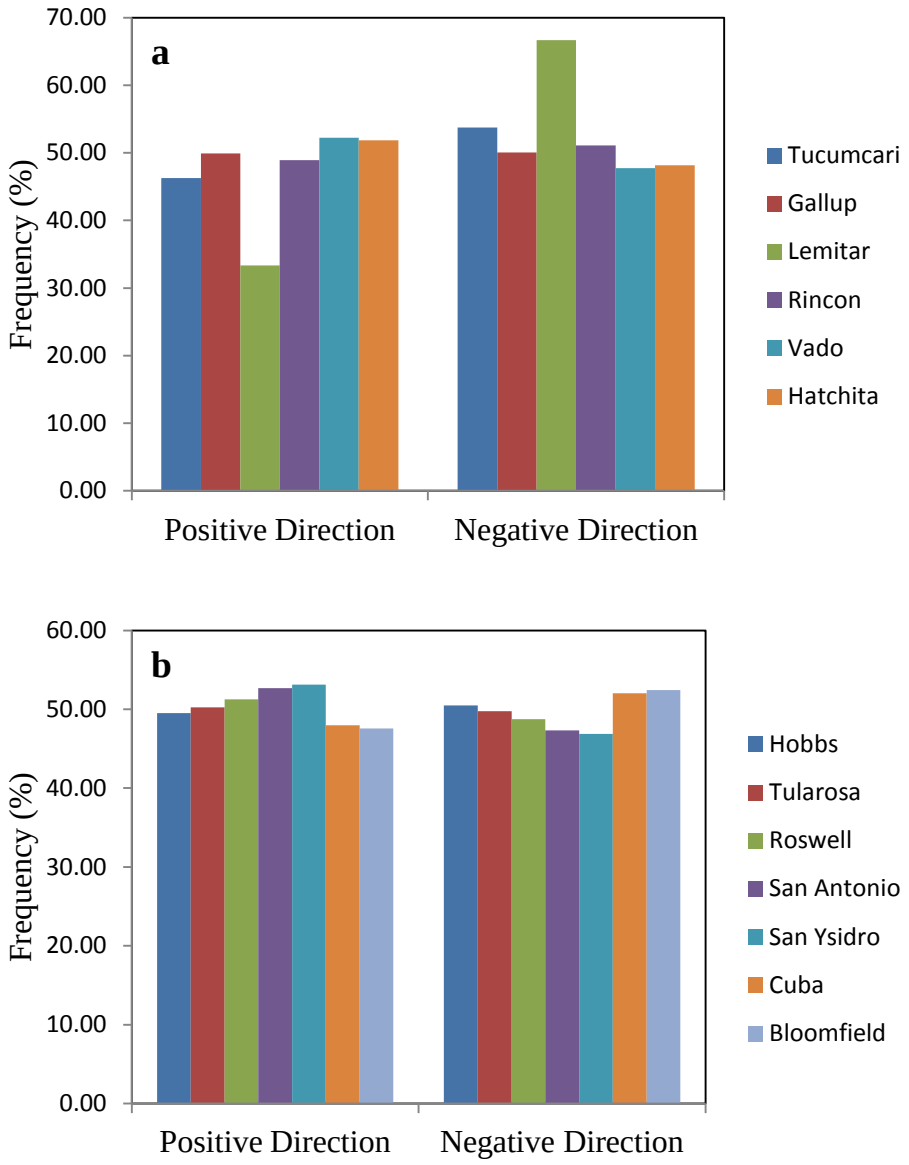

Figure 3.5 Directional distribution: a) functional class 1, b) functional class 2

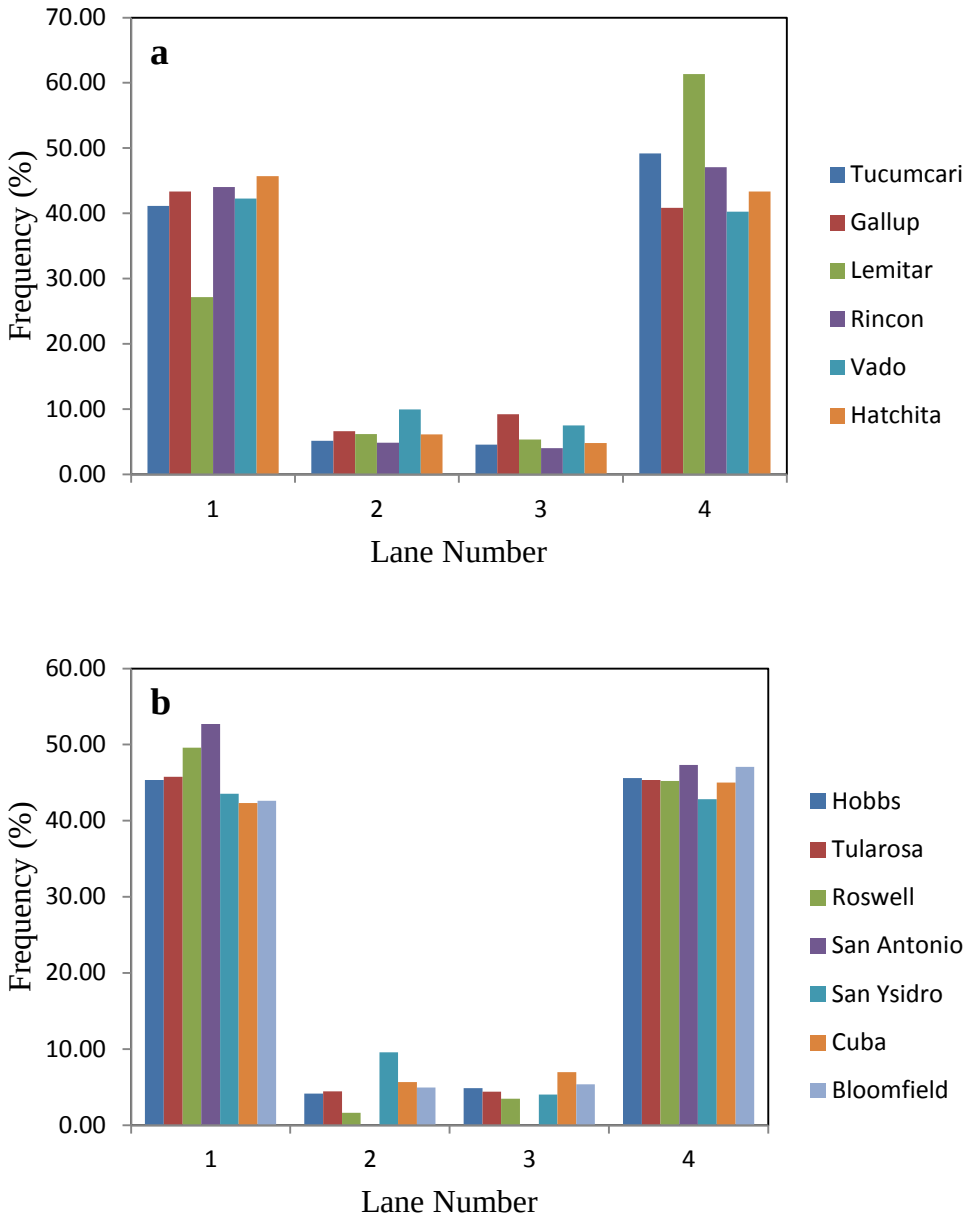

Figure 3.6 Lane distribution: a) functional class 1, b) functional class 2

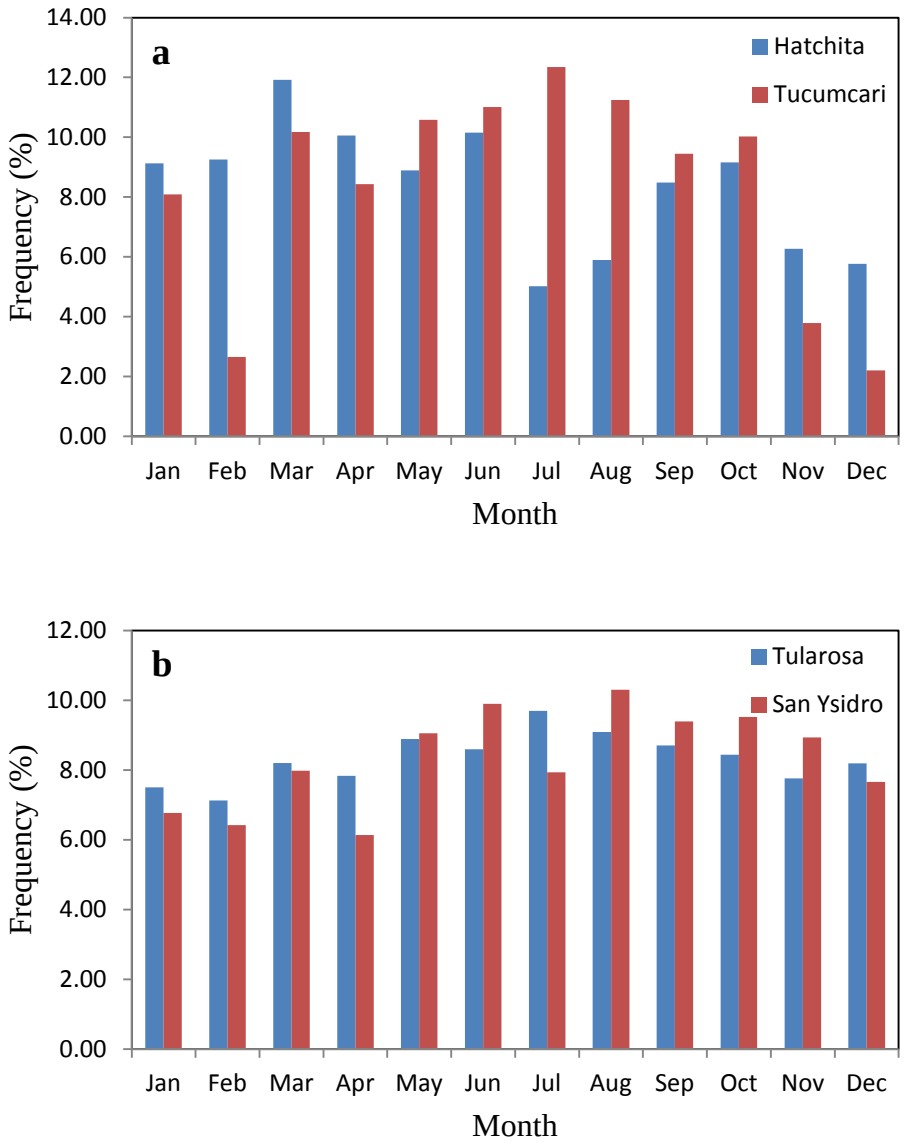

Figure 3.7 Monthly distribution: a) functional class 1, b) functional class 2

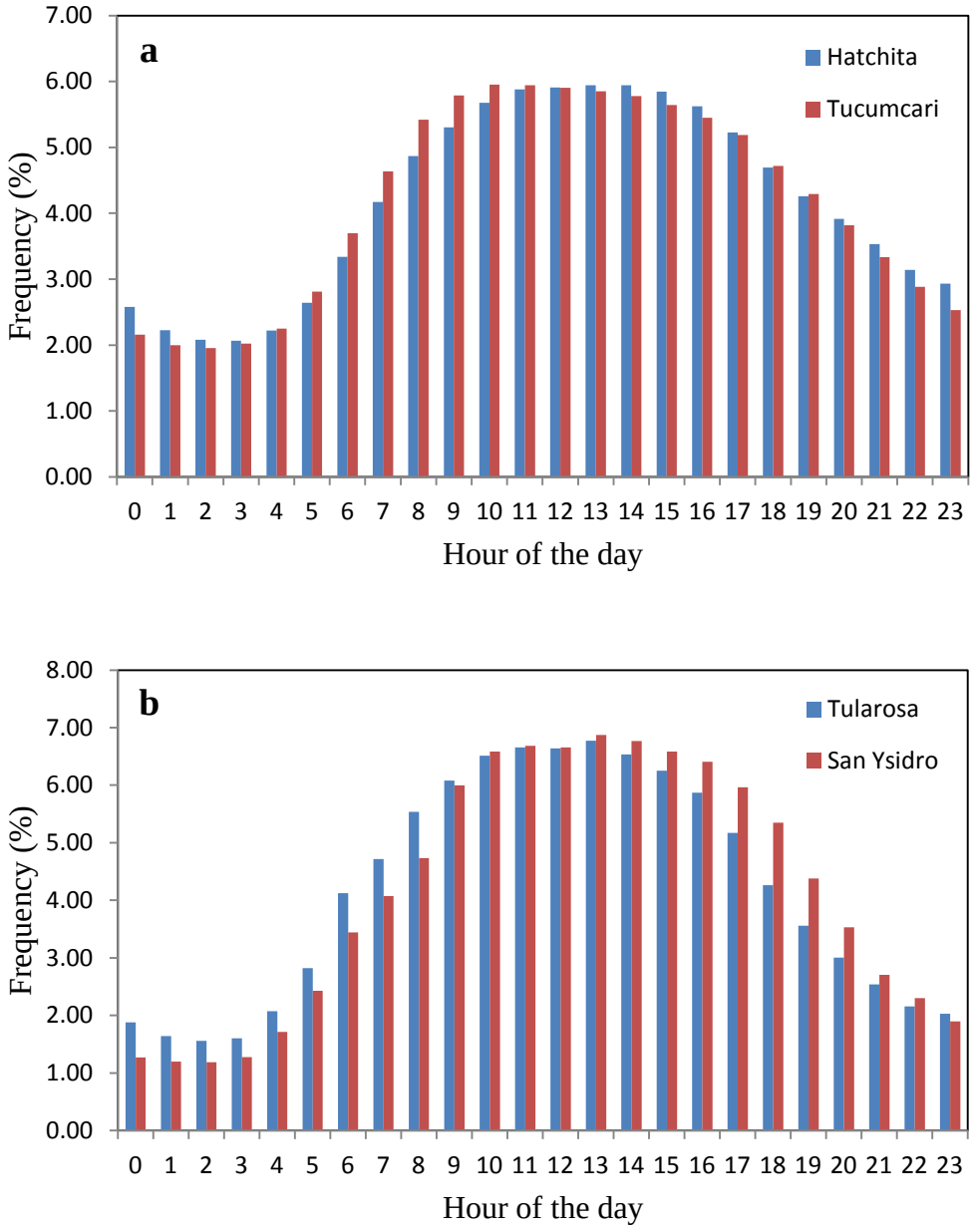

Figure 3.8 Hourly distribution: a) functional class 1, b) functional class 2

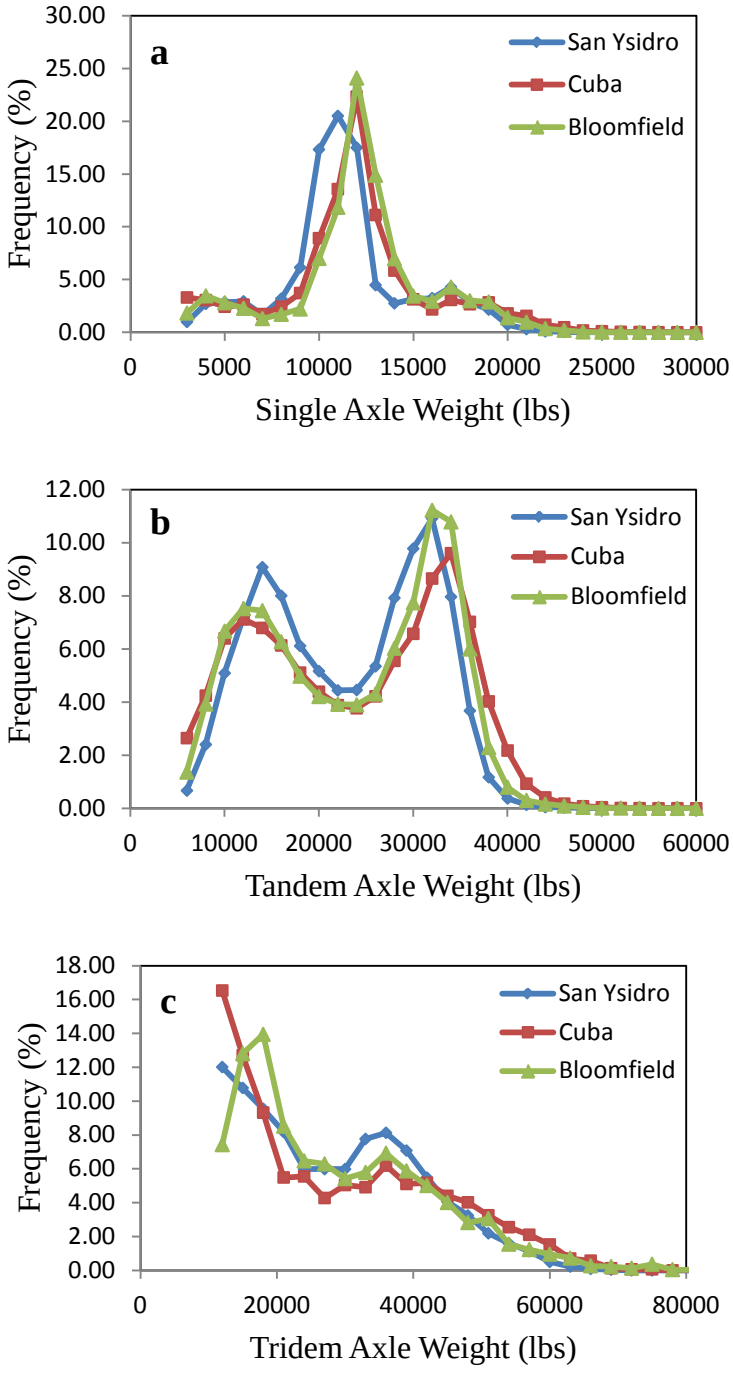

Figure 3.9 Axle load spectra of selected WIM sites: a) single class 9, b) tandem class 9, c) tridem class 10

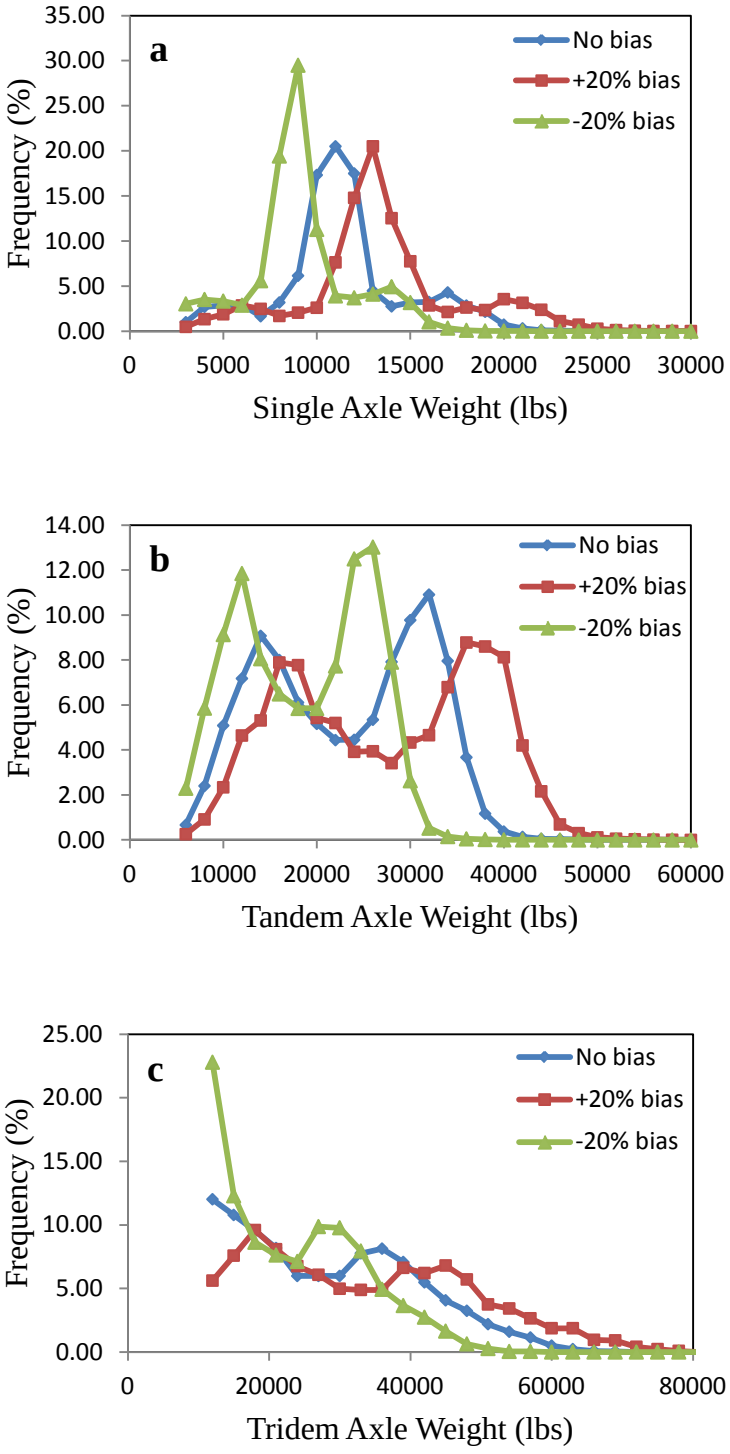

Figure 3.10 Effect of bias on axle load spectra at San Ysidro site:
a) single class 9, b) tandem class 9, c) tridem class 10

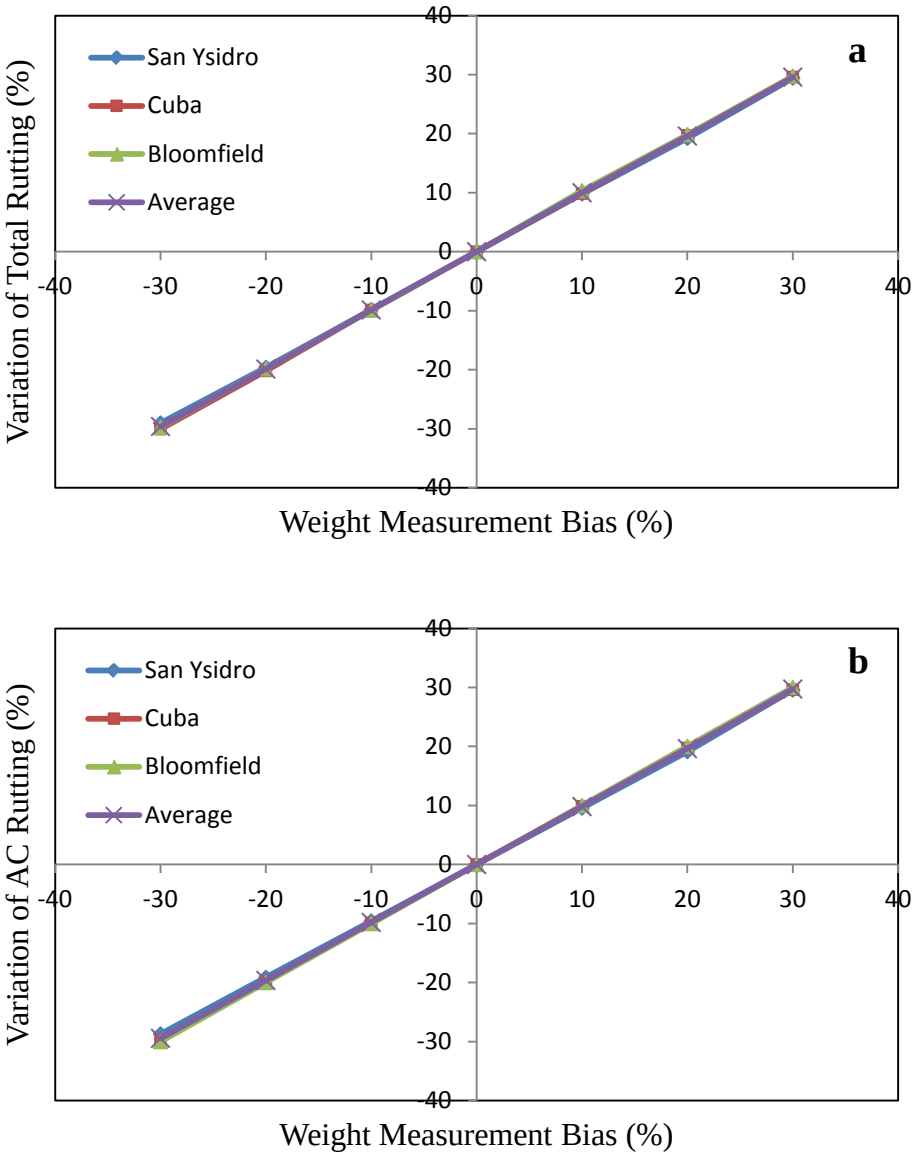

Figure 3.11 Influence of weight measurement bias on predicted rutting: a) total rutting, b) AC rutting

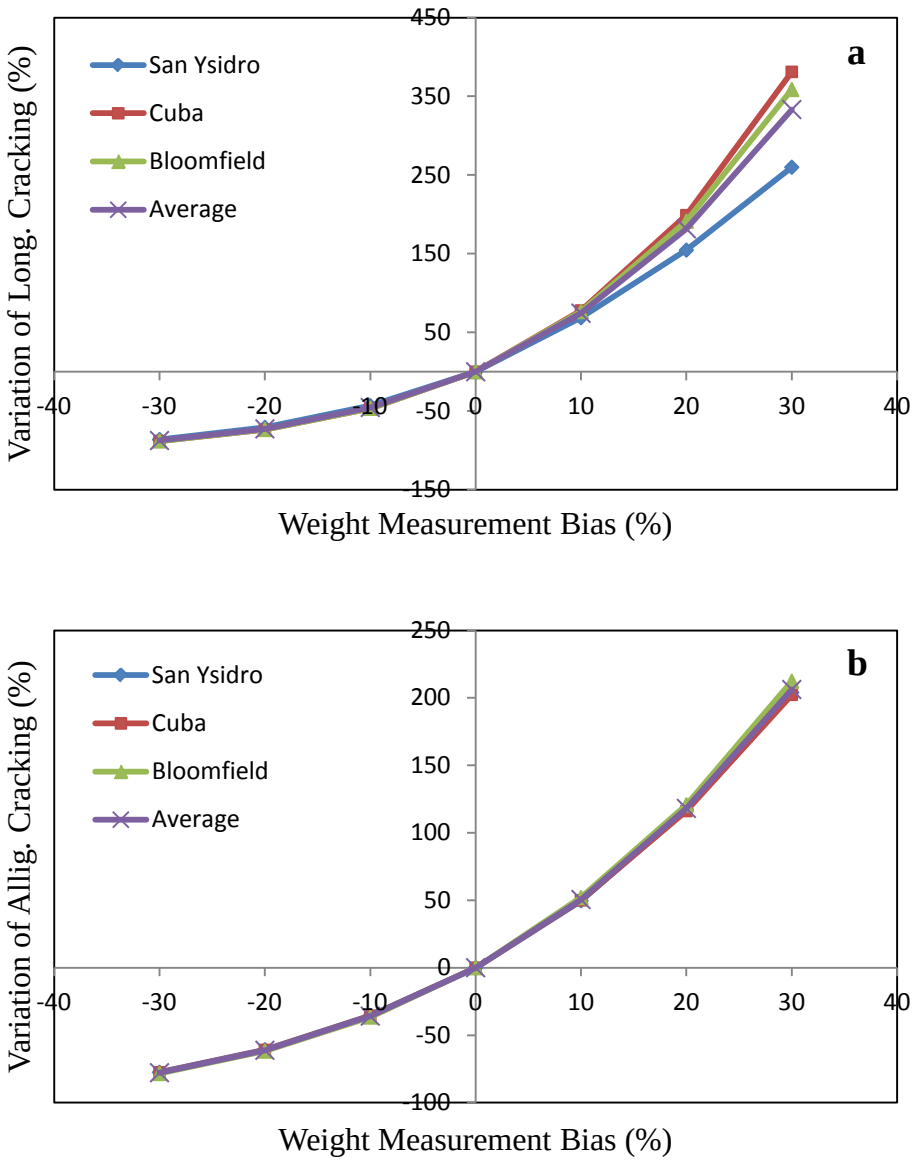

Figure 3.12 Influence of weight measurement bias on predicted cracking: a) longitudinal cracking, b) alligator cracking

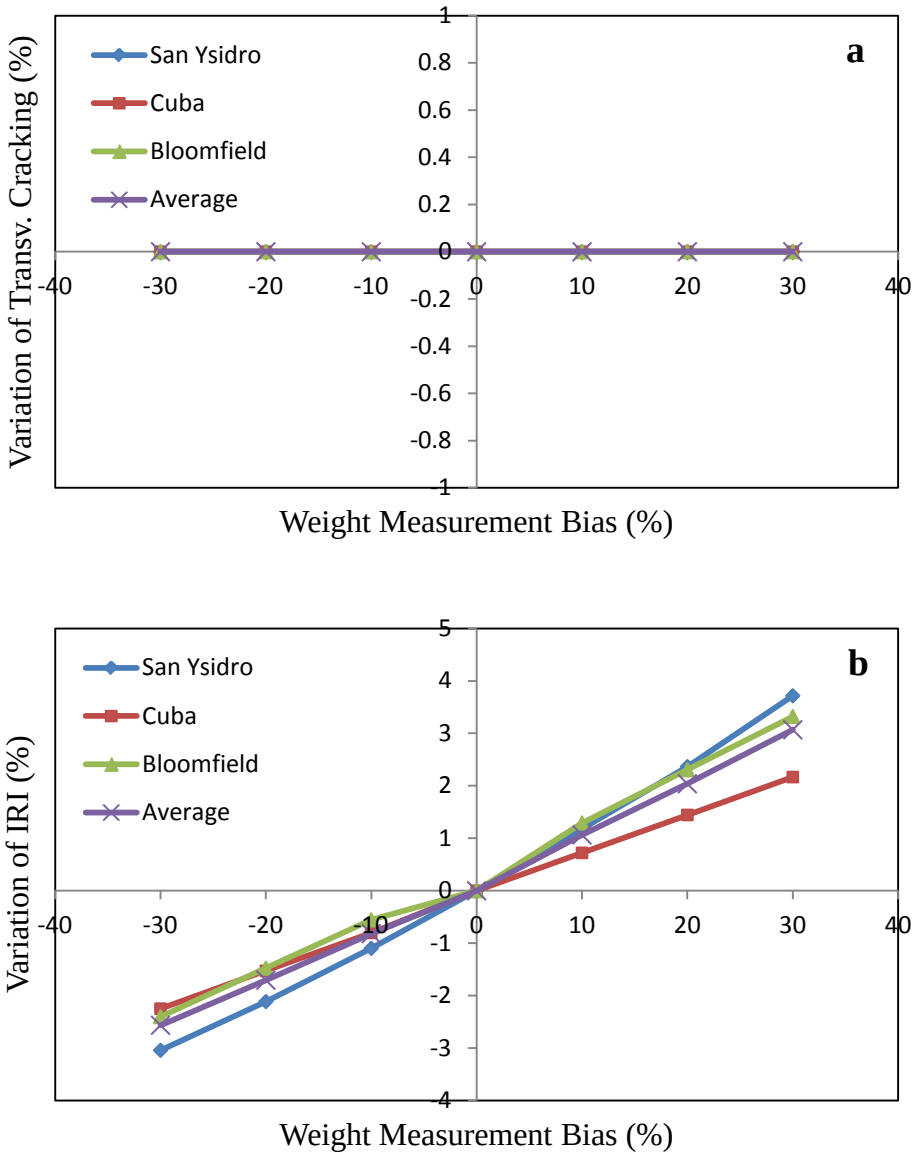

Figure 3.13 Influence of weight measurement bias on cracking and IRI: a) transverse cracking, b) IRI

Chapter 4

LOCAL CALIBRATION OF THE MEPDG FOR FLEXIBLE PAVEMENT IN NEW MEXICO

4.1 Introduction

The pavement distress prediction models of the new Mechanistic-Empirical Pavement Design Guide (MEPDG) were calibrated at a national level using pavement sections from the Long Term Pavement Performance (LTPP) database across North America. As a result, the default configuration of the MEPDG predicts the average performance of a flexible pavement in the United States but fails to predict accurately its performance at a particular location. Therefore, the calibration coefficients of these empirical models should be adjusted specifically for each state so differences in construction practices, maintenance policies, and material specifications from one location to another are considered.

The final goal of the local calibration process is to determine a set of calibration coefficients that eliminates bias and increases precision of the pavement performance models. The consequences are higher reliability levels in the design and the reduction of construction and maintenance costs. The local calibration process has two main steps: calibration and validation. Calibration is the mathematical process involving local pavement data sets in which the residual error (difference between MEPDG predicted and field observed values of distress) is minimized. Validation is necessary to confirm that the calibrated model can perform accurate predictions for cases other than those used in the calibration.

In this chapter, the following objectives are pursued:

- Collect data of all MEPDG inputs (traffic, climate, and materials) for a sufficient number of pavement sections throughout New Mexico.
- Determine for every distress model a set of calibration coefficients that minimize the residual error (difference between observed and predicted distresses).
- Validate the effectiveness of these calibration coefficients for a number of pavement sections that were not included in the local calibration process.

4.2 Pavement Sections for Calibration

The internal databases of New Mexico Department of Transportation (NMDOT) are the first source considered for collecting the traffic, climate, structure, materials, and performance data necessary to obtain a sufficient number of local pavement sections. Indeed, all these databases have been consolidated in the new NMDOT Flexible Pavement Database created at the University of New Mexico. A total of 29 sections are completed for a variety of roads across the state but their use is discarded because the corresponding distress data is inconsistent and unreliable. The reason for this is that NMDOT measures pavement performance with qualitative ratings rather than with quantitative measures of distress (depth of rutting or length of cracks). Nonetheless, these sections are kept aside in case that better performance data is obtained in the future. This leaves the LTPP database as the only source of data.

However, the LTPP database created under the Strategic Highway Research Program (SHRP) contains extensive amounts of data and is consistent and reliable being the main resource used by most state agencies in their calibration efforts. There are 11 complete flexible experiments within the state of New Mexico. The code, location, functional class,

construction date, and type of each of these sections are contained in Table 4.1. As shown, six sections are new flexible pavements while the other five are rehabilitated asphalt concrete pavements. Figure 4.1 shows the location of these sections across New Mexico (*LTPP Database Reference Manual, 2006*).

4.3 Data Collection

4.3.1 Traffic Data

The traffic information necessary to run the MEPDG is obtained from the following LTPP database tables:

- TRF_BASIC: Location and number of lanes.
- TRF_MEPDG_AADTT_LTPP_LN: Annual average daily truck traffic.
- TRF_MONITOR_LTPP_LN: AADTT and vehicle class distribution.
- TRF_MEPDG_VEH_CLASS_DIST: Vehicle class distribution.
- TRF_MEPDG_MONTHLY_ADJ_FACTORS: Monthly distribution factors.
- TRF_MONITOR_AXLE_DISTRIB: Axle load spectra.
- TRF_MEPDG_AX_PER_TRUCK: Number of axles of each type per truck class.

The directional distribution, the lane distribution, and the truck growth rate are obtained from NMDOT sources. Default values are used for other traffic inputs. Table 4.2 shows the AADTT for each section, the truck growth rate at the beginning of the design life, and the percentage of class 5, 8 and 9 trucks.

4.3.2 Climatic Data

The climatic data is obtained by interpolating the MEPDG weather files at the location of each section. The ground water table depth is assumed to be 100 ft as suggested by

NMDOT. The following LTPP tables are used to collect the coordinates and elevation of each section:

- CLM_SITE_VWS_LINK: Weather stations.
- CLM_VWS_OWS_LINK: Weather stations and distance to LTPP sections.
- CLM_OWS_LOCATION: Longitude, latitude and elevation.

Table 4.3 contains the coordinates and elevation where the climatic data is interpolated and the ground water table depth.

4.3.3 Structural Data

The number of layers, and the thickness and type of each pavement layer are included in Table 4.4. This information has been collected from the following LTPP tables:

- INV_ID: Location and elevation of sections.
- INV_AGE: Date of construction.
- INV_MAJOR_IMPROV: Date, thickness and type of rehabilitation.
- INV_LAYER: Number of layers, thickness and type of each layer.

4.3.4 Materials Data

In the flexible pavement sections used in this study, there are mainly three types of materials: asphalt concrete, engineered granular soil, and natural soil. The properties of these materials are extracted from the following LTPP tables:

- INV_GRADATION: Gradation analysis of layers.
- INV_PMA_ASPHALT: Binder grade of asphalt.
- INV_PMA_ORIG_MIX: Asphalt content and air voids of mixture.
- INV_UNBOUND: Properties of unbound granular soil.

- INV_SUBGRADE: Properties of natural soil.
- TST_AG04: Gradation of AC mixture aggregates.
- TST_AC05: Asphalt content, air voids, and specific gravity of mixture.
- TST_SS04_UG08: AASHTO class of soil.
- TST_SS01_UG01_UG02: Gradation of soil.
- TST_UG04_SS03: Plasticity index (PI) and liquid limit (LL).
- TST_UG05_SS05: Moisture content and maximum dry unit weight.

Table 4.5 contains the binder grade, asphalt content, air voids percent, unit weight, and aggregate gradation of the AC mixtures used in these sections. Tables 4.6 and 4.7 shows the AASHTO class, PI, LL, sieve analysis, maximum dry unit weight, optimum gravimetric water content, and R-value of the soils used for the granular base and the subgrade respectively.

4.3.5 Performance Data

Measures of total rutting, alligator cracking, longitudinal cracking, transverse cracking and international roughness index (IRI) at the LTPP sections are obtained from the following tables:

- MON_T_PROFILE_INDEX_SECTION: Total rutting.
- MON_DIS_AC_REV: Alligator, longitudinal, and transverse cracking.
- MON_PROFILE_MASTER: IRI.

Tables 4.8, 4.9, and 4.10 contains the measurements of total rutting, alligator cracking, and longitudinal cracking respectively that were taken between 1989 and 2007 at the LTPP experiments.

4.4 Calibration-Validation Methodology

Calibration of the performance prediction models is achieved by varying the coefficients such that the residual sum of squared errors is reduced. The distress values measured in the field are compared to those predicted by the MEPDG and the residual error is calculated at five particular times per section equally distributed through the pavement design life.

The possibility of using numerical nonlinear optimization techniques was explored but its application would be too difficult since the MEPDG prediction of distress is a very complex iterative process. Therefore, the only way to proceed is to run the MEPDG multiple times for different combinations of the calibration coefficients and calculate the corresponding sum of squared errors.

The split-sample approach is used in the calibration-validation process: 9 out of 11 LTPP sections are chosen randomly for use in the calibration of each distress model while the other 2 sections are kept aside to check whether the calibrated pavement performance model can reduce the error in the MEPDG prediction of distress for cases different to those used during calibration.

4.5 Permanent Deformation Model

4.5.1 Prediction of Permanent Deformation in the MEPDG

This section describes the empirical model used in the MEPDG to predict the permanent deformation occurring in the pavement layers (*MEPDG Documentation, 2004*).

The plastic strain of the asphalt concrete layer is given by the following equations:

$$\frac{\varepsilon_p}{\varepsilon_r} = k_z \ \beta_{r1} \ 10^{k1} \ T^{k2\,\beta r2} \ N^{k3\,\beta r3} \qquad \text{Eq. 4.1}$$

$$k_z = (C_1 + C_2\, d)\ 0.328196^d \qquad \text{Eq. 4.2}$$

$$C_1 = -0.1039\, h_{AC}^2 + 2.4868\, h_{AC} - 17.342 \qquad \text{Eq. 4.3}$$

$$C_2 = 0.0172\, h_{AC}^2 - 1.7331\, h_{AC} + 27.428 \qquad \text{Eq. 4.4}$$

where ε_p = Plastic strain of the asphalt concrete layer (in/in)

ε_r = Resilient strain of the asphalt concrete layer (in/in)

T = Asphalt concrete layer temperature (°F)

N = Number of axle load repetitions

d = Depth of the point where strain is being determined (in)

h_{AC} = Thickness of the asphalt concrete layer (in)

k_1 = -3.35412, k_2 = 1.5606, k_3 = 0.4791

β_{r1}, β_{r2}, β_{r3} = calibration coefficients to be optimized

This plastic strain value multiplied by the AC thickness provides the permanent deformation occurring at the asphalt concrete layer. The permanent deformation for granular bases and the subgrade is obtained using the following formula:

$$\delta_a = \beta_{s1}\ k_1\ \varepsilon_v\ h\ \frac{\varepsilon_0}{\varepsilon_r}\ e^{-\left(\frac{\rho}{N}\right)^{\beta}} \qquad \text{Eq. 4.5}$$

where δ_a = Permanent deformation of the unbound layer (in)

N = Number of axle load repetitions

ε_v = Average vertical strain in the unbound layer (in/in)

h = Thickness of the unbound layer (in)

ε_r = Resilient strain in the unbound layer (in/in)

ε_0, β, ρ = Material properties

k_1 = 2.03 for granular base and 1.35 for subgrade

β_{s1} = Calibration coefficient to optimize for both base and subgrade

The total permanent deformation of the section is the summation of the permanent deformation occurring in every single layer:

$$PD = \sum_{i=1}^{layers} \varepsilon_p^i \; h^i$$

$$= h_{AC} \; \varepsilon_r \; k_z \; \beta_{r1} \; 10^{k1} \; T^{k2\,\beta r2} \; N^{k3\,\beta r3}$$

$$+ \beta_{GB} \; k_{GB} \; \varepsilon_v \; h_{GB} \; \frac{\varepsilon_0}{\varepsilon_r} \; e^{-\left(\frac{\rho}{N}\right)^{\beta}_{GB}} \qquad \text{Eq. 4.6}$$

$$+ \beta_{SG} \; k_{SG} \; \varepsilon_v \; h_{SG} \; \frac{\varepsilon_0}{\varepsilon_r} \; e^{-\left(\frac{\rho}{N}\right)^{\beta}_{SG}}$$

where PD = Total permanent deformation (in)

$\varepsilon_p^{\,i}$ = Total plastic strain of layer i (in/in)

h^i = Thickness of layer i (in)

In the previous equation, there are five calibration coefficients: β_{r1}, β_{r2}, and β_{r3} for the asphalt concrete layer, β_{GB} for the granular base layer, and β_{SG} for the subgrade. These coefficients cannot be calibrated separately for each layer since individual rutting data of each pavement layer is not available. Therefore, only the total permanent deformation prediction can be calibrated. Measurement of rutting at each pavement layer would require cutting trenches in the pavement sections but it would make the local calibration process much easier and more accurate.

4.5.2 Calibration of the Permanent Deformation Model

LTPP sections 2006 and 6033 are chosen randomly to be kept aside for validation while the nine remaining sections are used in the calibration process.

In the total rutting equation, β_{r2} and β_{r3} are respectively exponents to the AC temperature and the number of axle loads which are large numbers. Therefore, β_{r2} and β_{r3} are

nonlinear calibration coefficients and the two most sensitive parameters of this model. The remaining calibration coefficients β_{r1}, β_{GB}, and β_{SG} are linear calibration factors.

It is decided to optimize β_{r2} and β_{r3} in a first iterative run. This is done by varying and permuting the two nonlinear calibration coefficients while the other three, β_{r1}, β_{GB}, and β_{SG} are set to the default value 1.0. The residual sum of squared errors which is the target to reduce is calculated for every set of β_{r2} and β_{r3} values.

Table 4.11 contains the sets of calibration coefficients considered in this first step and the corresponding sum of squared errors (SSE) and mean residual error (MRE) per section. As shown, the set of calibration coefficients $\beta_{r2} = 0.9$ and $\beta_{r3} = 1.2$ reduces the SSE from 0.9107 to 0.6724. Similarly the MRE per section is reduced from 0.1060 to 0.0911.

In a second iterative run, the calibration coefficients β_{r2} and β_{r3} are fixed to 0.9 and 1.2 respectively, while the values of β_{r1}, β_{GB}, and β_{SG} are varied and permuted. Table 4.12 shows the SSE and the MRE per section for every set of coefficients. It is observed that the set $\beta_{r1} = 1.0$, $\beta_{r2} = 0.9$, $\beta_{r3} = 1.2$, $\beta_{GB} = 0.8$, and $\beta_{SG} = 0.8$ reduces the sum of squared errors to 0.6217 and the mean residual error per section to 0.0876.

A total of 476 MEPDG runs were initially made but more were performed in order to refine the calibration coefficients and reduce the SSE even more.

Figure 4.2 plots measured total rutting versus predicted total rutting with default MEPDG settings. There is significant bias. Most of the data points fall on the right side of the line of equality suggesting that MEPDG tends to under-predict rutting.

With calibration, bias is eliminated. Now the line of equality is around the middle of the scatterplot. This is evident from Figure 4.3 which plots the measured total rutting versus the corresponding prediction with calibrated MEPDG.

4.5.3 Validation of the Permanent Deformation Model

Validation of the calibrated permanent deformation model requires running the MEPDG for LTPP sections 2006 and 6033 using the new set of calibration coefficients. Then, the corresponding SSE and MRE are calculated to check whether the new model reduces the residual error for the validation sections as well.

Figures 4.4 (a) and 4.4 (b) compare the field measurements of total rutting and the uncalibrated and calibrated MEPDG predictions through the pavement design life of sections 2006 and 6033, respectively. The new model improves the MEPDG prediction for section 2006 but it does not for section 6033. The SSE of these two sections increases from 0.3291 to 0.5121. If the squared error of the validation sections is added to that of the calibration sections, the new model still reduces the SSE from 1.2398 to 1.1338. This validation is considered acceptable, but more sections are needed for a better calibration.

4.6 Alligator (Bottom-Up) Cracking Model

4.6.1 Prediction of Alligator Cracking in the MEPDG

The approach used in the MEPDG to model fatigue cracking is based on the calculation of fatigue damage at the surface for top-down (longitudinal) cracking and at the bottom of the asphaltic layer for bottom-up (alligator) cracking (*MEPDG Documentation, 2004*). The fatigue damage is estimated using the following relationship known as Miner's Law:

$$D = \sum_{i=1}^{T} \frac{n_i}{N_i} \qquad \text{Eq. 4.7}$$

where D = Fatigue damage

T = Total number of periods

n_i = Actual number of axle load repetitions applied during period i

N_i = Number of load repetitions to fatigue cracking

The following mathematical relationship is used for predicting the number of load repetitions to fatigue cracking:

$$N_f = 0.00432\ C\ \beta_{f1}\ k_1\ \left(\frac{1}{\varepsilon_t}\right)^{k_2\ \beta_{f2}}\ \left(\frac{1}{E}\right)^{k_3\ \beta_{f3}} \quad \text{Eq. 4.8}$$

$$C = 10^M \quad \text{Eq. 4.9}$$

$$M = 4.84\ \left(\frac{V_b}{V_a+V_b} - 0.69\right) \quad \text{Eq. 4.10}$$

where N_f = Number of load repetitions to fatigue cracking

ε_t = Tensile strain at the critical location (in/in)

E = Stiffness modulus of the asphalt concrete (psi)

k_1 = 0.007566, k_2 = 3.9492, k_3 = 1.281

V_b = Effective binder content (%)

V_a = Percent of air voids (%)

β_{f1}, β_{f2}, β_{f3} = Calibration coefficients to be optimized

The critical location may be at the surface for top-down cracking or at the bottom of the asphalt concrete layer for bottom-up cracking. The final transfer function provides bottom-up fatigue cracking from the fatigue damage and is expressed as:

$$FC_{bottom} = \frac{1}{60}\ \left(\frac{C_3}{1+e^{C_1\ C'_1+C_2\ C'_2\ log_{10}(100\ D)}}\right) \quad \text{Eq. 4.11}$$

$$C'_2 = -2.40874 - 39.748\ (1 + h_{AC})^{-2.856} \quad \text{Eq. 4.12}$$

$$C'_1 = -2\ C'_2 \quad \text{Eq. 4.13}$$

where FC_{bottom} = Bottom-up fatigue cracking (% of the lane area)

D = Bottom-up fatigue damage

h_{AC} = Thickness of the asphalt concrete layer

C_1, C_2, C_3 = Calibration coefficients to be optimized

4.6.2 Calibration of the Alligator Cracking Model

Sections 1002 and 1022 are randomly chosen for validation. The remaining nine sections are used in the calibration process.

The coefficients β_{f1}, β_{f2}, and β_{f3} of the fatigue damage prediction equation cannot be calibrated because there is no available data to compare with. Calibration of these factors would require performing lab testing on the asphalt concrete mixtures used in the sections to determine the number of load repetitions necessary to initiate fatigue cracking. Therefore, the calibration coefficients β_{f1}, β_{f2}, and β_{f3} are set to default value 1.0.

In the bottom-up cracking transfer function, the calibration coefficients C_1 and C_2 are varied and permuted in order to find a combination of values that will reduce the SSE. The coefficient C_3 is fixed at the default value 6000. Table 4.13 shows the sum of squared errors and the mean residual error per section for several sets of calibration coefficients. It is found that C_1 = 0.625 and C_2 = 0.25 reduces the SSE from 1383.58 to 1227.87 and the MRE per section from 4.13 to 3.89.

The calibration is refined by varying the three coefficients and performing more MEPDG runs. The combination of coefficients C_1 = 0.73, C_2 = 0.09, and C_3 = 7200 further reduces the SSE to 1133.13 and the MRE to 3.74.

The graph predicted versus measured alligator cracking before calibration is plotted in Figure 4.5. It is observed that the alligator cracking predicted by MEPDG with default settings is almost zero. The measurements vary from zero to some high values. It seems that MEPDG tends to under-predict alligator cracking as well.

Figure 4.6 compares predicted versus measured alligator cracking after performing calibration. It is shown that the calibration process brings many data points closer to the line of equality. Prediction can still be improved with additional MEPDG runs.

4.6.3 Validation of the Alligator Cracking Model

In the validation process, sections 1002 and 1022 are run in the MEPDG with the calibrated alligator cracking model. Figures 4.7 (a) and 4.7 (b) compare the uncalibrated and calibrated MEPDG predictions with the measurements taken in the field during the design life of sections 1002 and 1022, respectively. Default MEPDG does not predict any alligator cracking at all for section 1002, in consequence the new calibration coefficients improve the prediction of future distress. In the case of section 1022, it seems that the default MEPDG prediction is more accurate but probably the new model will match better the distress measured in the future. The SSE of these two sections increases from 0.61 to 46.92 with the new model. But considering the eleven sections, the new calibration coefficients reduce the SSE from 1384.19 to 1180.05.

4.7 Longitudinal (Top-Down) Cracking Model

4.7.1 Prediction of Longitudinal Cracking in the MEPDG

The approach used in the MEPDG to predict longitudinal cracking is based on the estimation of the fatigue damage that was described previously in detail (*MEPDG Documentation, 2004*). The next transfer function calculates the longitudinal fatigue cracking:

$$FC_{top} = 10.56 \left(\frac{C_3}{1+e^{C_1 - C_2 \, log_{10}(100\,D)}} \right) \qquad \text{Eq. 4.14}$$

where FC_{top} = Top-down fatigue cracking (ft/mile)

D = Top-down fatigue damage

C_1, C_2, C_3 = Calibration coefficients to be optimized

4.7.2 Calibration of the Longitudinal Cracking Model

Sections 1003 and 6035 are reserved for validation. In the calibration of the longitudinal cracking model, the numerator of the corresponding transfer function (C_3) is kept constant at the default value 1000. The calibration coefficients C_1 and C_2 are varied and the MEPDG is run for different combinations of these parameters.

Table 4.14 shows the SSE and the MRE per section for different values of the C_1 and C_2 coefficients. The calibration coefficients C_1 = 5 and C_2 = 2.25 reduce the SSE from 34,814,457.96 to 33,612,603.89 and the MRE from 655.60 to 644.18. The improvement is not significant, and therefore, more MEPDG runs are performed varying the three coefficients. Finally, the set C_1 = 5.5, C_2 = 2.56, and C_3 = 1000 reduces the SSE to 26,601,745.13 and the MRE to 573.08.

Figures 4.8 and 4.9 illustrate the predicted versus measured longitudinal cracking values before and after calibration, respectively. Even though the top-down cracking data is too scattered, calibration still brings some data points closer to the line of equality, and thus, bias is reduced.

4.7.3 Validation of the Longitudinal Cracking Model

Sections 1003 and 6035 are run with the calibrated longitudinal cracking model for validation. Figures 4.10 (a) and 4.10 (b) compare the uncalibrated and calibrated MEPDG predictions with the values measured in the field for sections 1003 and 6035, respectively. The new calibration factors improve the longitudinal cracking prediction of both sections. The SSE is reduced from 27,816,784.48 to 17,759,263.90 for the validation

sections and from 62,631,242.44 to 44,361,009.03 for the eleven LTPP sections. This validation is considered successful.

Table 4.1 LTPP flexible pavement sections in New Mexico

State Code	SHRP Id	Road	Milepoint	Functional Class	Type of Experiment	Construction Date *
35	1002	US-70	310.1	2	GPS-6A	May, 1985
35	1003	US-70	320.9	2	GPS-1	May, 1983
35	1005	I-25	263.8	1	GPS-1	Sep, 1983
35	1022	US-550	125.1	2	GPS-1	Sep, 1986
35	1112	US-62	81.3	2	GPS-1	May, 1984
35	2006	US-550	89.5	2	GPS-2	Jun, 1982
35	2007	US-550	106.2	2	GPS-6A	Jun, 1981
35	2118	I-40	346.2	1	GPS-2	Dec, 1979
35	6033	I-25	159.3	1	GPS-6A	May, 1981
35	6035	I-40	96.7	1	GPS-6A	May, 1985
35	6401	I-40	107.7	1	GPS-6A	May, 1984

GPS-1: Asphalt Concrete on Unbound Granular Base
GPS-2: Asphalt Concrete on Bound Granular Base
GPS-6A: Existing AC Overlay on AC Pavement
* This is the date of last major improvement in the case of rehabilitated sections.

Figure 4.1 LTPP sections in New Mexico

Table 4.2 AADTT, truck growth, and classes 5, 8 and 9 at LTPP sections

SHRP Id	Traffic Open Date	Initial two-way AADTT	Growth Rate (%) *	Class 5 (%)	Class 8 (%)	Class 9 (%)
351002	Jun, 1985	736	0.1	14.5	13.1	67.7
351003	Jun, 1983	735	0.1	14.5	13.1	67.7
351005	Oct, 1983	2971	0.3	23.4	17.0	47.9
351022	Oct, 1986	911	1.0	30.4	13.5	42.6
351112	Jun, 1984	559	3.2	32.9	9.9	44.5
352006	Jul, 1982	844	0.4	23.5	17.7	42.8
352007	Jul, 1981	563	2.8	36.8	10.0	39.6
352118	Jan, 1980	831	7.3	4.8	5.6	79.2
356033	Jun, 1981	1885	0.5	39.9	17.9	32.6
356035	Jun, 1985	540	10.4	16.4	7.1	71.6
356401	Jun, 1984	1760	4.7	9.2	5.4	75.9

* The truck growth rate is assumed to be compound.

Table 4.3 Coordinates, elevation, and ground water table depth of LTPP sections

SHRP Id	Latitude (dd.mm)	Longitude (dd.mm)	Elevation (ft)	GWT Depth (ft)
351002	33.22	-104.55	3800	100
351003	33.23	-104.44	3800	100
351005	35.31	-106.14	5523	100
351022	36.22	-107.50	6727	100
351112	32.38	-103.31	3760	100
352006	36.11	-107.20	6742	100
352007	36.15	-107.36	7021	100
352118	35.10	-103.29	3927	100
356033	34.12	-106.55	4662	100
356035	35.50	-107.39	6200	100
356401	35.20	-107.29	5893	100

Table 4.4 Layer system of LTPP sections

SHRP Id	Type and Thickness of Layers
351002	AC Overlay (3.9 in); AC Existing (5.2 in); GB (5 in); SG (semi-infinite)
351003	AC (7.6 in); GB (5 in); SG (semi-infinite)
351005	AC (9.1 in); GB (7 in); SG (semi-infinite)
351022	AC (6.6 in); GB (10 in); SG (semi-infinite)
351112	AC (5.6 in); GB (4 in); SG (semi-infinite)
352006	AC (6.1 in); GB (11.5 in); SG (semi-infinite)
352007	AC Overlay (2.1 in); AC Existing (7.1 in); GB (6 in); SG (semi-infinite)
352118	AC (11.1 in); GB (18 in); SG (semi-infinite)
356033	AC Overlay (3.1 in); AC Existing (4.8 in); GB (4 in); GB (8 in); SG (semi-infinite)
356035	AC Overlay (3.1 in); AC Existing (5.1 in); GB (16 in); SG (semi-infinite)
356401	AC Overlay (3.7 in); AC Existing (3.5 in); GB (12 in); SG (semi-infinite)

AC: Asphalt Concrete, GB: Granular Base, SG: Subgrade

Table 4.5 Asphalt concrete properties of LTPP sections

SHRP Id	Binder Viscosity Grade	Effective Binder Content (%)	Air Voids (%)	Total Unit Weight (pcf)
351002	Pen 85-100	5.5	4.1	143.65
351003	Pen 85-100	5.9	4.8	143.8
351005	Pen 85-100	5.3	3.9	146
351022	Pen 85-100	5.9	3.7	147
351112	Pen 85-100	5.05	4.4	151.63
352006	AC 10	5.5	5.8	142.7
352007	Pen 85-100	6.1	4.6	145.95
352118	Pen 120-150	4.8	4.4	147.8
356033	Pen 85-100	6.1	3.2	143.8
356035	Pen 85-100	5.5	8.1	149
356401	Pen 85-100	5.4	4	153
SHRP Id	Cum. Retained 3/4 in (%)	Cum. Retained 3/8 in (%)	Cum. Retained #4 (%)	Passing #200 (%)
351002	0	20	43	5.8
351003	0	23	39.5	10.2
351005	0	27	48	6
351022	0	26	44	6
351112	0	20	36.5	7.75
352006	3.5	41	56	7.85
352007	0	30.5	44	5
352118	6	35.5	51	5
356033	0	21.7	43.3	6
356035	0	30	50	3
356401	1	20	42	8.5

Table 4.6 Granular base properties of LTPP sections

SHRP Id	AASHTO Class	PI	LL	Passing #4 (%)	Passing #40 (%)	Passing #200 (%)	γ_{dry} (pcf)	w_{opt} (%)	R-value*
351002	A-1-a	0.5	12	42	23.5	12.3	131.0	8.5	-
351003	A-2-4	10.5	28.5	41	18.5	12.3	139.5	6	-
351005	A-1-a	0	6	49.5	21	6.1	135	7.4	61
351022	A-1-b	0	6	59.5	35	9.3	138	6	-
351112	Gravel	5.5	23.5	70	48.5	16.8	121	10	61
352006	A-2-4	0	14	99	88.5	14.4	122.5	10.5	54
352007	A-3	1.5	22	99	77.5	28.4	122	10	-
352118	A-1-a	0	6	42.5	21.5	6.9	138.5	5.5	-
356033	A-1-b	1	11	59	23	8	119	11.5	77
356033	A-1-a	1	21	62.5	24.5	11.2	131.5	7.5	75
356035	Gravel	0	6	59.5	23.5	8	133	8	-
356401	A-1-b	6.5	23.5	47.5	20.5	12.8	142	5	-

The layer modulus is estimated from ICM inputs (Level 3).
* The layer modulus is estimated from the R-value (Level 2).

Table 4.7 Subgrade properties of LTPP sections

SHRP Id	AASHTO Class	PI	LL	Passing #4 (%)	Passing #40 (%)	Passing #200 (%)	γ_{dry} (pcf)	w_{opt} (%)	R-value*
351002	A-1-b	2.5	23	52.5	32	21.4	120.5	11.5	48
351003	A-2-4	6	23.5	52.5	34.5	27.6	130	9.5	-
351005	A-2-4	3	22.5	95.5	73.5	28.7	118	14	30
351022	A-2-4	2	19.5	97.5	73.5	8.4	122	11.5	49
351112	A-2-4	0	0	99.5	84	13.7	106	12.5	59
352006	A-2-4	0	14	100	82.5	25.6	122.5	10	53
352007	A-4	5	21	93	83	37	123	9.3	52
352118	A-2-4	2	14	93.5	85.5	21.4	114.5	12.5	51
356033	A-2-4	2.5	22	79	60.5	41	126	9.5	71
356035	A-4	3.5	23	91	78	43.7	121	11.5	24
356401	A-2-4	2	14	98.5	96	23.1	120	11.5	37

The layer modulus is estimated from ICM inputs (Level 3).

* The layer modulus is estimated from the R-value (Level 2).

Table 4.8 Total rutting (in) measured in LTPP sections

Yr	SHRP Id										
	1002	1003	1005	1022	1112	2006	2007	2118	6033	6035	6401
89	0.1969	0.1969	0.6299	0.1969	0.1969	0.4724	0.2362		0.2362	0.4724	0.2756
90								0.1969	0.2756	0.3543	0.3150
91	0.1575	0.1969	0.6693	0.1575	0.1969	0.6299	0.1969	0.1575	0.2362	0.3543	0.3543
92			0.5512	0.1969		0.4724			0.2362	0.3937	0.3937
93	0.1969	0.1181			0.1575			0.1575			
94											
95	0.3937	0.1969	0.6693	0.2756	0.2165		0.1969	0.2362	0.2756	0.4331	0.4331
96											
97	0.3543	0.1575	0.6693	0.2362	0.1969		0.1575	0.2756	0.5118	0.4331	0.4724
98											
99	0.3543	0.1969	0.7283	0.1969	0.1969		0.1575	0.3150	0.4724		0.4724
00					0.1969			0.3543			
01	0.3543		0.8268		0.2362				0.0394		
02	0.2756		0.7480		0.1772			0.2756			
03			0.8268		0.1969						
04					0.1969				0.1969		
05			0.8268								
06											
07								0.3543	0.2362		

Table 4.9 Alligator cracking (%) measured in LTPP sections

Yr	SHRP Id										
	1002	1003	1005	1022	1112	2006	2007	2118	6033	6035	6401
1991	0.00	0.00	0.00	0.00	0.00	0.00		0.00	0.00		3.17
1992											
1993											
1994	0.00	0.00	0.00	0.00	0.00		0.00	0.00	13.00	9.95	1.26
1995		1.77			0.00						
1996					0.00						
1997	0.00	0.02	0.00	0.00	0.00		0.00	0.12	13.00	7.07	4.24
1998											
1999	0.05	0.00	0.00	0.00	0.00		0.61	0.27	13.00		6.51
2000					0.00						
2001								3.97	12.63		
2002	0.75		0.00		0.00			0.00	25.70		
2003					0.00						
2004					0.00				0.00		
2005			0.00								
2006											
2007								0.00	0.00		

Table 4.10 Longitudinal cracking (ft/mi) measured in LTPP sections

Yr	SHRP Id										
	1002	1003	1005	1022	1112	2006	2007	2118	6033	6035	6401
1989											
1990											
1991	0.00	706.77	0.00	0.00	0.00	0.00		0.00	5442.83		1773.86
1992											
1993											
1994	0.00	491.97	0.00	0.00	0.00		398.43	0.00	381.10	1087.87	5855.12
1995		225.20			0.00						
1996					0.00						
1997	48.50	460.79	0.00	0.00	0.00		845.35	76.22	401.89	543.94	2885.98
1998											
1999	0.00	363.78	0.00	0.00	0.00		696.38	69.29	381.10		1739.21
2000					0.00						
2001								0.00	381.10		
2002	69.29		0.00		0.00			0.00			
2003					0.00						
2004					0.00				0.00		
2005			0.00								
2006											
2007								0.00	0.00		

Table 4.11 SSE and MRE of the rutting model for different β_{r2} and β_{r3}

Set #	β_{r2}	β_{r3}	SSE	MRE
1	0.8	0.8	2.0613	0.1595
2	0.8	0.9	1.9586	0.1555
3	0.8	1	1.7671	0.1477
4	0.8	1.1	1.4305	0.1329
5	0.8	1.2	0.9309	0.1072
6	0.9	0.8	1.9448	0.1550
7	0.9	0.9	1.7495	0.1470
8	0.9	1	1.4121	0.1320
9	0.9	1.1	0.9248	0.1069
10	**0.9**	**1.2**	**0.6724**	**0.0911**
11	1	0.8	1.7237	0.1459
12	1	0.9	1.3834	0.1307
13	**1**	**1**	**0.9107**	**0.1060**
14	1	1.1	0.7289	0.0949
15	1	1.2	3.3398	0.2031
16	1.1	0.8	1.3433	0.1288
17	1.1	0.9	0.8906	0.4719
18	1.1	1	0.8148	0.1003
19	1.1	1.1	3.7853	0.2162
20	1.1	1.2	21.9508	0.5206
21	1.2	0.8	0.8685	0.1035
22	1.2	0.9	0.9518	0.1084
23	1.2	1	4.4849	0.2353
24	1.2	1.1	24.3645	0.5484
25	1.2	1.2	110.2678	1.1668

Table 4.12 SSE and MRE of the rutting model for different β_{r1}, β_{GB}, and β_{SG}

Set #	β_{r1}	β_{r2}	β_{r3}	β_{GB}	β_{SG}	SSE	MRE
1	0.8	0.9	1.2	0.8	0.8	0.7150	0.0940
2	0.8	0.9	1.2	0.8	1	0.6510	0.0896
3	0.8	0.9	1.2	0.8	1.2	0.6335	0.0884
4	0.8	0.9	1.2	1	0.8	0.6944	0.0926
5	0.8	0.9	1.2	1	1	0.6500	0.0896
6	0.8	0.9	1.2	1	1.2	0.6524	0.0897
7	0.8	0.9	1.2	1.2	0.8	0.6823	0.0918
8	0.8	0.9	1.2	1.2	1	0.6596	0.0902
9	0.8	0.9	1.2	1.2	1.2	0.6818	0.0917
10	**1**	**0.9**	**1.2**	**0.8**	**0.8**	**0.6217**	**0.0876**
11	1	0.9	1.2	0.8	1	0.6391	0.0888
12	1	0.9	1.2	0.8	1.2	0.7033	0.0932
13	1	0.9	1.2	1	0.8	0.6352	0.0886
14	1	0.9	1.2	1	1	0.6724	0.0911
15	1	0.9	1.2	1	1.2	0.7564	0.0966
16	1	0.9	1.2	1.2	0.8	0.6592	0.0902
17	1	0.9	1.2	1.2	1	0.7163	0.4232
18	1	0.9	1.2	1.2	1.2	0.8202	0.1006
19	1.2	0.9	1.2	0.8	0.8	0.6899	0.0923
20	1.2	0.9	1.2	0.8	1	0.7890	0.0987
21	1.2	0.9	1.2	0.8	1.2	0.9350	0.1074
22	1.2	0.9	1.2	1	0.8	0.7376	0.0954
23	1.2	0.9	1.2	1	1	0.8566	0.1028
24	1.2	0.9	1.2	1	1.2	1.0225	0.1124
25	1.2	0.9	1.2	1.2	0.8	0.7961	0.0991
26	1.2	0.9	1.2	1.2	1	0.9348	0.1074
27	1.2	0.9	1.2	1.2	1.2	1.1203	0.1176

Table 4.13 SSE and MRE of the alligator cracking model for different C_1 and C_2

Set #	C_1	C_2	C_3	SSE	MRE
1	0.25	0.25	6000	8355.94	10.16
2	0.25	0.625	6000	7447.21	9.59
3	0.25	1	6000	8579.38	10.29
4	0.25	1.5	6000	11181.53	11.75
5	0.25	2	6000	14527.67	13.39
6	**0.625**	**0.25**	**6000**	**1227.87**	**3.89**
7	0.625	0.625	6000	1400.68	4.16
8	0.625	1	6000	1547.42	4.37
9	0.625	1.5	6000	1833.23	4.76
10	0.625	2	6000	2383.02	5.42
11	1	0.25	6000	1335.85	4.06
12	1	0.625	6000	1370.69	4.11
13	**1**	**1**	**6000**	**1383.58**	**4.13**
14	1	1.5	6000	1395.21	4.15
15	1	2	6000	1414.60	4.18
16	1.5	0.25	6000	1401.18	4.16
17	1.5	0.625	6000	1403.89	4.16
18	1.5	1	6000	1405.28	4.17
19	1.5	1.5	6000	1405.64	4.17
20	1.5	2	6000	1405.69	4.17
21	2	0.25	6000	1407.68	4.17
22	2	0.625	6000	1407.68	4.17
23	2	1	6000	1407.68	4.17
24	2	1.5	6000	1407.68	4.17
25	2	2	6000	1407.68	4.17

Table 4.14 SSE and MRE of the longitudinal cracking model for different C_1 and C_2

Set #	C_1	C_2	C_3	SSE	MRE
1	1	0.3	1000	277,227,886.44	1850.02
2	1	1	1000	491,663,106.44	2463.72
3	1	2.25	1000	1,003,746,096.80	3520.22
4	1	3.5	1000	1,319,859,564.48	4036.65
5	1	5	1000	1,548,756,568.03	4372.69
6	3	0.3	1000	40,133,542.18	703.90
7	3	1	1000	40,118,158.96	703.77
8	3	2.25	1000	222,374,099.13	1656.91
9	3	3.5	1000	640,972,187.17	2813.05
10	3	5	1000	953,108,144.95	3430.27
11	5	0.3	1000	47,770,755.93	767.96
12	5	1	1000	43,879,446.01	736.02
13	**5**	**2.25**	**1000**	**33,612,603.89**	**644.18**
14	5	3.5	1000	164,075,443.56	1423.24
15	5	5	1000	585,830,659.05	2689.33
16	7	0.3	1000	50,320,260.83	788.19
17	7	1	1000	49,690,503.44	783.24
18	7	2.25	1000	45,177,197.42	746.82
19	**7**	**3.5**	**1000**	**34,814,457.96**	**655.60**
20	7	5	1000	189,775,193.08	1530.65
21	10	0.3	1000	50,734,102.16	791.42
22	10	1	1000	50,702,029.07	791.17
23	10	2.25	1000	50,445,318.17	789.17
24	10	3.5	1000	48,883,159.46	776.85
25	10	5	1000	39,310,112.68	696.64

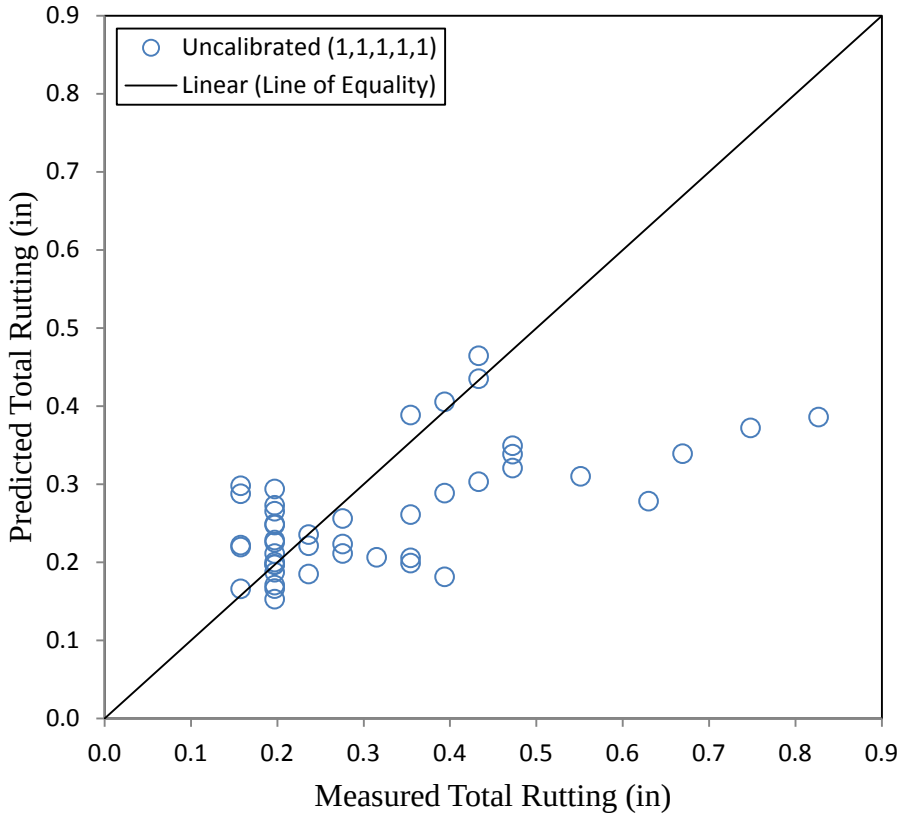

Figure 4.2 Predicted versus measured total rutting before calibration

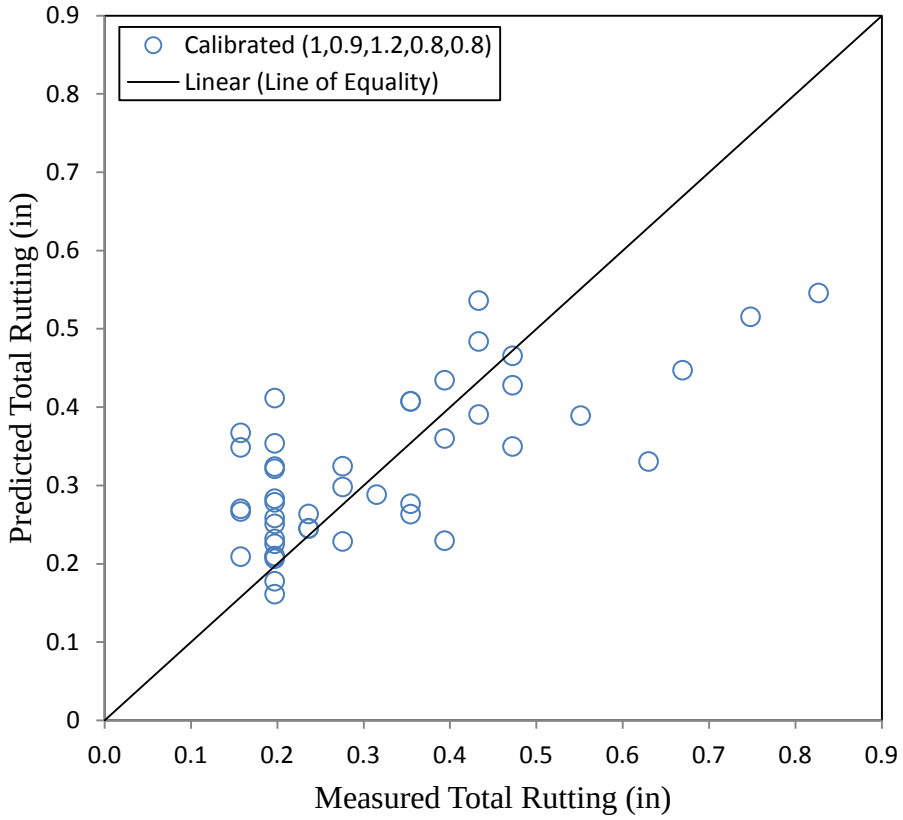

Figure 4.3 Predicted versus measured total rutting after calibration

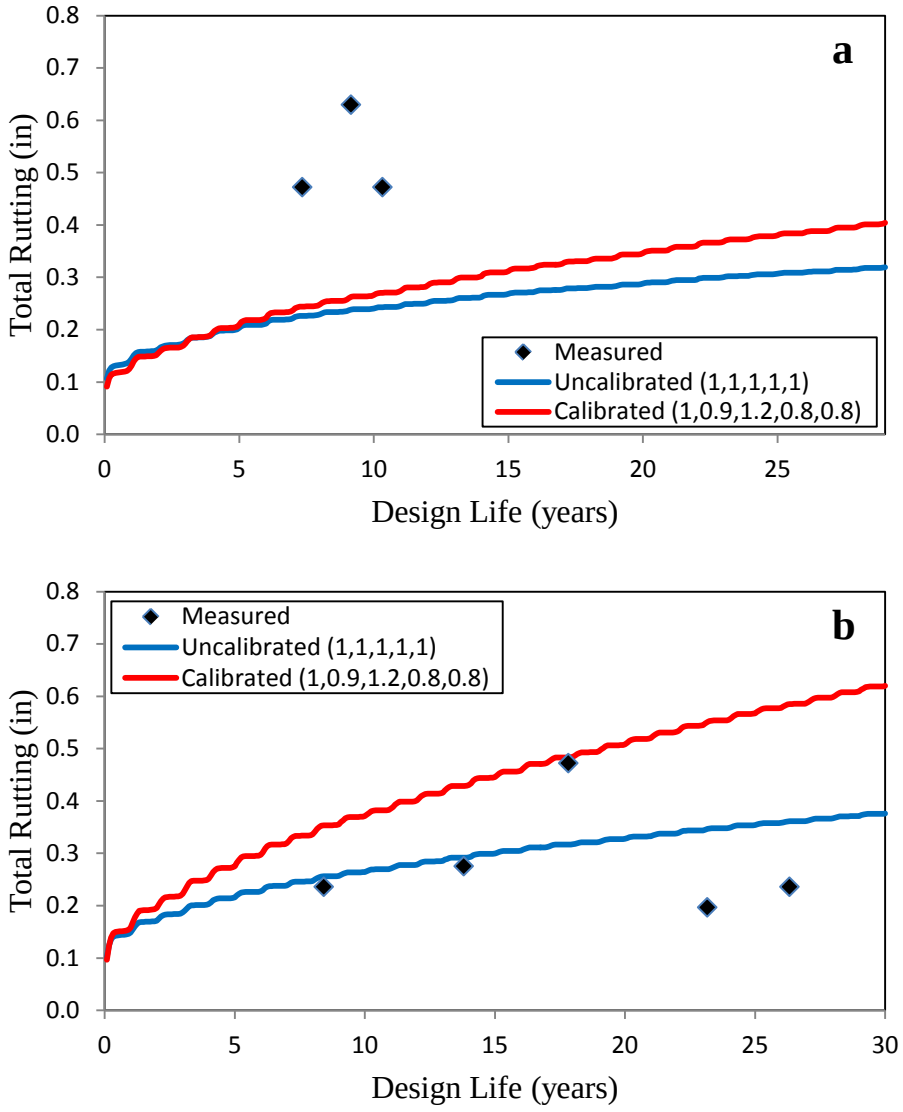

Figure 4.4 Validation of the calibrated permanent deformation model: a) LTPP section 2006, b) LTPP section 6033

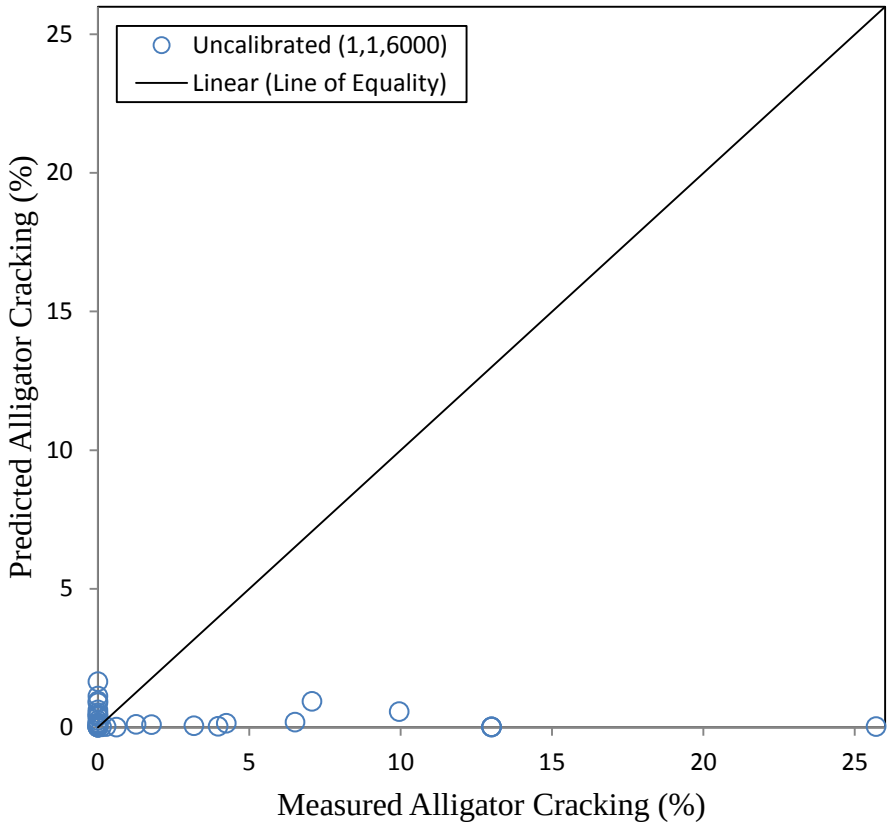

Figure 4.5 Predicted versus measured alligator cracking before calibration

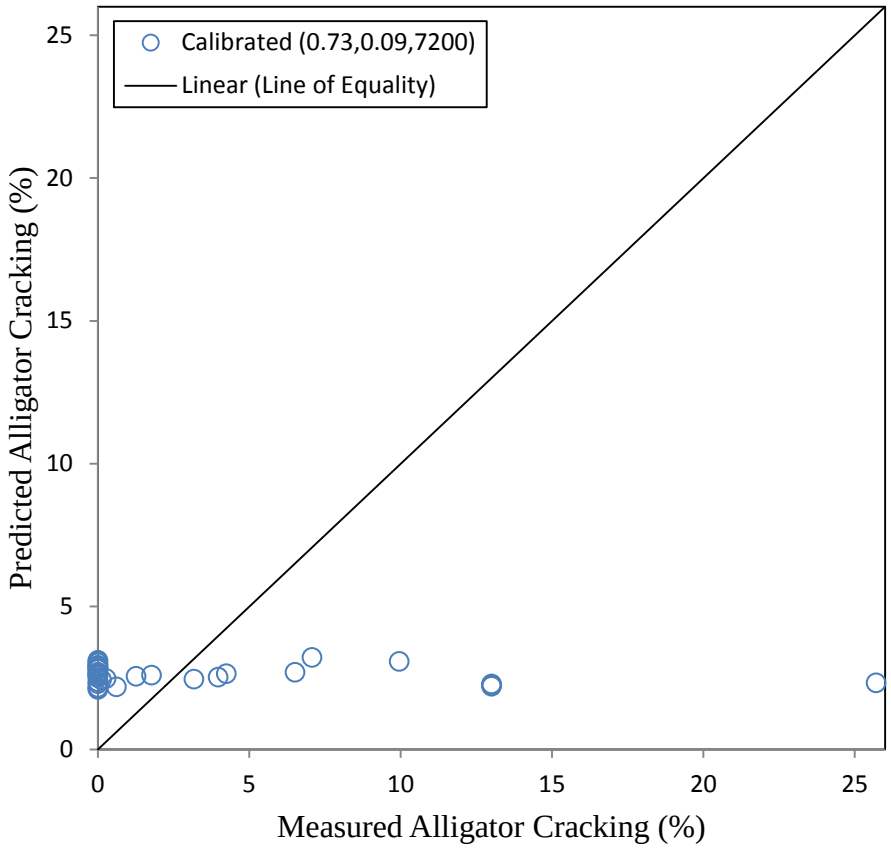

Figure 4.6 Predicted versus measured alligator cracking after calibration

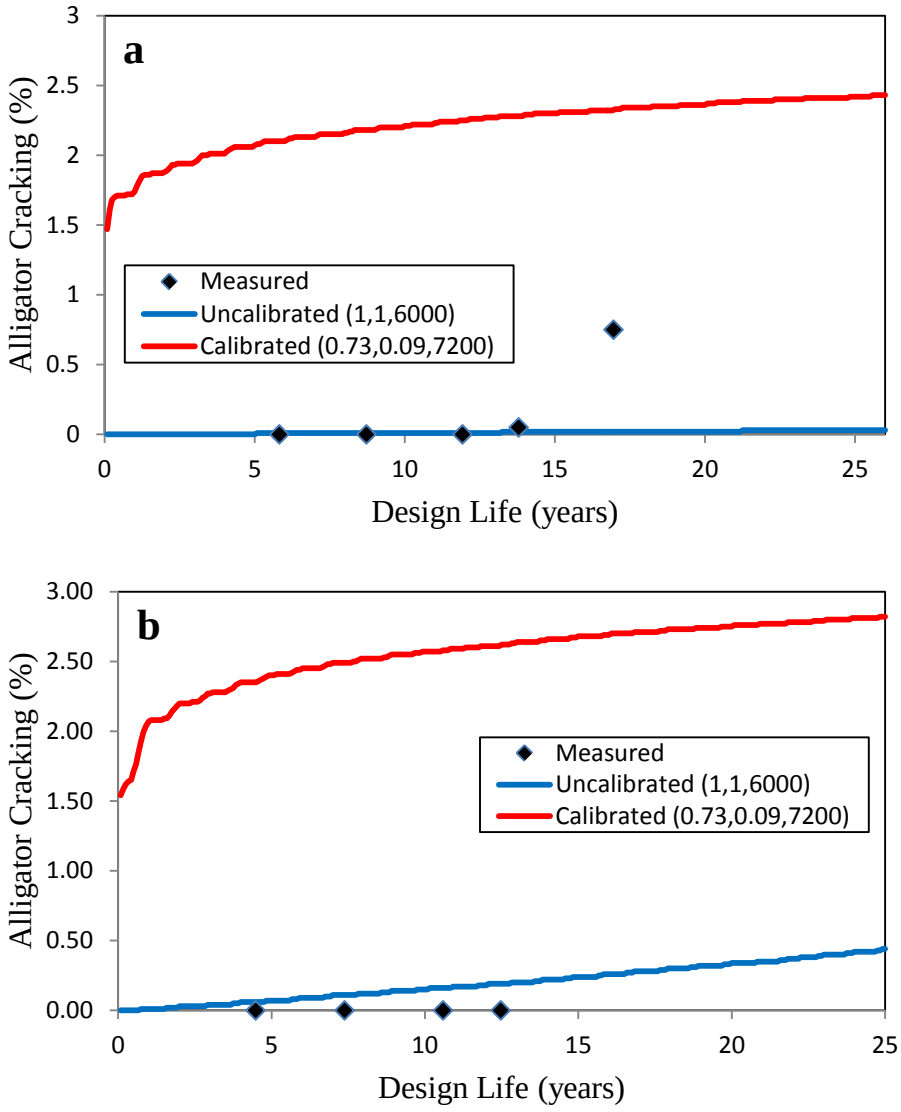

Figure 4.7 Validation of the calibrated alligator cracking model: a) LTPP section 1002, b) LTPP section 1022

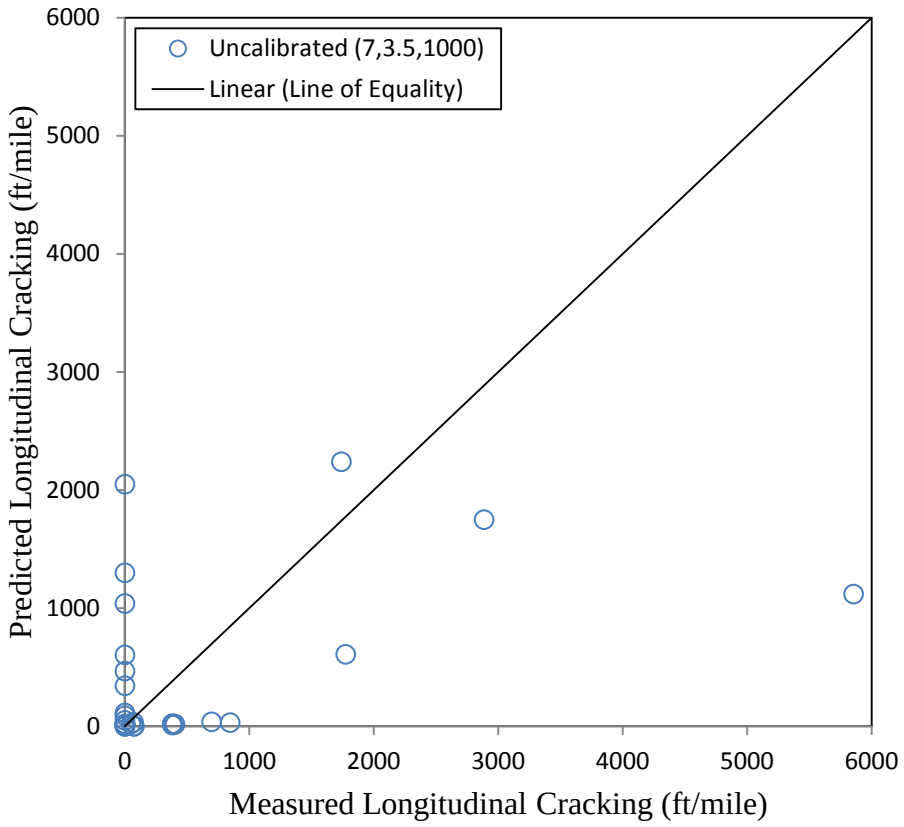

Figure 4.8 Predicted versus measured longitudinal cracking before calibration

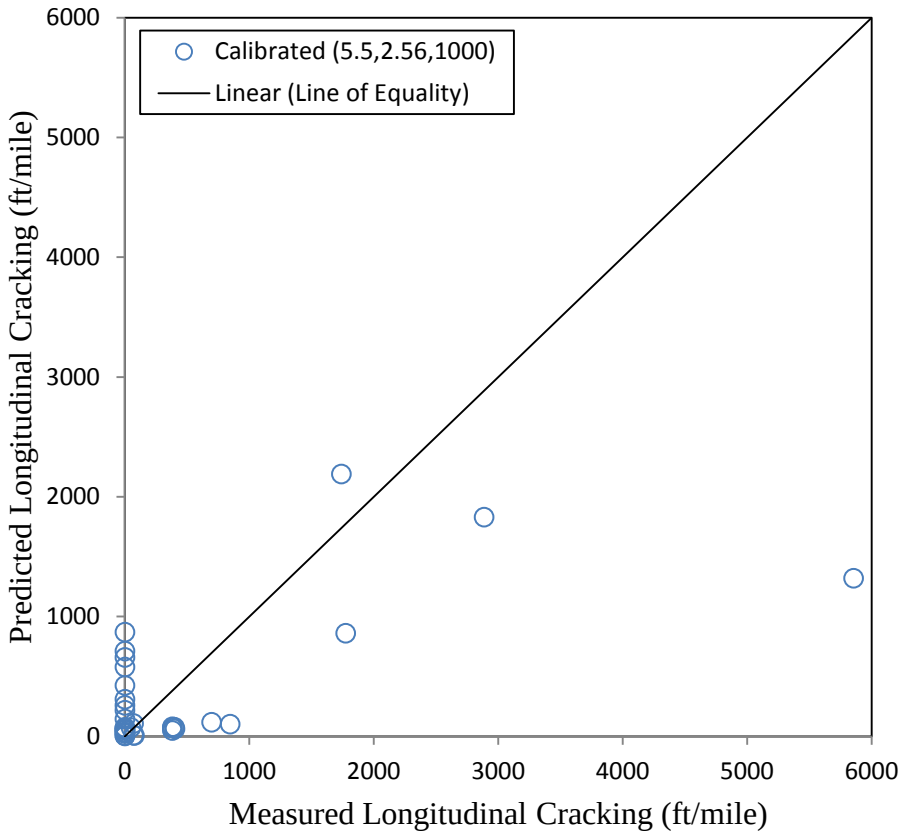

Figure 4.9 Predicted versus measured longitudinal cracking after calibration

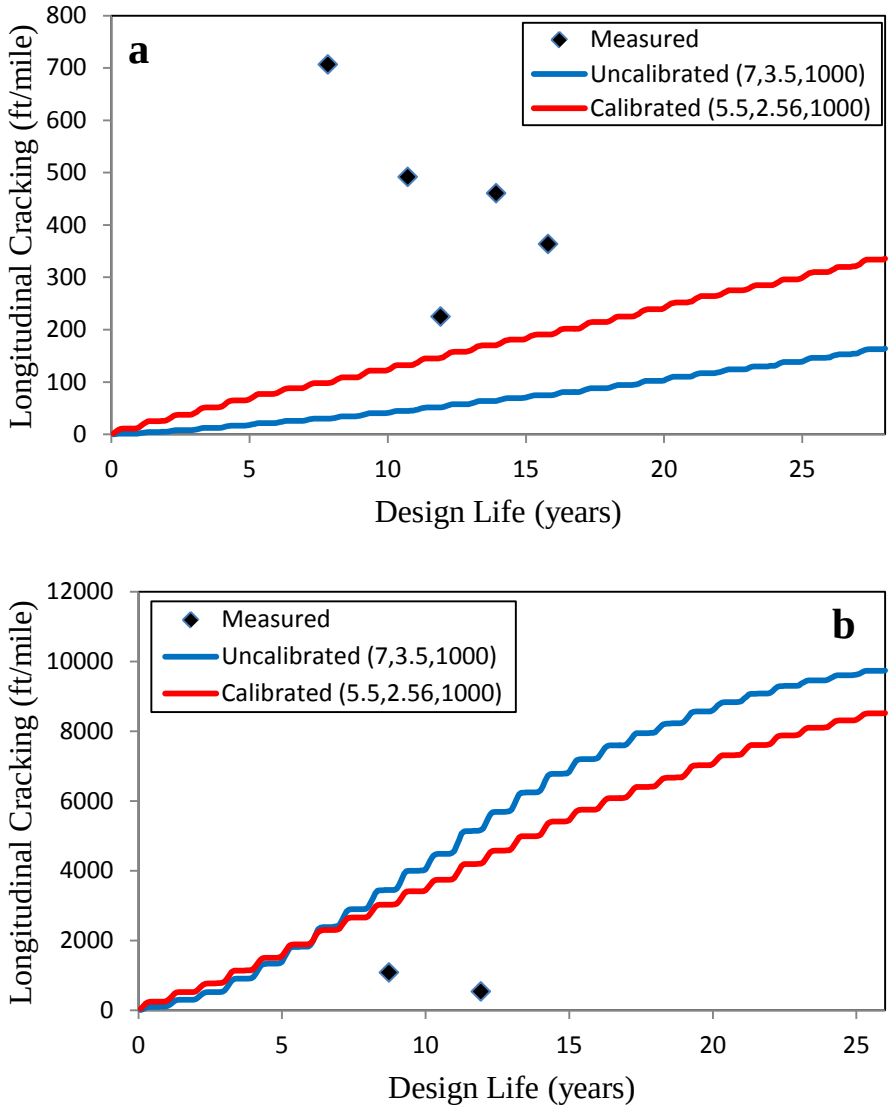

Figure 4.10 Validation of the calibrated longitudinal cracking model: a) LTPP section 1003, b) LTPP section 6035

Chapter 5

CONCLUSIONS AND RECOMMENDATIONS

5.1 General

In the first stage of this study, a procedure based on the 2001 Traffic Monitoring Guide is developed to check the quality of the WIM data collected in New Mexico. Results show that only 3 out of 15 WIM sites have collected reliable data. Axle load spectra and other MEPDG traffic inputs are developed using a set of subroutines that support the implementation of MEPDG in New Mexico. The influence of axle load spectra on MEPDG distress prediction is analyzed for the three WIM sections providing good data. The MEPDG traffic inputs obtained are used for the local calibration of the MEPDG under New Mexico conditions. Detailed data of traffic, climate, and materials are collected for 29 pavement sections in New Mexico, but their respective distress data are qualitative ratings that cannot be used for calibration. Therefore, only 11 sections from the LTPP database located in New Mexico can be used in this study. The calibration coefficients of the rutting, alligator cracking, and longitudinal cracking models are optimized by reducing the residual sum of squared errors. These calibration factors reduce the difference between MEPDG predictions and field measurements, and thus, they are recommended for flexible pavement design in New Mexico.

5.2 Conclusions

From the traffic loading characterization, the following conclusions can be made:

- The criteria based on gross vehicle weight and steering axle weight frequency distributions allow successfully evaluating the quality of WIM data. In New

Mexico, piezoelectric systems are not collecting reliable data, and therefore, calibration of these WIM sites is required. Bending plate systems are providing high-quality WIM data.

- Several subroutines have been created in Visual Basic Application for Microsoft Excel to process WIM data and develop successfully the traffic inputs required by the Mechanistic-Empirical Pavement Design Guide (MEPDG).
- It is recommended using these sets of subroutines for checking the quality of WIM data and developing the traffic inputs required in the MEPDG.
- Positive and negative bias of the weight measured at WIM sites can be simulated respectively by increasing and decreasing by a percentage the weight data collected. Positive bias results in a displacement of the axle load spectra to the right, while negative bias moves the axle load spectra to the left.
- The influence of weight measurement bias on predicted pavement performance can be analyzed using the axle load spectra for the cases of no bias, positive bias, and negative bias in the MEPDG in order to predict the corresponding distresses.
- The effect of weight measurement bias on predicted rutting is considerable but not critical. However, bias of weight data affects dramatically predicted longitudinal and alligator cracking (1% of bias can result in an increase of 9% in longitudinal cracking and 6% in alligator cracking). The influence of weight measurement bias on transverse cracking and IRI can be neglected.
- It is determinant to collect accurate and reliable WIM data since error in its measurement can lead to overestimate or underestimate the pavement thickness, and thus, to unnecessary costs of construction or maintenance.

The next conclusions are related to the local calibration of the MEPDG for flexible pavements in New Mexico:

- The qualitative distress ratings collected by the New Mexico Department of Transportation (NMDOT) are not useful for local calibration of the MEPDG because this data is not consistent and reliable. Therefore, there are only 11 LTPP sections that can be used in the calibration process.
- Initial verification runs suggest that there is significant bias in the permanent deformation prediction of default MEPDG. Only total rutting can be calibrated since there is no rut depth data for individual layers. Local calibration of the rutting calibration coefficients β_{r1}, β_{r2}, β_{r3}, β_{GB}, and β_{SG} is successfully achieved. The standard error of the estimate is low and bias is eliminated.
- The plot showing measured versus predicted alligator cracking before calibration indicates that the default MEPDG prediction does not match the observed values particularly well. Many field measurements have a value of zero which makes the local calibration process of this particular distress more difficult. Nonetheless, the alligator cracking calibration coefficients C_1, C_2, and C_3 are optimized such that the sum of squared errors is reduced and thus many data points are brought closer to the line of equality.
- The longitudinal cracking model is even more challenging because many data points fall very close to the origin (the values are almost zero). Calibration of the longitudinal cracking coefficients C_1, C_2, and C_3 does not produce as good results as those obtained for rutting and alligator cracking. However, the positive effect

of calibration is noticed with some points moving closer to the line of equality and the sum of squared errors being reduced.

5.3 Recommendations

For improving the characterization of traffic loading in mechanistic-empirical pavement design, the following recommendations are provided:

1) It is strongly encouraged to calibrate WIM sites at least twice a year in order to collect reliable weight data.

For most efficient and successful calibration of the MEPDG in New Mexico, the following recommendations should be implemented:

1) Local calibration requires a few more data sets in addition to LTPP sections. The NMDOT should establish at least 30 pavement sections for local calibration of the MEPDG. These sections should be new flexible pavements constructed with practices, techniques and materials currently used in the state. The new pavement sections should be located in segments near to WIM sites so the traffic loading can be accurately characterized. The 30 pavement sections should be distributed among different climatic regions (from cold to warm weather) and different functional class roads (from low to high traffic).
2) Measurements of distress data (rutting, alligator cracking, longitudinal cracking, thermal cracking, and IRI) must be collected every year at every section during its pavement design life following the Distress Identification Manual for the Long Term Pavement Performance Program. Eventually, these pavement sections will become damaged and rehabilitation will be carried out though an AC overlay.

Then, the monitoring effort should continue and local calibration of the MEPDG for rehabilitated pavements should be performed in the same manner.

3) Permanent deformation should be measured at every layer of the pavement section by performing trenches and/or cores. This will allow a much more precise and consistent calibration of the rutting model.
4) Creep compliance and thermal contraction coefficients of the asphalt concrete mixtures should be determined in the lab for the pavement sections. This will make local calibration of the thermal cracking model possible.

REFERENCES

MEPDG Documentation (2004). "Guide for Mechanistic-Empirical Design of New and Rehabilitated Pavement Structures". *National Cooperative Highway Research Program, Transportation Research Board, National Research Council*, Washington, D.C.

FHWA (2001). "Traffic Monitoring Guide". *U.S. Department of Transportation, Federal Highway Administration, Office of Highway Policy Information,* Washington, D.C.

Quinley, R. (2009). "WIM Data Analyst's Manual". *U.S. Department of Transporation, Report No. FHWA-IF-09-038, Federal Highway Administration,* Washington, D.C.

AASHTO (2001). "Guide for Vehicle Weights and Dimensions". *American Association of State Highway and Transportation Officials,* ISBN: 1560512962, Washington, D.C.

Cambridge Systematics Inc., Washington State Transportation Center, and Chaparral Systems (2004). "TrafLoad User's Manual". *National Cooperative Highway Research Program, Project 1-39,* Washington, D.C.

University of Arkansas (2009). "User's Guide of PrepME Database Software". *Arkansas State Highway and Transportation Department, Final Report, Project: TRC-0702,* Little Rock, Arkansas.

Flinner, M., and Horsey, H. (1995). "Traffic Data Editing Procedures: Traffic Data Quality (TDQ)". *Final Report, Transportation Pooled-Fund Study SPR-2 (182), Federal Highway Administration,* Washington, D.C.

AASHTO (2010). "Guide for the Local Calibration of the Mechanistic-Empirical Pavement Design Guide". *American Association of State Highway and Transportation Officials,* ISBN: 9781560514497, Washington, D.C.

AASHTO (1993). "Guide for Design of Pavement Structures". *American Association of State Highway and Transportation Officials,* ISBN: 978-1560510550, Washington, D.C.

Elkins, G., Schmalzer, P., Thomson, T., and Simpson, A. (2006). "Long-Term Pavement Performance Information Management System: Pavement Performance Database User Reference Guide". *U.S. Department of Transportation, Report No. FHWA-RD-03-088, Federal Highway Administration,* Washington, D.C.

Huang, Y. H. (2004). "Pavement Analysis and Design". *Pearson Prentice Hall, Pearson Eduaction Inc.,* Second Edition, ISBN: 0131424734, Upper Saddle River, NJ.

Brown, E. R., Kandhal, P. S., Roberts, F. L., Kim, Y. R., Lee, D. Y., and Kennedy, T. W. (2009). "Hot Mix Asphalt Materials, Mixture Design, and Construction". *National Asphalt Pavement Association Research and Education Foundation,* Third Edition, ISBN: 0914313021, Lanham, MD.

Haas, R., Hudson, W. R., and Zaniewski, J. (1994). "Modern Pavement Management". *Krieger Publishing Company,* ISBN: 0894645889, Malabar, FL.

Yoder, E. J., and Witczak, M. W. (1975). "Principles of Pavement Design". *John Wiley & Sons, Inc.,* Second Edition, ISBN: 0471977802, New York, NY.

Ramachandran, A. N., Taylor, K. L., Stone, J. R., and Sajjadi, S. S. (2011). "NCDOT Quality Control Methods for Weigh in Motion Data". *Public Works Management Policy 2011, Volume No. 16,* DOI: 10.1177/1087724X10383583, pp. 3-19, SAGE Publications.

Tran, N. H., and Hall, K. D. (2007a). “Development and Significance of Statewide Volume Adjustment Factors in Mechanistic-Empirical Pavement Design Guide”. *Transportation Research Record: Journal of the Transportation Research Board, No. 2037, Rigid and Flexible Pavement Design 2007,* ISBN: 9780309113014, pp. 97-105, Washington, D.C.

Tran, N. H., and Hall, K. D. (2007b). “Development and Influence of Statewide Axle Load Spectra on Flexible Pavement Performance”. *Transportation Research Record: Journal of the Transportation Research Board, No. 2037, Rigid and Flexible Pavement Design 2007,* ISBN: 9780309113014, pp. 106-114, Washington, D.C.

Ishak, S., Shin, H. C., Sridhar, B. K., and Zhang, Z. (2010). “Characterization and Development of Truck Axle Load Spectra for Future Implementation of Pavement Design Practices in Louisiana”. *Transportation Research Record: Journal of the Transportation Research Board, No. 2153,* ISSN: 0361-1981, pp. 121-129, Washington, D.C.

Smith, B. C., and Diefenderfer, B. K. (2010). “Analysis of Virginia-Specific Traffic Data for Use with the Mechanistic-Empirical Pavement Design Guide”. *Transportation Research Record: Journal of the Transportation Research Board, No. 2154, Pavement Management 2010 (Volume 2),* ISBN: 9780309142946, pp. 100-107, Washington, D.C.

Haider, S. W., Harichandran, R. S., and Dwaikat, M. B. (2010). “Effect of Axle Load Measurement Errors on Pavement Performance and Design Reliability”. *Transportation Research Record: Journal of the Transportation Research Board, No. 2160, Data Systems and Travel Survey Methods 2010,* ISBN: 9780309142885, pp. 107-117, Washington, D.C.

Tran, N. H., and Hall, K. D. (2007). “Evaluation of Weigh-In-Motion Data for Developing Axle Load Distribution Factors for Mechanistic Empirical Pavement Design Guide”. *Transportation Research Board Annual Meeting: TRB 86th Annual Meeting Compendium of Papers CD-ROM,* Paper No. 07-0698, 22 p, Washington, D.C.

Hoegh, K., Khazanovich, L., and Jensen, M. (2010). "Local Calibration of Mechanistic-Empirical Pavement Design Guide Rutting Model: Minnesota Road Research Project Test Sections". *Transportation Research Record: Journal of the Transportation Research Board, No. 2180, Bituminous Materials and Mixtures 2010, Volume 2,* ISBN: 9780309160506, pp. 130-141, Washington, D.C.

Li, J., Pierce, L. M., and Uhlmeyer, J. (2009). "Calibration of Flexible Pavement in Mechanistic-Empirical Pavement Design Guide for Washington State". *Transportation Research Record: Journal of the Transportation Research Board, No. 2095, Pavement Management 2009, Volume 3,* ISBN: 9780309126328, pp. 73-83, Washington, D.C.

Banerjee, A., Aguiar-Moya, J. P., and Prozzi, J. A. (2009). "Calibration of Mechanistic-Empirical Pavement Design Guide Permanent Deformation Models: Texas Experience with Long-Term Pavement Performance". *Transportation Research Record: Journal of the Transportation Research Board, No. 2094, Pavement Management 2009, Volume 2,* ISBN: 9780309126113, pp. 12-20, Washington, D.C.

Muthadi, N. R., and Kim, Y. R. (2008). "Local Calibration of Mechanistic-Empirical Pavement Design Guide for Flexible Pavement Design". *Transportation Research Record: Journal of the Transportation Research Board, No. 2087, Pavement Testing and Design 2008,* ISBN: 9780309126007, pp. 131-141, Washington, D.C.

Hall, K. D., Wang, K. C., and Xiao, D. X. (2011). "Calibration of the Mechanistic-Empirical Pavement Design Guide for Flexible Pavement Design in Arkansas". *Transportation Research Record: Journal of the Transportation Research Board, No. 2226, Pavement Management 2011, Volume 2*, ISBN: 9780309167369, pp. 135-141, Washington, D.C.

Wang, K., Li, Q., Hall, K., Nguyen, V., Gong, W., and Hou, Z. (2008). "Database Support for the New Mechanistic-Empirical Pavement Design Guide". *Transportation Research Record: Journal of the Transportation Research Board, No. 2087, Pavement Testing and Design 2008*, ISBN: 9780309126007, pp. 109-119, Washington, D.C.

Li, S., Jiang, Y., Zhu, K., and Nantung, T. (2007). "Truck Traffic Characteristics for Mechanistic-Empirical Flexible Pavement Design: Evidences, Sensitivities, and Implications". *Transportation Research Board Annual Meeting: TRB 86th Annual Meeting Compendium of Papers CD-ROM*, 21p, Washington, D.C.

Haider, S. W., and Harichandran, R. S. (2007). "Characterizing Axle Load Spectra by Using Gross Vehicle Weights and Truck Traffic Volumes". *Transportation Research Board Annual Meeting: TRB 86th Annual Meeting Compendium of Papers CD-ROM*, Paper No. 07-2342, 25p, Washington, D.C.

Oman, M. (2010). "MnROAD Traffic Characterization for Mechanistic-Empirical Pavement Design Guide Using Weigh-in-Motion Data". *Transportation Research Board Annual Meeting: TRB 89th Annual Meeting Compendium of Papers CD-ROM*, Paper No. 10-2903, 19p, Washington, D.C.

Sayyady, F., Stone, J. R., Taylor, K. L., Jadoun, F. M., and Kim, Y. R. (2010). "Clustering Analysis to Characterize Mechanistic-Empirical Pavement Design Guide Traffic Data in North Carolina". *Transportation Research Record: Journal of the Transportation Research Board, No. 2160, Data Systems and Travel Survey Methods 2010*, ISBN: 9780309142885, pp. 118-127, Washington, D.C.

Johanneck, L., Tompkins, D., Clyne, T., and Khazanovich, L. (2011). "Minnesota Road Research Data for Evaluation and Local Calibration of the Mechanistic-Empirical Pavement Design Guide's Enhanced Integrated Climatic Model". *Transportation Research Record: Journal of the Transportation Research Board, No. 2226, Pavement Management 2011, Volume 2,* ISBN: 9780309167369, pp. 30-40, Washington, D.C.

Orobio, A., and Zaniewski, J. P. (2011). "Sampling-Based Sensitivity Analysis of the Mechanistic-Empirical Pavement Design Guide Applied to Material Inputs". *Transportation Research Record: Journal of the Transportation Research Board, No. 2226, Pavement Management 2011, Volume 2,* ISBN: 9780309167369, pp. 85-93, Washington, D.C.

Grebenschikov, S., and Prozzi, J. A. (2011). "Enhancing Mechanistic-Empirical Pavement Design Guide Rutting-Performance Predictions with Hamburg Wheel-Tracking Results". *Transportation Research Record: Journal of the Transportation Research Board, No. 2226, Pavement Management 2011, Volume 2,* ISBN: 9780309167369, pp. 111-118, Washington, D.C.

Delgadillo, R., Wahr, C., and Alarcón, J. P. (2011). "Toward Implementation of the Mechanistic-Empirical Pavement Design Guide in Latin America: Preliminary Work in Chile". *Transportation Research Record: Journal of the Transportation Research Board, No. 2226, Pavement Management 2011, Volume 2,* ISBN: 9780309167369, pp. 142-148, Washington, D.C.

Li, J., Luhr, D. R., and Uhlmeyer, J. S. (2010). "Pavement Performance Modeling Using Piecewise Approximation". *Transportation Research Record: Journal of the Transportation Research Board, No. 2153, Pavement Management 2010, Volume 1,* ISBN: 9780309143004, pp. 24-29, Washington, D.C.

Mamlouk, M., and Zapata, C. E. (2010). "Necessary Assessment of Use of State Pavement Management System Data in Mechanistic-Empirical Pavement Design Guide Calibration Process". *Transportation Research Record: Journal of the Transportation Research Board, No. 2153, Pavement Management 2010, Volume 1,* ISBN: 9780309143004, pp. 58-66, Washington, D.C.

Saxena, P., Tompkins, D., Khazanovich, L., and Balbo, J. T. (2010). "Evaluation of Characterization and Performance Modeling Cementitiously Stabilized Layers in the Mechanistic-Empirical Pavement Design Guide". *Transportation Research Record: Journal of the Transportation Research Board, No. 2186, Soil Mechanics 2010,* ISBN: 9780309160599, pp. 111-119, Washington, D.C.

Cary, C. E., and Zapata, C. E. (2010). “Enhanced Model for Resilient Response of Soils Resulting from Seasonal Changes as Implemented in Mechanistic-Empirical Pavement Design Guide”. *Transportation Research Record: Journal of the Transportation Research Board, No. 2170, Geology and Properties of Earth Materials 2010,* ISBN: 9780309160391, pp. 36-44, Washington, D.C.

Kim, S., Ceylan, H., Gopalakrishnan, K., and Smadi, O. (2010). “Use of Pavement Management Information System for Verification of Mechanistic-Empirical Pavement Design Guide Performance Predictions”. *Transportation Research Record: Journal of the Transportation Research Board, No. 2153, Pavement Management 2010, Volume 1,* ISBN: 9780309143004, pp. 30-39, Washington, D.C.

El-Basyouny, M., and Jeong, M. G. (2010). “Probabilistic Performance-Related Specifications Methodology based on Mechanistic-Empirical Pavement Design Guide”. *Transportation Research Record: Journal of the Transportation Research Board, No. 2151, Construction 2010, Volume 1,* ISBN: 9780309142823, pp. 93-102, Washington, D.C.

Johanneck, L., and Khazanovich, L. (2010). “Comprehensive Evaluation of Effect of Climate in Mechanistic-Empirical Pavement Design Guide Predictions”. *Transportation Research Record: Journal of the Transportation Research Board, No. 2170, Geology and Properties of Earth Materials 2010,* ISBN: 9780309160391, pp. 45-55, Washington, D.C.

Schram, S. A., and Abdelrahman, M. (2010). “Integration of Mechanistic-Empirical Pavement Design Guide Distresses with Local Performance Indices”. *Transportation Research Record: Journal of the Transportation Research Board, No. 2153, Pavement Management 2010, Volume 1,* ISBN: 9780309143004, pp. 13-23, Washington, D.C.

Corley-Lay, J., Jadoun, F. M., Mastin, J. N., and Kim, Y. R. (2010). “Comparison of Flexible Pavement Distresses Monitored by North Carolina Department of Transportation and Long-Term Pavement Performance Program”. *Transportation Research Record: Journal of the Transportation Research Board, No. 2153, Pavement Management 2010, Volume 1,* ISBN: 9780309143004, pp. 91-96, Washington, D.C.

Katicha, S. W., Flintsch, G. W., McGhee, K. K., and Loulizi, A. (2010). “Use of Mechanistic-Empirical Pavement Design Guide for Mix Performance Evaluation Using the Dynamic Modulus”. *Transportation Research Record: Journal of the Transportation Research Board, No. 2180,* ISSN: 0361-1981, pp. 156-164, Washington, D.C.

Retherford, J. Q., and McDonald, M. (2010). “Reliability Methods Applicable to Mechanistic-Empirical Pavement Design Method”. *Transportation Research Record: Journal of the Transportation Research Board, No. 2154, Pavement Management 2010, Volume 2,* ISBN: 9780309142946, pp. 130-137, Washington, D.C.

Li, J., Pierce, L. M., Hallenbeck, M. E., and Uhlmeyer, J. S. (2009). “Sensitivity of Axle Load Spectra in the Mechanistic-Empirical Pavement Design Guide for Washington State”. *Transportation Research Record: Journal of the Transportation Research Board, No. 2093, Pavement Management 2009, Volume 1,* ISBN: 9780309126243, pp. 50-56, Washington, D.C.

Le, A. T., Lee, H. J., Park, H. M., and Lee, S. Y. (2009). “Development of a Permanent Deformation Model of Asphalt Mixtures for South Korean Pavement Design Guide”. *Transportation Research Record: Journal of the Transportation Research Board, No. 2095, Pavement Management 2009, Volume 3,* ISBN: 9780309126328, pp. 45-52, Washington, D.C.

Lu, Q., Zhang, Y., and Harvey, J. T. (2009). “Estimation of Truck Traffic Inputs for Mechanistic-Empirical Pavement Design in California”. *Transportation Research Record: Journal of the Transportation Research Board, No. 2095, Pavement Management 2009, Volume 3,* ISBN: 9780309126328, pp. 62-72, Washington, D.C.

Hajek, J., Billing, J. R., and Swan, D. J. (2011). “Forecasting Traffic Loads for M-E Pavement Design”. *Transportation Research Board Annual Meeting: TRB 90th Annual Meeting Compendium of Papers DVD,* Paper No. 11-1761, 20p, Washington, D.C.